SAND2018-13358J

On Mixed Integer Programming Formulations for the Unit Commitment Problem

Bernard Knueven
Discrete Math & Optimization, Sandia National Laboratories, Albuquerque, NM 87185, bknueve@sandia.gov

James Ostrowski
Industrial and Systems Engineering, University of Tennessee, Knoxville, TN 37996, jostrows@utk.edu

Jean-Paul Watson
Data Science & Cyber Analytics, Sandia National Laboratories, Livermore, CA 94551, jwatson@sandia.gov

We provide a comprehensive overview of mixed integer programming formulations for the unit commitment problem (UC). UC formulations have been an especially active area of research over the past twelve years, due to their practical importance in power grid operations, and this paper serves as a capstone for this line of work. We additionally provide publicly available reference implementations of all formulations examined. We computationally test existing and novel UC formulations on a suite of instances drawn from both academic and real-world data sources. Driven by our computational experience from this and previous work, we contribute some additional formulations for both production upper bound and piecewise linear production costs. By composing new UC formulations using existing components found in the literature and new components introduced in this paper, we demonstrate that performance can be significantly improved – and in the process, we identify a new state-of-the-art UC formulation.

Key words: Unit commitment, mixed integer programming, mathematical programming formulations

Nomenclature

Indices and Sets

$g \in \mathcal{G}$	Thermal generators
$l \in \mathcal{L}_g$	Piecewise production cost intervals for generator g: $1, \ldots, L_g$.
$s \in \mathcal{S}_g$	Start-up categories for generator g, from hottest (1) to coldest (S_g).
$t \in \mathcal{T}$	Hourly time steps: $1, \ldots, T$.
$[t, t') \in \mathcal{X}_g$	Feasible intervals of non-operation for generator g with respect to its minimum downtime, i.e., $[t, t') \in \mathcal{T} \times \mathcal{T}$ such that $t' \geq t + DT_g$, including times (as necessary) before and after the planning horizon $\mathcal{T}$.
$n \in \mathcal{N}$	Set of buses: $1, \ldots, N$.
$g \in \mathcal{G}_n$	Thermal generators at bus n.
$k \in \mathcal{K}$	Set of branches (lines): $1, \ldots, K$.
$k \in \delta^+(n)$	Lines to bus n, $\subseteq \mathcal{N}$.

$k \in \delta^-(n)$ Lines from bus n, $\subseteq \mathcal{N}$.

Parameters

B_k Susceptance of branch k.

C_g^l Cost coefficient for piecewise segment l for generator g (\$/MWh).

$\overline{C}_g^l$ Cost of generator g producing $\overline{P}^l$ MW of power (\$/h).

C_g^R Cost of generator g running and operating at minimum production $\underline{P}_g$ (\$/h).

C_g^s Start-up cost in category s for generator g (\$).

C_g^w Shutdown cost for generator g (\$).

C_{LP} Penalty cost for failing to meet or exceed load (\$/MWh).

C_{RP} Penalty cost for failing to meet reserve requirement (\$/MWh).

$D_n(t)$ Load (demand) at time t at bus n (MW).

D_g Number of hours generator g is required to be off at $t = 1$ (h).

DT_g Minimum down time for generator g (h).

F_k Transmission capacity of branch k (MW).

$k(n)$ From bus for branch k, $\in \mathcal{N}$.

$k(m)$ To bus for branch k, $\in \mathcal{N}$.

$p_g(0)$ Power output of generator g at time 0, $\in [0, \overline{P}_g]$ (MW).

$\overline{P}_g$ Maximum power output for generator g (MW).

$\overline{P}_g^l$ Maximum power available for piecewise segment l for generator g (MW).

$\underline{P}_g$ Minimum power output for generator g (MW).

$R(t)$ System-wide spinning reserve at time t (MW).

RD_g Ramp-down rate for generator g (MW/h).

RU_g Ramp-up rate for generator g (MW/h).

SD_g Shutdown rate for generator g (MW/h).

SU_g Start-up rate for generator g (MW/h).

TC_g Time down after which generator g goes absolutely cold, i.e., enters state S_g.

$\underline{T}_g^s$ Time offline after which the start-up category s is available ($\underline{T}_g^1 = DT_g$, $\underline{T}_g^{S_g} = TC_g$).

$u_g(0)$ State of generator g at time 0, $\in \{0, 1\}$.

U_g Number of hours generator g is required to be on on at $t = 1$ (h).

UT_g Minimum run time for generator g (h).

$\underline{W}_n(t)$ Aggregate renewables generation that is must-take at bus n at time t (MW).

$\overline{W}_n(t)$ Aggregate renewables generation available at bus n at time t (MW).

Variables

$p_g(t)$	Power generated for generator g at time t (MW), ≥ 0.
$p'_g(t)$	Power generated above minimum for generator g at time t (MW), ≥ 0.
$\overline{p}_g(t)$	Maximum power available for generator g at time t (MW), ≥ 0.
$\overline{p}'_g(t)$	Maximum power available above minimum for generator g at time t (MW), ≥ 0.
$p_{W,n}(t)$	Aggregate renewable generation used at bus n at time t (MW), ≥ 0.
$p^l_g(t)$	Power from piecewise interval l for generator g at time t (MW), ≥ 0.
$r_g(t)$	Spinning reserves provided by generator g at time t (MW), ≥ 0.
$u_g(t)$	Commitment status of generator g at time t, $\in \{0,1\}$.
$\tilde{u}_g(t)$	Commitment transition status of generator g at time t, $\in \{0,1\}$.
$v_g(t)$	Start-up status of generator g at time t, $\in \{0,1\}$.
$w_g(t)$	Shutdown status of generator g at time t, $\in \{0,1\}$.
$c^p_g(t)$	Production cost over $\underline{P}_g$ for generator g at time t (\$), ≥ 0.
$c^{SU}_g(t)$	Start-up cost for generator g at time t (\$), ≥ 0.
$c^{SD}_g(t)$	Shutdown cost for generator g at time t (\$), ≥ 0.
$\delta^s_g(t)$	Start-up in category s for generator g at time t, $\in \{0,1\}$.
$x_g(t,t')$	Indicator arc for shutdown at time t, start-up at time t', uncommitted for $i \in [t,t')$, for generator g, $\in \{0,1\}$, $[t,t') \in \mathcal{X}_g$.
$\theta_n(t)$	Voltage angle at bus n at time t (radians).
$f_k(t)$	Power flow on branch k from bus $k(n)$ to $k(m)$ at time t (MW).
$s_n(t)$	Load mismatch at bus n at time t (MW).
$s_R(t)$	Reserve shortfall at time t (MW), ≥ 0.

1. Introduction

Unit commitment (UC) is a foundational problem in real-world power systems operations and planning. The UC problem is to determine an operating schedule – which specifies unit on/off statuses and associated production levels – for a fleet of thermal power generators to meet forecasted load at minimum total production cost, while satisfying a range of physical (e.g., Kirchhoff's laws) and operational (e.g., unit production ramping limits) constraints. Variants of UC are used in power systems operations for day-ahead market clearing, and day-ahead and intra-day reliability processes. Simplified versions of these UC variants also see widespread use in power systems planning, specifically in production cost models.

Beginning with the PJM (Pennsylvania-Jersey-Maryland) independent system operator in 2005, power systems operators in the United States have transitioned from solving UC via heuristics based on Lagrangian relaxation to formulating UC as mixed-integer (linear) programs (MIPs) (O'Neill 2017) that are solved via commercial branch-and-cut engines such as CPLEX (International Business Machines Corporation 2018) and Gurobi (Gurobi Optimization, Inc. 2018). The savings associated with this transition are estimated at $5 billion USD annually in the United States alone (O'Neill 2017). For a recent high-level overview on UC and its importance in power systems operations and planning, we refer to Anjos et al. (2017).

The typical real-world day-ahead UC problem is solved for an hourly time resolution over 36 to 48 hours, and considers hundreds to thousands of thermal generators and transmission systems with up to tens of thousands of buses and lines. Because the size of the transmission system can make solving the UC problem prohibitively difficult in practice, typically only a small subset of transmission constraints are considered in the day-ahead UC variant (Chen et al. 2016). While system operators commonly have up to three hours to solve their day-head UC, much of that time is consumed verifying the input data (e.g., market bids and offers), performing post-solve feasibility checks (e.g., considering AC power flow), re-solving after integration of feasibility cuts, performing a pricing run, and finally publishing the results. Consequently, it is strongly desirable in practice to have a UC solution available in 10 to 15 minutes.

The importance of UC in practice and the size of real-world power systems has led to significant interest from both the research and practitioner communities in developing improved mathematical programming formulations of UC, in order to reduce branch-and-cut solve times. It is well-known that the choice of MIP formulation for any given optimization problem can have a significant impact on practical computational difficulty, and UC is no exception. Consequently, there has been significant research focus over the past twelve years in developing improved UC MIP formulations, i.e., focusing on "tighter" formulations with improved linear programming (LP) relaxations in order to reduce the tree exploration time associated with branch-and-cut. In this context, this paper makes the following contributions:

- We catalog existing formulations in the literature for the UC problem as originally defined by Carrion and Arroyo (2006), who additionally introduce the base MIP UC formulation that we consider herein. Improvements to this base formulation have been the subject of many subsequent papers, and such improvements are closely tracked by industry.
- We computationally examine the performance 41 different UC formulations on 68 instances considering three generator fleets of increasing size. This analysis carefully quantifies the performance of UC formulations reported in the literature, and identifies the present state-of-the-art.
- We make publicly available on GitHub (please contact the authors until the paper has completed the review process) the reference implementations for all of the UC formulations we consider, expressed in the Pyomo (`www.pyomo.org`) algebraic modeling language Hart et al. (2011, 2017), and additionally release all instances. The release of these reference implementations will allow the community to consider additional combinations we have not considered on their own test instances. The availability of tested MIP model and instances for UC will significantly reduce the time required to examine alternative novel UC formulations, ensures that accurate and controlled computational experiments can be conducted across the community, and provides a performance baseline against which the efficacy of novel UC formulations can be assessed.
- Driven by the computational experience from Damcı-Kurt et al. (2016), Knueven et al. (2017) and preliminary work for this paper, we introduce two formulation enhancements. One is a set of strong variable upper bound inequalities for a ramping-constrained generator. The other is a tightening of the piecewise linear production costs. The later allows us to derive, in an online supplement (Knueven et al. 2018c), a convex hull result for a generator with piecewise linear production costs, start-up and shutdown ramping constraints, and minimum uptime/downtime constraints.
- We introduce two novel UC formulations, one of which represents new combinations of components from existing UC formulations, and the other drawls on new components and existing formulations. We demonstrate that the later formulation significantly improves of the performance of any previously reported UC formulation, establishing a new state-of-the-art UC formulation.

In all, this paper puts forth a new benchmark for the unit commitment problem. While we do not consider various extensions of UC, e.g., stochastic or robust variants, different

reserve products, or improvements to the network model, nearly every extension has at its core formulations of the generation units, the variants of which is the primary focus of this paper. We therefore believe the results herein are broadly relevant to extensions of the unit commitment problem.

The remainder of this paper is organized as follows. We begin in Section 2 by introducing the basic UC model and key issues in its formulations. In Section 3, we detail the key formulation variants introduced for UC to date. Our computational experiments are based on several complete UC formulations introduced by researchers over the past twelve years; these are documented in Section 4, placed in the notational context of Section 3. We additionally consider some new UC formulations, as described in Section 5. Our computational experiments are summarized in Section 6, and we conclude with a summary of our findings and contributions in Section 7.

2. Overview

We formulate the general unit commitment problem as follows

$$\min \sum_{g \in \mathcal{G}} \sum_{t \in \mathcal{T}} c_g(t) \tag{1a}$$

$$\text{s.t.} \sum_{g \in \mathcal{G}} A_g(p_g, \overline{p}_g, u_g) + N(s) = L \tag{1b}$$

$$(p_g, \overline{p}_g, u_g, c_g) \in \Pi_g \qquad \forall g \in \mathcal{G}. \tag{1c}$$

Here c_g is the vector cost associated with $p_g, \overline{p}_g, u_g$, such that the objective function (1a) is to minimize system operation cost. The vectors p_g, $\overline{p}_g$, and u_g represent the feasible generation schedule, maximum power available, and the on/off status for generator g, respectively. The matrix $A_g(p_g, \overline{p}_g, u_g)$ determines how the generator interacts with the system requirements, which are written in matrix form as equation (1b). Here the variable s is other potential decision variables involving the operation of the system. Finally, constraint (1c) defines the feasible region for each generator's schedule and the cost associated with that schedule. Because generators usually have a discrete component to their operation (they are either on and operating above some minimum level $\underline{P}$ or off), the set Π_g is often non-convex. In reality the system constraints (1b) are non-convex as networks usually use alternating current; in practice this is often approximated using a linear set of constraints. For the

purposes of this paper will we assume the system constraints are linear in nature, and we consider only a minor variation with regards to how the reserve is modeled.

Most of the research for MIP formulations of UC has focused on better descriptions of the non-convex set Π_g. We will refer to the $\text{conv}(\Pi_g)$ as the *generator polytope*. Tighter descriptions for Π_g tend to increase the linear-programming relaxation bound of (1), which often reduces computation times by reducing the enumeration necessary to find and prove an optimal solution. However, in general tighter descriptions tend to use more variables and/or constraints, so which description to use in practice is a balance between the tightness and the compactness for the given choices. Further, modern commercial MIP solvers have sophisticated cut-generation and pre-solve routines which can serve to tighten a formulation automatically.

Common constraints for Π_g are minimum/maximum generation levels when on, production ramping limits, minimum up-times and down-times, piecewise linear convex production costs, and time-dependent start-up costs. Most of the UC literature involves finding a *locally ideal* or *locally tighter* formulation for a subset of the constraints in Π_g, that is, just considering one (or two) of the types of constraints above and deriving a result for that (or those) constraint type(s).

Regarding the minimum uptime/downtime constraints, Lee et al. (2004) shows a convex hull description of these constraints alone is exponential in the space of the u variables, though the constrains can be separated in linear (in T) time. Malkin (2003) and Rajan and Takriti (2005) show these same minimum uptime/downtime constraints have a linear-sized convex hull when one adds the start-up variable $v(t)$, indicating the generator is switched on at time t. Subsequent work has shown the uptime/downtime constraints provided by Malkin (2003) and Rajan and Takriti (2005) to be computationally beneficial (Ostrowski et al. 2012, Morales-España et al. 2013a), and are usually one of the core components of a modern unit commitment model.

Frangioni et al. (2009) demonstrates how to tighten the piecewise linear production costs using *perspective cuts*. These serve to accurately model the production costs not just in the space of the p variables, but in the space of the (p, u) variables. The formulation given is the convex hull of the piecewise linear production costs with the addition of basic minimum/maximum power constraints. Sridhar et al. (2013) gives similar results for a broad class of potential piecewise linear formulations, and Wu (2016) confirms this

result for the SOS2-type formulation as gives an additional locally ideal reformation of the piecewise linear constraints from Carrion and Arroyo (2006). Chen and Wang (2017) gives yet another locally ideal formulation which is a modification of the SOS2-type formulation. In this paper we will present another formulation which is locally ideal for the piecewise production cost, generation limits, start-up and shutdown ramps, and the minimum up-time/down-time constraints. An extension of the result from Knueven et al. (2018b) will show this is also tight when time-dependent start-up costs are added.

Morales-España et al. (2013a) presents a tightening of the generation limits when there are start-up and shutdown ramping limits, which are the maximum the generator can produce when turning on and turning off, respectively. A follow-up paper, Gentile et al. (2017), shows that a slight modification of this formulation is locally ideal for the generation limits, start-up/shutdown ramp limits, and minimum up/down times.

Morales-España et al. (2013a) also introduces and computationally evaluates a reformulation for the time-dependent start-up costs, which had been typically modeled as in Nowak and Römisch (2000). Knueven et al. (2018b) proves the formulation from Morales-España et al. (2013a) is tighter than that of Nowak and Römisch (2000) and introduces a new formulation that is as tight, but smaller, than a locally ideal formulation for time-dependent start-up costs. Knueven et al. (2018b) further shows that any formulation ideal in the uptime/downtime constraints of Malkin (2003) and Rajan and Takriti (2005) will have an integer optimal solution when the start-up cost formulation introduced therein is added. Queyranne and Wolsey (2017) give a convex hull description for time-dependent start-up costs which requires $O(T^2)$ constraints.

The ramping constraints are perhaps the most studied. Ostrowski et al. (2012) introduces strengthening inequalities for ramping, some of which are shown to be facets of certain projections of Π_g. Damcı-Kurt et al. (2016) defines the convex hull for the two-period ramp-up polytope and the two-period ramp-down polytope, as well as several classes of facet-defining inequalities for the ramp-up and ramp-down constraints, respectively. Pan and Guan (2016) gives the convex hull description for $T = 3$ with minimum up/down time constraints, production limits, ramping limits, and start-up/shutdown limits, and facet-defining inequalities for this polytope when $T > 3$. Pan and Guan (2017) extends this result for general T for a couple special cases, and gives convex hull descriptions for the ramping-up polytope (that is, minimum up/down time constraints, production limits,

ramp-up limits, and start-up limit) and ramping-down polytope for general T. However, all these formulations require an exponential number of constraints when expressed with the p, u, v (and/or w) variables.

As was the case with the minimum up-time/down-time constraints, an extended formulation may prevent such exponential blow-up in the number of constraints. Knueven et al. (2017) shows the generator polytope $\text{conv}(\Pi_g)$ can be expressed with $O(T^3)$ variables and constraints. Guan et al. (2018) give two different extended formulations for the generator polytope. However, all of the extended formulations for the whole of $\text{conv}(\Pi_g)$ tend to be too large for direct incorporation into a UC MIP model.

So while a perfect formulation for a generator exists, it is not practical to use within a MIP formulation for UC. The question then is an engineering one–what formulation is good in practice? That is, determine a formulation which typically performs well when solving UC with a modern commercial MIP solver. This has often been discussed in the literature as a trade-off between tightness and compactness. A "tight" formulation for a generator is either a convex hull description for Π_g or a set of equations which are thought to provide a good approximation for $\text{conv}(\Pi_g)$, where as a "compact" formulation is one which describes Π_g without using "too many" variables and constraints. The thought is that a tight formulation will provide a better bound for the MIP solver to exploit, at the cost of increasing the size of the linear programming relaxation, whereas a compact formulation will result in faster node solve times, at the cost of weakening the lower bound given by the linear programming relaxation.

However, this paradigm is not an entirely accurate presentation of the landscape. Modern commercial MIP solvers have both sophisticated heuristics and cut-generation routines which work on finding better incumbent solutions and lower bounds, respectively. Because of this, many UC problems can be solved to a reasonable optimality gap a the root node or with only minimal enumeration. Differences in formulation may affect the cut-generation routines or the heuristics in ways that are difficult to anticipate. For example, it has been observed that tighter formulations often improve the performance of MIP heuristics (Rothberg 2018). For these reasons, it is important to evaluate UC formulations empirically, as it is difficult to know a priori the effect of making a formulation tighter or more compact.

3. Formulations

Throughout much of this section, we discuss formulations for constraints and variables describing Π_g. When describing the formulation for a single generator, we will drop the subscript g for clarity and ease of presentation. Most of the constraints described here could be applied to every generator $g \in \mathcal{G}$; we will explicitly point out when this is not the case. In a similar fashion, most constraints can be applied to every time period, so we will often forgo the qualifier $\forall t \in \mathcal{T}$, and put an additional qualifier on the time step t if necessary. In general, the variables $v(t)$ and $w(t)$ for $t < 1$ should be based on historical data, and for $t > T$ they can be assumed to be 0.

3.1. State variables and minimum up-time/down-time constraints

3.1.1. Three- (and two-) binary formulations Garver (1962) first proposed using three binary variables to represent the state of the generator: $u(t)$ for if the generator is on at time t, $v(t)$ if the generator is turned on at time t, and $w(t)$ if the generator is turned off at time t. Garver (1962) also first formulated the logical constraints, which relate the three binary variables:

$$u(t) - u(t-1) = v(t) - w(t) \qquad t \in \mathcal{T}. \tag{2}$$

Common to all models is the need to enforce the initial uptime and downtime constraints based on the generator g's history. As some generators can have very long minimum up-times and down-times, these are formulated as:

$$\sum_{i=1}^{\min\{U,T\}} u(i) = \min\{U, T\} \tag{3a}$$

$$\sum_{i=1}^{\min\{D,T\}} u(i) = 0. \tag{3b}$$

Any reasonable formulation of these constraints should cause the solver to preprocess away the involved variables in short order. Note that if U or D are 0 these sums become empty, thus eliminating these constraints.

A now common way to formulate minimum up-time and down-time are the turn on/turn off inequalities proposed by Malkin (2003) and Rajan and Takriti (2005):

$$\sum_{i=t-UT+1}^{t} v(i) \leq u(t) \qquad t \in \{UT, \ldots, T\} \tag{4}$$

$$\sum_{i=t-DT+1}^{t} w(i) \leq 1 - u(t) \qquad t \in \{DT, \dots, T\}. \tag{5}$$

Malkin (2003) and Rajan and Takriti (2005) independently showed that these constraints are facets of the convex hull of the uptime/downtime polytope, which together with (2) and variable bounds are an ideal formulation for up-time/down-time. A more recent and general proof can be found in Queyranne and Wolsey (2017), which extends this result to minimum up-time and down-times which vary across the planning horizon, as well as *maximum* up-times and down-times. One may use equation (2) to project out either the v or w variables while not losing strength. Typically the w variables are projected out as there are costs usually associated with start-up but not shutdown. The resulting logical and minimum down-time constraints, respectively, are

$$v(t) \geq u(t) - u(t-1) \qquad \forall t \in \mathcal{T} \tag{6}$$

$$\sum_{i=t-DT+1}^{t} v(i) \leq 1 - u(t-DT) \qquad t \in \{DT, \dots, T\}. \tag{7}$$

While not often used, this version of the logical and minimum down-time constraints was tested computationally in Yang et al. (2017) (which completely projects out the shutdown variables w), and a version of equation (7) was computationally tested in Atakan et al. (2018). Note that in what follows, if only the two-binary variables $u(t)$ and $v(t)$ are used, we can always use the substitution provided by (2) to eliminate $w(t)$ from the expression.

3.1.2. State transition variables Atakan et al. (2018) suggest replacing the variable $u(t)$ with a state-transition variable $\tilde{u}(t)$ which encodes if the generator g remains operational at time t. (The state transition variables for start-up and shutdown are equivalent to Garver's.) They also give the mathematical relationship

$$u(t) = \tilde{u}(t) + v(t), \tag{8}$$

which allows for the transformation of constraints for Garver's three-binary variables to those for the state-transition variables.

In particular, the logic constraint (2) becomes

$$\tilde{u}(t) - \tilde{u}(t-1) = v(t-1) - w(t) \qquad t \in \mathcal{T}, \tag{9}$$

and Atakan et al. (2018) uses constraints (4) and (7) with this transformation applied for minimum up-time/down-time:

$$\sum_{i=t-UT+1}^{t-1} v(i) \leq \tilde{u}(t) \qquad t \in \{UT, \dots, T\} \tag{10}$$

$$\sum_{i=t-DT}^{t} v(i) \leq 1 - \tilde{u}(t-DT) \qquad t \in \{DT, \dots, T\}. \tag{11}$$

The historical stay-on and turn-on at $t=0$, $\tilde{u}(0)$ and $v(0)$, can be inferred from the initial information. Similarly, constraints such as (3) can be formulated to enforce the initial run-time or off-time.

There are many other potential ways to formulate the minimum up-time/down-time constraints using two or three binary variables, but the ones presented above are most common in the MIP UC literature. Hedman et al. (2009) gives an overview of other possible formulations. We detail additional formulations for uptime and downtime from Dillon et al. (1978), Takriti et al. (2000), and Carrion and Arroyo (2006) in the online supplement (Knueven et al. 2018c, Section B.1).

3.2. Power and reserve variables

There are two suggestions in the literature for formulating the power output of a generator: (1) $p_g(t)$ to represent the power produced by generator g at time t, and (2) $p'_g(t)$, which represents the power produced above $\underline{P}_g$ by generator g at time t. The former formulation has been more common, though the later was suggested by Garver (1962) and has recently been put forward by Morales-España et al. (2013a). The two variable choices are equivalent mathematically through the linear relationship

$$p_g(t) = p'_g(t) + \underline{P}_g u_g(t). \tag{12}$$

For the reserve contribution, here again the literature suggests two possible approaches. One, introduced by Carrion and Arroyo (2006), is to model the maximum power available for generator g at time t, which we will call $\overline{p}_g(t)$. The other, introduced by Morales-España et al. (2013a), is to model the reserves contributed by generator g at time t, which we refer to as $r_g(t)$. For this paper we introduce a third possibility, which is to have a variable for

the maximum power available above minimum for generator g at time t, referred to as $\overline{p}'_g(t)$. Here we have the linear relationships

$$\overline{p}_g(t) = \overline{p}'_g(t) + \underline{P}_g u_g(t) \tag{13}$$

$$\overline{p}'_g(t) = p'_g(t) + r_g(t) \tag{14}$$

$$\overline{p}_g(t) = p_g(t) + r_g(t), \tag{15}$$

so like with power these three variable choices are mathematically equivalent. Note we also have the relationships

$$p_g(t) \leq \overline{p}_g(t) \tag{16}$$

$$p'_g(t) \leq \overline{p}'_g(t), \tag{17}$$

both of which can be appropriately translated using the equations above.

The linear relationships provided by equations (12)–(15) allow for the translation of constraints involving one group of variables into constraints involving another through simple substitution. In the proceeding we will use the constrains as they were presented in the papers that introduced them; applying the transformations directly when they allow for cancellations which reduce the number of non-zeros or simplify the constraint. Practically, formulations with $p'_g(t)$ are more difficult to implement if $\underline{P}_g$, $\overline{P}_g$ are functions of time.

3.3. Generation limits and upper bounds

The simplest generation limits, when stated in terms of the $p, \overline{p}$ variables is given by Carrion and Arroyo (2006)

$$\underline{P}_g u_g(t) \leq p_g(t) \leq \overline{p}_g(t) \leq \overline{P}_g u_g(t). \tag{18}$$

Additionally, to ensure total capacity is not exceeded as the generator g is shutting down, Arroyo and Conejo (2000) define the constraint

$$\overline{p}_g(t) \leq \overline{P}_g(u_g(t) - w_g(t+1)) + SD_g w_g(t+1). \tag{19}$$

Morales-España et al. (2013a) proposes using the start-up and shutdown ramping limits to tighten the variable upper bounds:

$$p'_g(t) + r_g(t) \leq (\overline{P}_g - \underline{P}_g)u_g(t) - (\overline{P}_g - SU_g)v_g(t) - (\overline{P}_g - SD_g)w_g(t+1) \quad g \in \mathcal{G}^{>1} \tag{20}$$

$$p'_g(t) + r_g(t) \leq (\overline{P}_g - \underline{P}_g)u_g(t) - (\overline{P}_g - SU_g)v_g(t) \qquad g \in \mathcal{G}^1 \quad (21a)$$

$$p'_g(t) + r_g(t) \leq (\overline{P}_g - \underline{P}_g)u_g(t) - (\overline{P}_g - SD_g)w_g(t+1) \qquad g \in \mathcal{G}^1, \quad (21b)$$

where $\mathcal{G}^{>1} := \{g \in \mathcal{G} \mid UT_g > 1\}$ and $\mathcal{G}^1 := \{g \in \mathcal{G} \mid UT_g = 1\}$. With the $\overline{p}$ variables constraint (20) can be equivalently expressed

$$\overline{p}_g(t) \leq \overline{P}_g u_g(t) - (\overline{P}_g - SU_g)v_g(t) - (\overline{P}_g - SD_g)w_g(t+1) \qquad g \in \mathcal{G}^{>1}, \quad (22)$$

and (21) can similarly be translated. Note that (21b) is the same expression as (19) through (13) and (14). Damcı-Kurt et al. (2016) showed that (21a) and (21b) are facets of the two-period ramp-up and ramp-down polytopes, respectively. Here the two-period ramp-up and ramp-down polytopes are simply the generator polytope for $T = 2$ while only considering the ramp-up and ramp-down constraints, respectively.

For $g \in \mathcal{G}^1$, when $SU_g \neq SD_g$, constraints (21) can be tightened (Gentile et al. 2017)

$$p'_g(t) + r_g(t) \leq (\overline{P}_g - \underline{P}_g)u_g(t) - (\overline{P}_g - SU_g)v_g(t) - [SU_g - SD_g]^+ w_g(t+1) \quad g \in \mathcal{G}^1 \quad (23a)$$

$$p'_g(t) + r_g(t) \leq (\overline{P}_g - \underline{P}_g)u_g(t) - (\overline{P}_g - SD_g)w_g(t+1) - [SD_g - SU_g]^+ v_g(t) \quad g \in \mathcal{G}^1, \quad (23b)$$

where $[\cdot]^+ := \max\{\cdot, 0\}$. Note that when $UT_g = 1$, it is possible for $v_g(t) = 1$ and $w_g(t+1) = 1$. This modification ensures that in this case both constraints are tight. Gentile et al. (2017) also gave a convex hull result using these tightened constraints along with (20). In particular, if $r_g(t)$ is fixed to zero and $UT_g > 1$, then (2), (4), (5), and (20), along with the basic $[0, 1]$ bounds on the binary variables, provides a convex hull description for these constraints (in particular, minimum up-time/down-time, start-up/shutdown ramps, and generation limits), for a single generator. If $UT_g = 1$, then (2), (4), (5), and (23), along with the variable bounds is a convex hull description for a single generator with these constraints. In either case, adding ramping constraints, piecewise linear production costs, and/or time-dependent start-up costs will result in a description that, in general, is no longer a convex hull description.

3.4. Ramping constraints

Ramping constraints are given by Arroyo and Conejo (2000) as

$$\overline{p}(t) - p(t-1) \leq RUu(t-1) + SUv(t) \quad (24)$$

$$p(t-1) - p(t) \leq RDu(t) + SDw(t). \quad (25)$$

These ramping constraints encode the physical limit that a generator's power output must not vary excessively within a certain time period. When the p' variables are used along with (20) or (21), Morales-España et al. (2013a) demonstrated these could be encoded more simply as

$$p'(t) + r'(t) - p'(t-1) \leq RU \tag{26}$$

$$p'(t-1) - p'(t) \leq RD. \tag{27}$$

3.4.1. Strengthening Ramping Ostrowski et al. (2012) introduced strengthened inequalities for ramping, under certain assumptions on the generator. Two ramp-up inequalities are proposed. The first holds for $g \in \mathcal{G}$ with $RU > SD - \underline{P}$ and $UT \geq 2$:

$$\begin{aligned} p(t) - p(t-1) \leq\ & RUu(t) - \underline{P}w(t) - (RU - SD + \underline{P})w(t+1) \\ & + (SU - RU)v(t) \qquad t \in \{1, \ldots, T-1\}, \end{aligned} \tag{28}$$

and the other when $RU > SD - \underline{P}$, $UT \geq 2$, and $DT \geq 2$:

$$\begin{aligned} p(t) - p(t-2) \leq\ & 2RUu(t) - \underline{P}w(t-1) - \underline{P}w(t) \\ & + (SU - RU)v(t-1) + (SU - 2RU)v(t) \qquad t \in \{2, \ldots, T-2\}. \end{aligned} \tag{29}$$

Though not mentioned in (Ostrowski et al. 2012), the $p(t)$ variable in (28) and (29) can be replaced with $\overline{p}(t)$ without loosing validity. Ostrowski et al. (2012) also proposes three ramp-down inequalities. The first is analogous to (28), and holds for $g \in \mathcal{G}$ with $RD > SU - \underline{P}$ and $UT \geq 2$:

$$\begin{aligned} p(t-1) - p(t) \leq\ & RDu(t) + SDw(t) - (RD - SU + \underline{P})v(t-1) \\ & - (RD - \underline{P})v(t) \qquad t \in \mathcal{T}, \end{aligned} \tag{30}$$

the second, when $RD > SU - \underline{P}$, $UT \geq 3$, and $DT \geq 2$:

$$\begin{aligned} p(t-1) - p(t) \leq\ & RDu(t+1) + SDw(t) + RDw(t+1) \\ & - (RD - SU + \underline{P})v(t-1) - (RD + \underline{P})v(t) \\ & - RDv(t+1) \qquad t \in \{1, \ldots, T-1\}, \end{aligned} \tag{31}$$

and the last, again when $RD > SU - \underline{P}$, $UT \geq 3$, and $DT \geq 2$:

$$\begin{aligned} p(t-2) - p(t) \leq\ & 2RDu(t) + SDw(t-1) + (SD + RD)w(t) \\ & - 2RDv(t-2) - (2RD + \underline{P})v(t-1) \\ & - (2RD + \underline{P})v(t) \qquad\qquad t \in \{2, \dots, T-2\}. \end{aligned} \tag{32}$$

Ostrowski et al. (2012) showed that (28)–(32) are facets for projections of the generator polytope onto the time periods and variables involved in these equations.

Damcı-Kurt et al. (2016) suggest a different formulation for the ramp-up and ramp-down inequalities, namely

$$p(t) - p(t-1) \leq (SU - \underline{P} - RU)v(t) + (\underline{P} + RU)u(t) - \underline{P}u(t-1) \tag{33}$$

$$p(t-1) - p(t) \leq (SD - \underline{P} - RD)w(t) + (\underline{P} + RD)u(t-1) - \underline{P}u(t). \tag{34}$$

Damcı-Kurt et al. (2016) demonstrate that these inequalities are facets of the two-period ramp-up and ramp-down polytopes, respectively. Validity is not affected if $p(t)$ is replaced with $\overline{p}(t)$ in (33). These inequalities are sparser when expressed using the $p'(t)$ variables:

$$\overline{p}'(t) - p'(t-1) \leq (SU - \underline{P} - RU)v(t) + RUu(t) \tag{35}$$

$$p'(t-1) - p'(t) \leq (SD - \underline{P} - RD)w(t) + RDu(t-1). \tag{36}$$

These inequalities are as sparse as (24) and (25) while having some guarantee on their strength. We detail a two-period ramp-up and ramp-down inequalities from Damcı-Kurt et al. (2016) in the online supplement (Knueven et al. 2018c, Section B.3). Damcı-Kurt et al. (2016) also give two additional exponential classes of two-period ramp-up and ramp-down inequalities; however, such inequalities require separation and hence will not be covered here. Similarly, Pan and Guan (2016) provide several exponential classes of two- and three-period ramping inequalities which are valid and facet-defining for the generator polytope, but as they also require separation we will not consider them here.

3.4.2. The Generator Polytope Knueven et al. (2017) introduces a perfect formulation for a generator with ramping constraints, and Guan et al. (2018) introduces three additional extended formulations for a ramping-constrained generator. While extended formulations for the generator polytope have been an interesting topic of research the past several years,

like the exponential classes of ramping inequalities from (Damcı-Kurt et al. 2016, Pan and Guan 2016, 2017), they are probably not appropriate for direct incorporation into the UC MIP because the additional variables and/or constraints become too burdensome. Thus we will not consider them for our computational comparisons to follow as they should be implemented in a more advanced way, such as using them as a separator for cut generation. However, we discuss these results in the online supplement (Knueven et al. 2018c, Section B.4).

3.5. Variable upper bounds with ramp limits

When ramping constraints are added, there maybe be an exponential number of variable upper bound inequalities in the three- or two-binary space which are tight (that is, they describe facets of the convex hull of the generator polytope), even when $SU = SD$ and $RU = RD$ (Damcı-Kurt et al. 2016, Pan and Guan 2016). However, computational experience with separating cuts from the generator polytope suggests that upper bound inequalities are often important in practice (Damcı-Kurt et al. 2016, Knueven et al. 2017), so they are worthy of special attention.

For notational ease, let $T^{RU} = \left\lfloor \frac{\overline{P}-SU}{RU} \right\rfloor$ and $T^{RD} = \left\lfloor \frac{\overline{P}-SU}{RD} \right\rfloor$. That is, T^{RU} (T^{RD}) is the number of time periods the generator spends ramping to go from SU ($\overline{P}$) to $\overline{P}$ (SD). Ostrowski et al. (2012) proposes tighter upper bounds on $p(t)$ based on the ramp-down trajectory of the generator

$$p(t) \leq \overline{P}u(t) - \sum_{i=0}^{K^{SD}(t)} (\overline{P} - (SD + iRD))w(t+1+i), \tag{37}$$

where $K^{SD}(t) = \min\{T^{RD}, UT-1, T-t-1\}$. This constraint enforces the maximum limit on the generator as it is shutting down, that is, if $w(t+2) = 1$, and the generator remains off past $t + K(t)$, then the upper bound on $p(t)$ is $SD + RD$, reflecting generator g's ramp-down and shutdown constraints.

Pan and Guan (2016) introduce several variable upper bound, the linear class of which is based on the ramp-up and shutdown trajectory of the generator

$$\overline{p}(t) \leq \overline{P}u(t) + (\overline{P} - SD)w(t+1) - \sum_{i=0}^{\min\{UT-2, T^{RU}\}} (\overline{P} - SU - iRU)v(t-i). \tag{38}$$

The has a nearly symmetric effect to that of (37), enforcing the maximum limit on the generator as it is starting up. This inequality additionally included the shutdown limit,

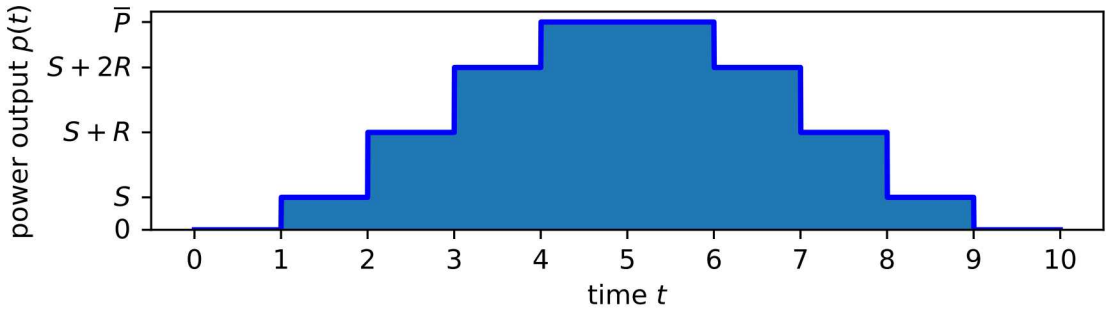

Figure 1 **Feasible region defined by inequalities** (39) **for a generator that turns on at** $t=1$ **and turns off at** $t=9$ **with** $UT=6$, $R=RU=RD$, $S=SU=SD$, $\underline{P}=0$, **and** $T^{RU}=T^{RD}=2$.

so it can also be seen as a generalization of (20). Note that because this inequality just involves the ramp-up trajectory with the shutdown limit, we can replace $p(t)$ with $\overline{p}(t)$ as we have done here.

Note that in both cases care must be taken with the minimum uptime UT. In particular, the minimum uptime must be such that if one of the v's or w's in inequalities (37) or (38) is 1, this implies $u(t)=1$. Like with (20), it must also be the case that at most one of the v's or w's in each inequality can be 1 to maintain validity. Finally, these type of inequalities need only "look back" (38) or "look forward" (37) enough time steps to capture T^{RU} or T^{RD}. In the online supplement we detail how (37) is derived from (Ostrowski et al. 2012, Eq. (19)) and how (38) is derived from (Pan and Guan 2016, Eq. (28)), and we also present some additional variable upper bounds (Knueven et al. 2018c, Section B.5).

By combining the insights from (37) and (38), one can derive similar polynomial classes of variable upper bounds. As an example, provided $UT \geq T^{RU}+T^{RD}+2$, the following inequality

$$p(t) \leq \overline{P}u(t) - \sum_{i=0}^{T^{RU}} (\overline{P} - (SU + iRU))v(t-i) - \sum_{i=0}^{T^{RD}} (\overline{P} - (SD + iRD))w(t+1+i) \tag{39}$$

is valid for all $t \in [T^{RU}, T - T^{RD}]$. The logic of (39) is similar to that of (37) and (38). Because $UT \geq T^{RD}+T^{RD}+2$, at most one of the v's or w's on the right-hand side is 1. When one of these variables is 1, the bound on $p(t)$ is adjusted downward to take into account the maximum power allowed by that ramp-up or ramp-down trajectory. Note that when $UT < T^{RU}+T^{RD}+2$, one can truncate the sums in (39) to ensure that at most one v or w is 1 and any v or w being 1 implies $u(t)=1$, given the minimum uptime UT. Figure 1 demonstrates how the inequalities (39) encode the ramping trajectory for a

ramping-constrained generator. We discuss an extension to when $UT = T^{RU} + T^{RD} + 1$ in the online supplement (Knueven et al. 2018c, Section B.5).

By combining some of the inequalities and ideas above we can create a set of strong variable upper bound inequalities which are complementary. Consider again inequality (38). If $UT - 2 < T^{RU}$, we may not cover the entire start-up ramping trajectory. In this case, we can augment (38) by shifting the terms

$$\overline{p}(t) \leq \overline{P}u(t) - \sum_{i=0}^{\min\{UT-1, T^{RU}\}} (\overline{P} - SU - iRU)v(t-i), \tag{40}$$

which with (38) covers an additional time period. Given (38) and (40), we notice the shutdown ramp trajectory is not considered. Here we can use a modified version of (39). Let $K^{SD}(t)$ be as in (37) and $K^{SU}(t) = \min\{T^{RU}, UT - 2 - [K^{SU}(t)]^+, t-1\}$, then

$$p(t) \leq \overline{P}u(t) - \sum_{i=0}^{K^{SD}(t)} (\overline{P} - (SD + iRD))w(t+1+i) - \sum_{i=0}^{K^{SU}(t)} (\overline{P} - (SU + iRU))v(t-i), \quad \text{if } K^{SD}(t) > 0 \tag{41}$$

where $K^{SD}(t)$ and $K^{SU}(t)$ serve to include as many v's and w's as possible given UT and the beginning and ending time period. If $K^{SU}(t) < T^{RU}$, we add the term $-[(SU + (K^{SU}(t) + 1)RU)) - (SD + T^{RD}RD)]^+ v(t - (K^{SU}(t) + 1))$ for additional tightening similar to (23b). Here we give preference to having more w's so as to correctly capture the shutdown ramp trajectory, given that the start-up ramp trajectory is covered by (38) or (40). Notice that if we are not near the beginning or end time periods and $UT \geq T^{RU} + T^{RD} + 2$, then (41) is exactly (39). If $K^{SD}(t) \leq 0$, this inequality should be omitted as it is dominated by (38).

3.6. Piecewise Linear Production Costs

For the purposes of this paper we will assume production costs (the marginal cost per MW of power) are piecewise linear and convex. While in reality the production costs follow a nonlinear (often quadratic) curve, in most electricity markets in the United States generators bid in piecewise offers. Further, we suspect that the general results in this paper would hold true for various potential MIQP formulations of UC where the marginal production cost is represented using a convex quadratic function. Frangioni et al. (2009) gives a method for solving a MIQP formulation for UC as a MILP using cutting-planes.

Garver (1962) included piecewise production costs in his original formulation. For each segment $l \in \mathcal{L}$, and $t \in \mathcal{T}$, the variable $p^l(t)$ represents the contribution to output from

piecewise segment l. Like Garver, we will assume throughout that $\overline{P}^l > \underline{P}$ for every l, and for convenience we define $\overline{P}^0 = \underline{P}$. (A simple preprocessing of the data will ensure this is the case.) Garver's formulation can then be written as

$$p^l(t) \leq (\overline{P}^l - \overline{P}^{l-1})u(t) \qquad l \in \mathcal{L}, \tag{42}$$

$$\sum_{l \in \mathcal{L}} p^l(t) = p'(t) \tag{43}$$

$$\sum_{l \in \mathcal{L}} C^l p^l(t) = c^p(t). \tag{44}$$

In actuality, Garver (1962) opted to use equation (43) to substitute out the p' variables, which do not explicitly appear in his model. However, with the basic limits on the $p'(t)$ variables, $p'(t) \leq (\overline{P} - \underline{P})u(t)$, this formulation is *locally ideal*, that is, (42), (43), and $p'(t) \leq (\overline{P} - \underline{P})u(t)$ along with the unit bounds on $u(t)$ are a convex hull description for these constraints (Wu 2016). This is essentially one of the production cost formulations from Wu (2016), except with (12) applied to (43). Finally, we substitute $\sum_{l \in \mathcal{L}} C^l p^l(t)$ for $c^p(t)$ in the objective function whenever $c^p(t)$ appears in and only in an equality constraint.

Carrion and Arroyo (2006) suggest a slightly simpler formulation, replacing (42) with

$$p^l(t) \leq (\overline{P}^l - \overline{P}^{l-1}) \qquad l \in \mathcal{L}. \tag{45}$$

Notice that (45) is the same as (42), except the binary on/off variable is not in the former. Because of this, this formulation does not have the locally ideal property (Sridhar et al. 2013).

Knueven et al. (2018a) tightens the bounds on $p^l(t)$ with the start-up and shutdown variables using the start-up and shutdown ramp:

$$p^l(t) \leq (\overline{P}^l - \overline{P}^{l-1})u(t) - C^v(l)v(t) - C^w(l)w(t+1) \qquad l \in \mathcal{L}, \tag{46}$$

where

$$C^v(l) := \begin{cases} 0 & \overline{P}^l \leq SU \\ \overline{P}^l - SU & \overline{P}^{l-1} < SU < \overline{P}^l \\ \overline{P}^l - \overline{P}^{l-1} & \overline{P}^{l-1} \geq SU \end{cases}, \qquad C^w(l) := \begin{cases} 0 & \overline{P}^l \leq SD \\ \overline{P}^l - SD & \overline{P}^{l-1} < SD < \overline{P}^l \\ \overline{P}^l - \overline{P}^{l-1} & \overline{P}^{l-1} \geq SD \end{cases},$$

for generators with $UT > 1$. When $UT = 1$, (46) must be replaced with:

$$p^l(t) \leq (\overline{P}^l - \overline{P}^{l-1})u(t) - C^v(l)v(t) \qquad l \in \mathcal{L} \tag{47a}$$

$$p^l(t) \leq (\overline{P}^l - \overline{P}^{l-1})u(t) - C^w(l)w(t+1) \qquad l \in \mathcal{L}. \tag{47b}$$

Notice that both (46) and (47) enforce that the piecewise production variables never exceed SU (SD) when the generator is turning on (off). Of course, these additional terms are not necessary for validity, they only serve to tighten the model. Finally, when $UT = 1$ and $SU \neq SD$, one can improve (47), in a similar fashion to (23a) and (23b):

$$p^l(t) \leq (\overline{P}^l - \overline{P}^{l-1})u(t) - C^v(l)v(t) - [C^v(l) - C^w(l)]^+ w(t+1) \qquad l \in \mathcal{L} \tag{48a}$$

$$p^l(t) \leq (\overline{P}^l - \overline{P}^{l-1})u(t) - C^w(l)w(t+1) - [C^w(l) - C^v(l)]^+ v(t) \qquad l \in \mathcal{L}. \tag{48b}$$

We show in the online supplement (Knueven et al. 2018c, Section A) that when $UT \geq 2$, (46) can be used to build an ideal formulation for a generator with piecewise production costs, minimum up/down times and start-up/shutdown ramping limits. In a similar fashion, we also show when $UT = 1$, (48) can be used to build an ideal formulation for a generator with start-up/shutdown ramping limits and piecewise production costs. We additionally show the start-up cost formulation from Knueven et al. (2018b) can be added to this without loosing strength. The inclusion of such strengthening for the piecewise linear costs may improve extended LMP calculation when the generator is turning on or turning off (Chen and Wang 2017, Hua and Baldick 2017). The generalization to considering the ramping trajectories when starting-up or shutting-down, as in (39), in the limits on $p^l(t)$ is straightforward but tedious.

Another common way to model convex piecewise production costs is by considering the typical epigraph formulation using $p'(t)$ and $c^p(t)$. That is (Atakan et al. 2018):

$$c^p(t) \geq C^l(p'(t) - (\overline{P}^{l-1} - \underline{P})) + \overline{C}^{l-1} \qquad \forall l \in \mathcal{L}. \tag{49}$$

Just a before, we can devise a locally ideal version for these production costs. This is sometimes called the *perspective formulation* (Frangioni and Gentile 2006, Frangioni et al. 2009). The form used here for convex piecewise linear production costs is given by (Hua and Baldick 2017):

$$c^p(t) \geq C^l p'(t) + (\overline{C}^{l-1} - C^l(\overline{P}^{l-1} - \underline{P}))u(t) \qquad \forall l \in \mathcal{L}. \tag{50}$$

As before, notice how the status variable u serves to adjust upward the production costs when $u(t)$ is fractional, which tightens the formulation. Notice that if the p variables are used this constraint simplifies a bit:

$$c^p(t) \geq C^l p(t) + (\overline{C}^{l-1} - C^l \overline{P}^{l-1}) u(t) \qquad \forall l \in \mathcal{L}. \tag{51}$$

We detail SOS2-type formulations for piecewise production costs in the online supplement (Knueven et al. 2018c, Section B.6).

3.7. Time-dependent start-up costs

When a thermal unit is switched off, the heat still left over begins to dissipate. However, if the unit is started-up while there is still heat remaining, it will cost less to bring it back up to operating temperature, and hence on-line.

Most UC models use an approximated and discretize version of these time-dependent start-up costs by considering different start-up types for each generator, often just hot, cold, and sometimes warm. In principle however, the formulations given below apply to an arbitrary number of start-up types.

3.7.1. Formulations with Additional Variables A common approach for start-up cost modeling is to add new variables to keep track of the generator's off-time and new constraints to tie these to the typical 3-binary variables.

On possibility is to use indicator variables for each start-up type $s \in \mathcal{S}_g$, for each $g \in \mathcal{G}$ and each $t \in \mathcal{T}$. This was originally proposed in Muckstadt and Wilson (1968), and has been more recently considered in Simoglou et al. (2010). We will use the more general formulation from Morales-España et al. (2013a)

$$\delta^s(t) \leq \sum_{i=\underline{T}^s}^{\underline{T}^{s+1}-1} w(t-i) \qquad s \in \mathcal{S} \setminus \{S\} \tag{52}$$

$$v(t) = \sum_{s=1}^{S} \delta^s(t) \tag{53}$$

$$c^{SU}(t) = \sum_{s=1}^{S} C^s \delta^s(t), \tag{54}$$

where $c^{SU}(t)$ can be eliminated from the formulation by substituting it for $\sum_{s=1}^{S} C^s \delta^s(t)$ (we always make this substitution for cost variables in the objective function which are defined by equalities). These same indicator variables can be used to track the power output during

different start-up and shutdown types, more accurately reflecting the generator's output as it comes on-line or goes off-line (Morales-España et al. 2013b). We also note that we can project out $\delta^S(t)$, the variable representing the coldest start-up type, by replacing (53) and (54) with

$$v(t) \geq \sum_{s=1}^{S-1} \delta^s(t) \tag{55}$$

$$c^{SU}(t) = c^S v(t) - \sum_{s=1}^{S-1} (C^S - C^s)\delta^s(t), \tag{56}$$

respectively. Convex hull results for time-dependent start-up costs using these variables can be found in Queyranne and Wolsey (2017) and Silbernagl (2016); however, in both cases a quadratic number of constraints is required. Additionally, both convex hull descriptions are somewhat cumbersome in their formulations.

Another formulation using indicators is presented in Knueven et al. (2018b). It uses the down-time arcs $x(t,t')$, but only for $[t,t') \in \mathcal{X}$ such that $t' - TC < t \leq t' - DT$:

$$\sum_{t'=t-TC+1}^{t-DT} x(t',t) \leq v(t) \tag{57}$$

$$\sum_{t'=t+DT}^{t+TC-1} x(t,t') \leq w(t) \tag{58}$$

$$c^{SU}(t) = c^S v(t) - \sum_{s=1}^{S-1} (C^S - C^s) \left(\sum_{t'=t-\underline{T}^{s+1}+1}^{t-\underline{T}^s} x(t',t) \right). \tag{59}$$

If $\underline{T}^s < \underline{T}^{s+1} - 1$ for some $s \in \mathcal{S} \setminus \{S\}$, then some of these arcs may be redundant, in the sense that there is more than one of them per start-up type for a given time period. However, Knueven et al. (2018b) showed this formulation to be as strong for increasing (non-decreasing) start-up costs as a perfect formulation. Like the other indicator variable formulations, this one too can be used to model power output for different start-up and shutdown types. We detail additional start-up cost formulations in the online supplement (Knueven et al. 2018c, Section B.7).

3.8. Shutdown costs

Shutdown costs are often 0, but in the case there are shutdown costs, the can be modeled in one of two ways. If the w variables are included, then the shutdown cost is simply

$$c^{SD}(t) = C^w w(t). \tag{60}$$

We handle the additional cases in the online supplement (Knueven et al. 2018c, Section B.8).

3.9. System Constraints

For the purposes of this paper, we will hold the system constraints constant, up to substitution of the variables used to describe the generators.

3.9.1. Renewables We will consider only aggregate renewables available at each bus n at time t, $p_{W,n}(t)$, and further assume they have zero marginal cost. To the extent that renewables bid into the market, they could be modeled as thermal generators as described above. Allowing for some (none to all) portion of the renewables to be must-take, this is modeled simply as

$$\underline{W}_n(t) \leq p_{W,n}(t) \leq \overline{W}_n(t) \qquad \forall t \in \mathcal{T}, \forall n \in \mathcal{N}, \tag{61}$$

where either parameter $\underline{W}_n(t)$ or $\overline{W}_n(t)$ may be 0 depending on policy and availability.

3.9.2. Network Constraints We will use the B, θ DC approximation for the transmission network, when one is provided. Consider the following network constraints:

$$f_k(t) = B_k \left(\theta_{k(n)}(t) - \theta_{k(m)}(t)\right) \qquad \forall k \in \mathcal{K}, \forall t \in \mathcal{T} \tag{62a}$$

$$-F_k \leq f_k(t) \leq F_k \qquad \forall k \in \mathcal{K}, \forall t \in \mathcal{T} \tag{62b}$$

$$-\pi \leq \theta_n(t) \leq \pi \qquad \forall n \in \mathcal{N}, \forall t \in \mathcal{T} \tag{62c}$$

$$\theta_1(t) = 0 \qquad \forall t \in \mathcal{T}. \tag{62d}$$

Equation (62a) is Kirchhoff's law; equation (62b) are the capacity constraints for the branches. We additionally bound the voltage angles to be no more than π in magnitude (62c) and fix the first bus to be the reference bus (62d). The flow balance constraints are:

$$\sum_{g \in \mathcal{G}_n} p_g(t) + p_{W,n}(t) + \sum_{k \in \delta^+(n)} f_k(t) - \sum_{k \in \delta^-(n)} f_k(t) + s_n(t) = D_n(t) \quad \forall n \in \mathcal{N}, \forall t \in \mathcal{T}, \tag{63}$$

where the constraint is satisfied if $s_n(t) = 0$. It is common for system operators to relax certain constraints – for example, if a demand cannot be met without an extraordinarily high cost, it may make sense for economic reasons to relax demand, and put a high penalty on $s_n(t) \neq 0$. This is modeled in a linear way using the typical auxiliary variables $s_n^+(t)$

and $s_n^-(t)$ to represent (respectively) the positive and negative part of the slack at bus n at time t, along with the constraints

$$s_n(t) = s_n^+(t) - s_n^-(t) \qquad \forall n \in \mathcal{N}, \forall t \in \mathcal{T} \tag{64a}$$

$$s_n^+(t),\ s_n^-(t) \geq 0 \qquad \forall n \in \mathcal{N}, \forall t \in \mathcal{T}. \tag{64b}$$

The penalty cost c_{LP} can then be put on both the $s_n^+(t)$ and $s_n^-(t)$ variables in the objective function. If appropriate, the variables $p_g(t)$ are replaced by the equivalent expression $p'_g(t) + \underline{P}u_g(t)$, depending on the variables used to represent generator output.

Finally, if there is only one bus (i.e., the network constraints are relaxed), (62) falls away, and the sums involving the $f_k(t)$ variables in equation (63) are empty, resulting in a simple system-wide demand constraint.

3.9.3. Reserve Requirement For this paper will we just consider a simple, system-wide spinning reserve requirement $R(t)$. Other ancillary services tend to vary by market.

The reserve requirement in (Carrion and Arroyo 2006, Ostrowski et al. 2012) is modeled as additional power above demand:

$$\sum_{g \in \mathcal{G}} \overline{p}_g(t) + s_R(t) \geq \sum_{n \in \mathcal{N}} D_n(t) + R(t), \qquad \forall t \in \mathcal{T} \tag{65}$$

whereas in (Morales-España et al. 2013a) the reserve requirement is modeled separately from total demand:

$$\sum_{g \in \mathcal{G}} r_g(t) + s_R(t) \geq R(t) \qquad \forall t \in \mathcal{T}. \tag{66}$$

Which one is used depends on how reserve production is modeled for the generators. If the $\overline{p}_g(t)$ or $\overline{p}'_g(t)$ variables are used, then equation (65) is the natural choice for the reserve requirement, substituting $\overline{p}'_g(t) + \underline{P}_g u_g(t)$ for $\overline{p}_g(t)$ if the $\overline{p}'_g(t)$ variables are used. Conversely, if the $r_g(t)$ variables are use to model reserve production, then equation (66) is more sensible. In either case note the relationship between these variables: $r_g(t) = \overline{p}_g(t) - p_g(t) = \overline{p}'_g(t) - p'_g(t)$. In both cases we also relax the global reserve requirement and add the penalty term $c_R s_R(t)$ to the objective for each $t \in \mathcal{T}$.

3.10. Objective Function

Finally, the objective is minimizing system operation cost:

$$\min \sum_{t\in\mathcal{T}} \left(\sum_{g\in\mathcal{G}} \left(c_g^p(t) + C_g^R u_g(t) + c_g^{SU}(t) + c_g^{SD}(t) \right) + \sum_{n\in\mathcal{N}} C_{LP} \left(s_n^+(t) + s_n^-(t) \right) + C_{RP} s_R(t) \right), \tag{67}$$

where when $c_g^p(t)$, $c_g^{SU}(t)$, or $c_g^{SD}(t)$ are expressed using equality constraints, we make the appropriate substitution directly into (67).

4. State-of-the-Art UC Formulations

Our analysis considers a range of UC formulations from the literature. Where possible, we mirror the authors' original formulation. However, some papers in the literature do not deal with every aspect of the UC problem discussed above. For example, many papers do not consider a network (Carrion and Arroyo 2006, Ostrowski et al. 2012, Morales-España et al. 2013a, Yang et al. 2017, Atakan et al. 2018), and even the seminal papers (Ostrowski et al. 2012, Morales-España et al. 2013a) do not consider piecewise production costs. We attempt to fill in these missing pieces by making a judgment about what would have been state-of-the-art at the time the source paper was published, and explicitly mention these differences as they arise. In this way, we hope to track the improvements in UC formulations over the past twelve years. When we state variable names when describing these formulations, they should be assumed to be T-dimensional vectors, e.g., $u_g \in \mathbb{Z}^T$, $p_g \in \mathbb{R}^T$. Similarly, the indexing set for those variables included in a model is implied.

For brevity, in the main text of this paper we only consider recent UC formulations that we show are computationally competitive performance. However, we additionally considered six other formulations from the literature, labeled **CA**, **OAV-O**, **OAV-UD**, **OAV**, **OAV-T**, and **ALS**. The first is from (Carrion and Arroyo 2006), the last from (Atakan et al. 2018), while the rest are variants tested in (Ostrowski et al. 2012). In general, these formulations are not competitive, as detailed with full computational results in the online supplement (Knueven et al. 2018c, Section C). This leaves two competitive UC formulations, which we denote **MLR** and **KOW**, which represent the current state-of-the-art.

Morales-España et al. (2013a) proposes many changes to the base UC formulation as compared to Carrion and Arroyo (2006), including the use of $p'_g(t)$ and $r_g(t)$ variables for power and reserves, start-up type indicator variables $\delta_g^s(t)$, and tighter bounds on generator

Table 1 Specification of the formulation proposed in Morales-España et al. (2013a)

Morales-España et al. (MLR)	
objective:	(67)
variables:	$u_g, v_g, w_g, \delta_g^s, p'_g, r_g, c_g^p, p_{W,n}, f_k, \theta_n, s_n^+, s_n^-, s_n, s_R$
uptime/downtime:	(2), (3), (4), (5)
generation limits:	(20), (21)
ramp limits:	(26), (27)
piecewise production:	(50)
start-up cost:	(52), (53), (54)
shutdown cost:	(60)
system constraints:	(62), (63), (64), (66)

Table 2 Specification of the formulation proposed in Knueven et al. (2018a)

Knueven et al. (KOW)	
objective:	(67)
variables:	$u_g, v_g, w_g, x_g, p'_g, r_g, p_g^l, p_{W,n}, f_k, \theta_n, s_n^+, s_n^-, s_n, s_R$
uptime/downtime:	(2), (3), (4), (5)
generation limits:	(20), (21)
ramp limits:	(26), (27)
piecewise production:	(43), (44), (46) if $UT_g > 1$, else (47)
start-up cost:	(57), (58), (59)
shutdown cost:	(60)
system constraints:	(62), (63), (64), (66)

production. We add the perspective formulation for piecewise cost curves (50) and the (B,θ) network formulation, which was referenced in (Morales-España et al. 2013a) but not considered therein for simplicity. Table 1 gives the complete formulation, which we refer to as **MLR**.

Knueven et al. (2018a) report a UC formulation similar to that of Morales-España et al. (2013a), with start-up costs formulated as in (Knueven et al. 2018b) in addition to a tighter description for piecewise production costs. As with **MLR**, we add the (B, θ) network formulation. The resulting formulation has the property that identical generators which are not ramping-constrained (i.e., $RU_g, RD_g \geq \overline{P}_g - \underline{P}_g$), can be exactly aggregated. Such aggregation can result in significant speed-ups for UC instances with identical generators, as symmetry issues are mitigated. Table 2 gives the complete formulation, which we refer to as **KOW**.

5. Novel Formulations

We now introduce two UC formulations that draw on various ideas presented above, yielding novel combinations of formulation components that have not been explicitly considered previously in the literature. The first formulation builds what should be a tight formulation,

Table 3 Specification of the "tight" formulation

Tight (T)	
objective:	(67)
variables:	$u_g, v_g, w_g, x_g, p'_g, \overline{p}'_g, p^l_g, p_{W,n}, f_k, \theta_n, s^+_n, s^-_n, s_n, s_R$
uptime/downtime:	(2), (3), (4), (5)
generation limits:	(17), (23), (38), (40) if $T^{RU}_g > UT_g - 2$, (41)
ramp limits:	(35), (36)
piecewise production:	(43), (44), (46) if $UT_g > 1$, else (48)
start-up cost:	(57), (58), (59)
shutdown cost:	(60)
system constraints:	(62), (63), (64), (65)

while sacrificing some compactness yet also exhibiting good computational performance. We refer to this formulation, presented in Table 3, as **T**. The differentiating features of the **T** formulation are the enhanced generation limits discussed in Section 3.5 and the tighter formulation for piecewise production cost discussed in Section 3.6. The **T** formulation also uses the two-period ramping limits from the ramp-up and ramp-down polytopes introduced in Damcı-Kurt et al. (2016) and the tight start-up cost formulation introduced in Knueven et al. (2018b). Finally, as with formulation **KOW**, formulation **T** has the property that identical generators with redundant ramping constraints can be aggregated exactly.

The second formulation we consider is also drawn from some of the tighter UC formulations reported in the literature, but emphasizes compactness at the potential loss of tightness. We refer to this formulation, presented in Table 4, as **Co**. This formulation is probably most similar to **MLR** (Morales-España et al. 2013a), with two exceptions: (1) we use the $\overline{p}'_g(t)$ variables for the reserve production because they empirically yield improved performance in practice relative to the $r_g(t)$ variables and (2) we use the ramping limits described in (Damcı-Kurt et al. 2016) used in formulation **T** in place of the ramping limits used in **MLR**. As with the **MLR** formulation, we use the perspective formulation to model piecewise production costs.

6. Computational Experiments

We now analyze the performance of various UC formulations, considering a variety of realistic test instances. All UC models were expressed using the Python-based Pyomo algebraic modeling library (`www.pyomo.org`) (Hart et al. 2011, 2017). In order to facilitate the comparison of a wide range of UC formulations, we developed a modular modeling framework that allows users to easily combine disparate formulation components from the

Table 4 Specification of the "compact" formulation

Compact (Co)	
objective:	(67)
variables:	$u_g, v_g, w_g, \delta_g^s, p'_g, \overline{p}'_g, c_g^p, p_{W,n}, f_k, \theta_n, s_n^+, s_n^-, s_n, s_R$
uptime/downtime:	(2), (3), (4), (5)
generation limits:	(17), (20), (21)
ramp limits:	(35), (36)
piecewise production:	(50)
start-up cost:	(52), (53), (54)
shutdown cost:	(60)
system constraints:	(62), (63), (64), (65)

literature to form both existing and novel UC models. This framework, in addition to all supporting code and problem instances, are available on GitHub (please contact the authors until the paper has completed the review process). While it is beyond the present scope to evaluate all possible UC formulations that can be expressed in the framework, our aim in this software release is to enable researchers and practitioners to quickly evaluate potential novel UC formulations by providing reference implementations of most of the formulation ideas found in the existing literature. Additionally, we solicit and will actively integrate new formulations for UC model components, as well as novel combinations that prove to be effective in practice.

6.1. Instances

We now describe the set of UC instances we consider in our computational experiments. We use realistic UC instances, based on real-world data, in order to avoid pathological issues that many of the synthetic instances reported in the UC literature possess. For example, the instances from (Carrion and Arroyo 2006, Ostrowski et al. 2012, Morales-España et al. 2013a) have excessive symmetry, which ends up dominating the solve time when not properly addressed, e.g., by the approaches reported by (Ostrowski et al. 2015, Knueven et al. 2018a,b). In all cases we consider a 48-hour scheduling horizon, mirroring the more difficult day-ahead (as opposed to reliability or intra-day UC) power systems operations context.

We consider three test sets, each based on realistic data. The first set, "RTS-GMLC," consists of twelve instances (corresponding to distinct days) associated with the newly introduced RTS-GMLC system (`https://github.com/GridMod/RTS-GMLC`) (Barrows et al. 2018). We consider variants both with and without the transmission network, for a total of 24 instances. The RTS-GMLC system is relatively small, with 73 thermal units.

Reserves are set at 3% of system load. The second set, "CAISO," is based on publicly available data available from the California Independent System Operator (CAISO) in the US. For the CAISO set, we consider five demand/renewable profiles and four system reserve levels, yielding a total of 20 instances. All CAISO instances consist of 410 thermal generators. Because it is sensitive critical infrastructure, we do not consider the transmission network. The third and final test set, "FERC," is based on data publicly available obtained from the US Federal Energy Regulatory Commission (FERC) (Krall et al. 2012), with demand, reserve quantities, and wind profiles taken from the PJM system operator in the US. The generator fleet from (Krall et al. 2012) is itself based on market data from PJM. Twelve demand/renewable profiles are considered, and the renewable data is scaled up to 30% penetration to create twelve additional instances. The FERC instances are the largest we consider, with approximately 900 thermal generators. In total, we solve 68 UC instances for each formulation considered in the computational experiments reported below. Further details on the test sets is available in the online supplement (Knueven et al. 2018c, Section D).

6.2. Novel UC Formulations

To demonstrate the utility of our modular framework for composing UC formulations, we sampled at random 1,000 formulations and solved each of the resulting formulations on each of our twenty-four RTS-GMLC instances. The formulations were sampled without replacement by selecting at random each of the eight components of a generator formulation (status variables, power variables, reserve variables, generation limits, ramping limits, production costs, uptime/downtime constraints, and start-up costs) based on the formulations discussed herein and the online supplement (Knueven et al. 2018c). Formulations with incompatible components were discarded. Each run used the Gurobi 8.0.1 (Gurobi Optimization, Inc. 2018) solver, limited to a single thread, with a 60 second time limit and a 0.0 optimality gap threshold. From these 1,000 formulations, we selected the two such UC formulations which scored in both the top 1% of shifted geometric mean optimality gap and geometric mean time. To compute the shifted geometric mean optimality gap, we add 1 to the optimality gap and compute the geometric mean of the resulting values. The two selected formulations are shown in Tables 5 and 6. Though we did not explicitly count the number of formulations our framework enables, we were able to generate 100,000

Table 5 Specification of the first randomly sampled UC formulation

Random1 (R1)	
objective:	(67)
variables:	$\tilde{u}_g, v_g, w_g, \delta_g^s, p'_g, \overline{p}'_g, c_g^p, p_{W,n}, f_k, \theta_n, s_n^+, s_n^-, s_n, s_R$
uptime/downtime:	(3), (9), (10), (11)
generation limits:	(17), (20), (21)
ramp limits:	(35), (36)
piecewise production:	(50)
start-up cost:	(52), (55), (56)
shutdown cost:	(60)
system constraints:	(62), (63), (64), (65)

Table 6 Specification of the second randomly sampled UC formulation

Random2 (R2)	
objective:	(67)
variables:	$u_g, v_g, w_g, \delta_g^s, p'_g, \overline{p}'_g, c_g^p, p_{W,n}, f_k, \theta_n, s_n^+, s_n^-, s_n, s_R$
uptime/downtime:	(2), (3), (4), (5)
generation limits:	(17), (23), (38), (40) if $T_g^{RU} > UT_g - 2$, (41)
ramp-up limits:	(24) if $RU_g \leq SD_g - \underline{P}_g$ or $UT_g < 2$, else (28)
ramp-down limits:	(25) if $RD_g \leq SU_g - \underline{P}_g$ or $UT_g < 2$, else (30) if $UT_g < 3$ or $DT_g < 2$, else (31)
2-ramp-up limits:	(29) if $RU_g > SD_g - \underline{P}_g$, $UT_g \geq 2$, and $DT_g \geq 2$
2-ramp-down limits:	(32) if $RD_g > SU_g - \underline{P}_g$, $UT_g \geq 3$, and $DT_g \geq 2$
piecewise production:	(50)
start-up cost:	(52), (53), (54)
shutdown cost:	(60)
system constraints:	(62), (63), (64), (65)

different formulations for UC, so we have explored no more than 1% of the search space with our sampling.

Inspection indicates that the first random formulation (denoted **R1**) is a modification of that introduced in Atakan et al. (2018) (see Table 6), but replaces the generation limits with those from Morales-España et al. (2013a), the modified start-up costs also from Morales-España et al. (2013a) (as presented in Section 3.7.1), and the perspective production cost formulation. Conversely, the second random formulation (denoted **R2**) is a mixture of diverse UC formulation ideas from the literature. Inspection indicates that **R2** essentially draws aspects from both the **T** and **Co** formulations, sharing the same set of variables as formulation **Co**, and adding the Morales-España et al. (2013a) start-up cost formulation and the perspective production cost formulation. However, **R2** further brings in the combination of generation limits used in formulation **T** and all of the ramping limits from Ostrowski et al. (2012), making it one of the denser formulations in terms of the number of power variables.

6.3. Results

All computational experiments were conducted on a Dell PowerEdge T620 with two Intel Xeon E5-2670 processors, 256GB of RAM, and running the Ubuntu 16.04.4 Linux operating system. Gurobi 8.0.1 was the MIP solver used in all tests, with the default settings preserved except for the time limit. Hence we attempt to solve all instances to a 0.01% relative optimality gap. No other intensive jobs were running on the system at the time the experiments were carried out.

We report the performance of each of the six UC formulations examined in summary tables, which report the following quantities: wall clock time, optimality gap, number of time outs (instances for which the time limit was reached), number of times a solution was found in the fastest overall time, and number of times a solution was found in the second fastest overall time. To rank the UC formulations, "times best" refers to the fastest solve time or if every formulation times out, the lowest optimality gap. "Times second" similarly refers to the second fastest solve or if every or all but one formulation times out, the second lowest optimality gap. In columns labeled "Time (s)" we report the geometric mean solve time in seconds, substituting the time limit for instances which time out. In columns labeled "Opt gap (%)" we report a shifted geometric mean optimality gap, where for each instance solved we replace the terminating optimality gap reported by the solver with the default tolerance of 0.01%. Because the optimality gap can be (close to) 0, we first add 1 to the optimality gap, compute the geometric mean, and subtract 1 from the result; the latter is the reported mean. We adjust the terminating optimality gap as the solver often terminates with a gap significantly less than 0.01%, and we do not wish to bias the reporting with this behavior. Thus, if every instance timed out, "Time (s)" would report the time limit, and conversely if every instance solved "Opt gap (%)" would report 0.01%. Full summary tables and detailed results are respectively provided in the online supplement (Knueven et al. 2018c), Sections E and G.

6.3.1. RTS-GMLC Summary computational results for the RTS-GMLC instances are reported in Table 7. Due to their relatively small size, we set the time limit for each solve of these instances to 300 seconds. We first note that two state-of-the-art formulations from the UC literature – **MLR** and **KOW** – perform very similarly, likely because they share many formulation components. Both the **MLR** and **KOW** formulations are outperformed by the **T** and **Co** formulations. Between formulations **T** and **Co**, **Co** is on average faster,

Table 7 Summary computational results for RTS-GMLC instances.

Formulation	Time (s)	Opt gap (%)	Time outs	Times best	Times 2nd
MLR	86.19	0.0165%	5	0	0
KOW	94.81	0.0165%	4	0	1
T	50.65	0.0121%	2	4	4
Co	43.11	0.0121%	**1**	1	4
R1	**32.37**	**0.0114%**	**1**	**14**	6
R2	36.94	0.0114%	**1**	4	**8**

Table 8 Summary computational results for CAISO instances.

Formulation	Time (s)	Opt gap (%)	Time outs	Times best	Times 2nd
MLR	117.1	0.0119%	2	0	1
KOW	79.02	0.0102%	2	4	**7**
T	**56.90**	**0.0100%**	**0**	**15**	3
Co	100.6	**0.0100%**	**0**	0	5
R1	147.4	0.0102%	1	0	1
R2	104.1	0.0100%	1	1	3

but **T** yields the fastest solve times more often. Even though **T** has an additional time-out over **Co**, their shifted geometric mean optimality gaps are identical. Finally, we observe that the best of the randomly sampled UC formulations – **R1** and **R2** – outperform even the **T** and **Co** formulations. Together, these two formulations together claim the majority of first and second place spots available across the formulations, and further possess the shortest geometric mean solve times and lowest shifted geometric mean optimality gap. It is worth emphasizing that these two random UC formulations were based on tests on the RTS-GMLC instances, so this result is not entirely surprising. However, the result does highlight that novel UC formulations can yield performance above that of state-of-the-art formulations reported in the literature.

6.3.2. CAISO Summary computational results for the CAISO instances are reported in Table 8. A time limit of 300 seconds for each solve of these instances was imposed, identical to that used for the RTS-GMLC experiments. The results indicate that formulation **MLR** is competitive on these instances, but is outperformed by **KOW** and the other four formulations introduced in this paper. Formulations **R1** and **R2** perform somewhat similarly on these instances, with **R2** leading in terms of time-to-solution. Formulation **R2**'s single time-out has a optimality gap of just over 0.01%, which is why its reported shifted geometric mean optimality gap is 0.0100%. However, in contrast to the results on

Table 9 Summary computational results for FERC instances.

Formulation	Time (s)	Opt gap (%)	Time outs	Times best	Times 2nd
MLR	340.5	0.0555%	3	4	1
KOW	390.2	0.0117%	2	3	5
T	**268.6**	**0.0104%**	**1**	**8**	4
Co	309.5	0.0596%	3	4	5
R1	308.9	0.0480%	3	3	**6**
R2	373.1	0.0665%	4	0	1

RTS-GMLC, the clear winner on the CAISO instances is formulation **T**, which yields the smallest geometric mean runtime and is fastest on three quarters of the instances. Further, as documented in the online supplement, the largest solve time given formulation **T** was 129.9 seconds, compared to a maximum time of 261.9 seconds for **Co** and 300+ seconds for the other four formulations.

6.3.3. FERC Summary computational results for the FERC instances are reported in Table 9. Because the FERC instances have over twice the number of thermal generators as the CAISO instances, we increase the solve time limit to 600 seconds. The results indicate that UC formulations using some variant of the start-up cost formulation from Morales-España et al. (2013a) (**MLR**, **Co**, **R1**, and **R2**) all perform similarly. In contrast, the start-up cost formulation from Knueven et al. (2018b) appears to be essential to achieving high-quality solutions across the FERC instance set, i.e., as can be seen for results obtained by the UC formulations **KOW** and **T**. Variant **T** slightly outperforms **KOW** in terms of geometric mean time to solution. Further, even on the one FERC instance for which formulation **T** hits the solve time limit, the terminating optimality gap is only 0.018%.

6.3.4. Summary Analysis Across the three test instance sets considered, the newly introduced "Tight" formulation **T** performs the best – establishing what we believe to be a new state-of-the-art in UC performance. Formulation **T** has the fewest time-outs overall, and is consistently the fastest on the larger and more difficult CAISO and FERC instances. In the worst case for **T**, Gurobi returns with a terminating gap of 0.05%, which is the best-worst case performance across all UC formulations examined. The performance of **T** is weakest on the RTS-GMLC instances, and in particular on the RTS-GMLC instances with a network. Upon closer examination, we believe this discrepancy is likely due to the lower number of nodes explored in the branch-and-cut process relative to the more

Table 10 Selected results for changing various components of the tight formulation T. For each row, we swap equations for the component in formulation T (e.g. uptime/downtime) with that defined by the equations given.

	RTS-GMLC		CAISO		FERC	
	Time (s)	Opt gap (%)	Time (s)	Opt gap (%)	Time (s)	Opt gap (%)
T	50.65	0.0121%	56.90	0.0100%	268.6	0.0103%
uptime/downtime						
RT 2bin: (4)(7)	48.29	0.0120%	51.30	0.0100%	235.1	0.0100%
generation limits						
MLR: (20)(21)	51.29	0.0122%	52.44	0.0100%	254.8	0.0100%
GMR: (20)(23)	51.37	0.0122%	52.42	0.0100%	254.1	0.0100%
ramping limits						
MLR: (26)(27)	49.28	0.0119%	48.53	0.0100%	242.6	0.0100%
piecewise production						
CA: (43)(44)(45)	48.93	0.0119%	57.87	0.0100%	230.2	0.0100%

compact formulations, i.e., **Co**, **R1**, and **R2**. Our analysis of solver logs suggests that Gurobi has difficulty generating cuts at the root node of the branch-and-cut tree when the (B, θ) linearized network representation is considered. Typically, system operators do not use this network representation when solving UC in practice, and instead rely on a Power Transfer Distribution Factor (PTDF) or related network formulations (Van den Bergh et al. 2014, Chen and Wang 2017). Because the vast majority of transmission lines will not have binding thermal limits in an optimal UC solution, those likely not to be at their limits can be dropped from the formulation (Chen et al. 2016) or treated as lazy constraints. Further, one can generate cover inequalities for the PTDF transmission constraints, which may tighten the relaxation (Wu 2016).

6.4. Detailed Analysis of the "Tight" Formulation

We undertook a detailed computational study to determine what aspects of formulation **T** are essential to its superior performance, and conversely which aspects could possibly be improved upon. For brevity, we report the full results in the online supplement (Knueven et al. 2018c, Section F), but provide selected results in Table 10. Overall, the results clearly indicate that there is some room for improvement over the base formulation **T**. Examining Table 10, formulating the uptime and downtime constraints using only two binary variables (in this case $u_g(t)$ and $v_g(t)$) resulted in a surprising performance improvement on the larger CAISO and FERC instances, with no degradation in performance on the RTS-GMLC instances.

Further examining Table 10, we see computational performance is moderately improved when considering the simpler MLR or GMR generation limits from Morales-España et al. (2013a) and Gentile et al. (2017), respectively. Interestingly the simple ramping limits from Morales-España et al. (2013a) improved the performance of **T**; this is likely because with the variable upper bounds used in **T**, the ramping constraints become mostly redundant. Finally, perhaps the formulate production costs from Carrion and Arroyo (2006) also exhibited some improvement in the FERC test instances over the tight but more complicated formulation introduced in this paper. However, because of the risk of over-fitting for these test cases, we will not explore combinations of these options, though they may prove beneficial for the practitioner.

7. Conclusion

This paper has undertaken a thorough examination of the state-of-the-art in formulations for the unit commitment problem, with subsequent computational analysis. The computational results presented herein suggests that with a modern formulation, realistic UC problems with up to a thousand generators and 48 time periods are easily solvable with modest hardware and a modern commercial MIP solver. The current challenges therefore in deterministic UC are (1) the interaction between unit commitment and the transmission system (Van den Bergh et al. 2014, Wu 2016), (2) virtual transactions, which may weaken our ability to tighten system constraints (Chen et al. 2016), (3) realistic modeling of the transmission system, including the need for reactive power support (Castillo et al. 2016), and (4) better modeling of the ancillary products, which tend to vary by market. Additional model changes will have to be considered with the continued increase in uncertain energy supply due to renewables, which could entail stochastic variants of UC, robust variants of UC, or additional reserve products, though all of these would have the deterministic formulations presented here at their core.

Acknowledgments

J. Ostrowski was supported by DOE (ASCR) award DE-SC0018175. B. Knueven and J.-P. Watson were supported by the U.S. Department of Energy (DOE), Office of Science, Office of Advanced Scientific Computing Research (ASCR), Applied Mathematics program under contract number KJ0401000 through the project "Multifaceted Mathematics for Complex Energy Systems", and the Grid Modernization Initiative of the U.S. DOE, under project 1.4.26, as part of the Grid Modernization Laboratory Consortium, a strategic partnership between DOE and the national laboratories to bring together leading experts, technologies, and

resources to collaborate on the goal of modernizing the nation's grid. Sandia National Laboratories is a multimission laboratory managed and operated by National Technology & Engineering Solutions of Sandia, LLC, a wholly owned subsidiary of Honeywell International Inc., for the U.S. Department of Energy's National Nuclear Security Administration under contract DE-NA0003525. This paper describes objective technical results and analysis. Any subjective views or opinions that might be expressed in the paper do not necessarily represent the views of the U.S. Department of Energy or the United States Government.

References

Anjos MF, Conejo AJ, et al. (2017) Unit commitment in electric energy systems. *Foundations and Trends® in Electric Energy Systems* 1(4):220–310.

Arroyo JM, Conejo AJ (2000) Optimal response of a thermal unit to an electricity spot market. *IEEE Transactions on Power Systems* 15(3):1098–1104.

Atakan S, Lulli G, Sen S (2018) A state transition MIP formulation for the unit commitment problem. *IEEE Transactions on Power Systems* 33(1):736–748.

Barrows C, Bloom A, Ehlen A, Jorgenson J, Krishnamurthy D, Lau J, McBennett B, O'Connell M, Preston E, Staid AS, Watson JP (2018) The IEEE reliability test system: A proposed 2018 update. Working Paper.

Carrion M, Arroyo JM (2006) A computationally efficient mixed-integer linear formulation for the thermal unit commitment problem. *IEEE Transactions on Power Systems* 21(3):1371–1378, ISSN 0885-8950.

Castillo A, Laird C, Silva-Monroy CA, Watson JP, O'Neill RP (2016) The unit commitment problem with AC optimal power flow constraints. *IEEE Transactions on Power Systems* 31(6):4853–4866.

Chen Y, Casto A, Wang F, Wang Q, Wang X, Wan J (2016) Improving large scale day-ahead security constrained unit commitment performance. *IEEE Transactions on Power Systems* 31(6):4732–4743.

Chen Y, Wang F (2017) MIP formulation improvement for large scale security constrained unit commitment with configuration based combined cycle modeling. *Electric Power Systems Research* 148:147–154.

Damcı-Kurt P, Küçükyavuz S, Rajan D, Atamtürk A (2016) A polyhedral study of production ramping. *Mathematical Programming* 158(1-2):175–205.

Dillon TS, Edwin KW, Kochs HD, Taud R (1978) Integer programming approach to the problem of optimal unit commitment with probabilistic reserve determination. *IEEE Transactions on Power Apparatus and Systems* (6):2154–2166.

Frangioni A, Gentile C (2006) Perspective cuts for a class of convex 0–1 mixed integer programs. *Mathematical Programming* 106(2):225–236.

Frangioni A, Gentile C, Lacalandra F (2009) Tighter approximated MILP formulations for unit commitment problems. *IEEE Transactions on Power Systems* 24(1):105–113.

Garver LL (1962) Power generation scheduling by integer programming-development of theory. *Power Apparatus and Systems, Part III. Transactions of the American Institute of Electrical Engineers* 81(3):730–734, ISSN 0097-2460.

Gentile C, Morales-Espana G, Ramos A (2017) A tight MIP formulation of the unit commitment problem with start-up and shut-down constraints. *EURO Journal on Computational Optimization* 5(1–2):177–201.

Guan Y, Pan K, Zhou K (2018) Polynomial time algorithms and extended formulations for unit commitment problems. *IISE Transactions* 50(8):735–751.

Gurobi Optimization, Inc (2018) Gurobi optimizer reference manual. URL `http://www.gurobi.com`.

Hart WE, Laird CD, Watson JP, Woodruff DL, Hackebeil GA, Nicholson BL, Siirola JD (2017) *Pyomo–optimization modeling in Python*, volume 67 (Springer Science & Business Media), second edition.

Hart WE, Watson JP, Woodruff DL (2011) Pyomo: Modeling and solving mathematical programs in Python. *Mathematical Programming Computation* 3(3):219–260.

Hedman KW, O'Neill RP, Oren SS (2009) Analyzing valid inequalities of the generation unit commitment problem. *Power Systems Conference and Exposition, 2009. PSCE'09. IEEE/PES*, 1–6 (IEEE).

Hua B, Baldick R (2017) A convex primal formulation for convex hull pricing. *IEEE Transactions on Power Systems* 32(5):3814–3823.

International Business Machines Corporation (2018) IBM CPLEX Optimizer. URL `https://www-01.ibm.com/software/commerce/optimization/cplex-optimizer/`.

Knueven B, Ostrowski J, Wang J (2017) The ramping polytope and cut generation for the unit commitment problem. *INFORMS Journal on Computing* To appear.

Knueven B, Ostrowski J, Watson JP (2018a) Exploiting identical generators in unit commitment. *IEEE Transactions on Power Systems* 33(4).

Knueven B, Ostrowski J, Watson JP (2018b) A novel matching formulation for startup costs in unit commitment. URL `http://www.optimization-online.org/DB_FILE/2017/03/5897.pdf`.

Knueven B, Ostrowski J, Watson JP (2018c) Online supplement for *On Mixed Integer Programming Formulations for the Unit Commitment Problem* .

Krall E, Higgins M, O'Neill RP (2012) RTO unit commitment test system. *Federal Energy Regulatory Commission* URL `https://ferc.gov/legal/staff-reports/rto-COMMITMENT-TEST.pdf`.

Lee J, Leung J, Margot F (2004) Min-up/min-down polytopes. *Discrete Optimization* 1(1):77–85, ISSN 1572-5286.

Malkin P (2003) Minimum runtime and stoptime polyhedra. *CORE, Université catholique de Louvain* Working Paper.

Morales-España G, Latorre JM, Ramos A (2013a) Tight and compact MILP formulation for the thermal unit commitment problem. *IEEE Transactions on Power Systems* 28(4):4897–4908.

Morales-España G, Latorre JM, Ramos A (2013b) Tight and compact MILP formulation of start-up and shut-down ramping in unit commitment. *IEEE Transactions on Power Systems* 28(2):1288–1296.

Muckstadt JA, Wilson RC (1968) An application of mixed-integer programming duality to scheduling thermal generating systems. *IEEE Transactions on Power Apparatus and Systems* (12).

Nowak MP, Römisch W (2000) Stochastic lagrangian relaxation applied to power scheduling in a hydro-thermal system under uncertainty. *Annals of Operations Research* 100(1-4):251–272.

O'Neill RP (2017) Computational issues in ISO market models. Workshop on Energy Systems and Optimization.

Ostrowski J, Anjos MF, Vannelli A (2012) Tight mixed integer linear programming formulations for the unit commitment problem. *IEEE Transactions on Power Systems* 27(1):39.

Ostrowski J, Anjos MF, Vannelli A (2015) Modified orbital branching for structured symmetry with an application to unit commitment. *Mathematical Programming* 150(1):99–129.

Pan K, Guan Y (2016) A polyhedral study of the integrated minimum-up/-down time and ramping polytope. *arXiv preprint arXiv:1604.02184* URL `https://arxiv.org/pdf/1604.02184`.

Pan K, Guan Y (2017) Convex hulls for the unit commitment polytope. *arXiv preprint arXiv:1701.08943* URL `https://arxiv.org/pdf/1701.08943`.

Queyranne M, Wolsey LA (2017) Tight MIP formulations for bounded up/down times and interval-dependent start-ups. *Mathematical Programming* 164(1-2):129–155.

Rajan D, Takriti S (2005) Minimum up/down polytopes of the unit commitment problem with start-up costs. *IBM Research Report* RC23628 (W0506-050).

Rothberg E (2018) Personal correspondence, Chief Executive Officer and Co-founder, Gurobi Optimization.

Silbernagl M (2016) *A polyhedral analysis of start-up process models in unit commitment problems*. Ph.D. thesis, Technische Universität München.

Simoglou CK, Biskas PN, Bakirtzis AG (2010) Optimal self-scheduling of a thermal producer in short-term electricity markets by MILP. *IEEE Transactions on Power Systems* 25(4):1965–1977.

Sridhar S, Linderoth J, Luedtke J (2013) Locally ideal formulations for piecewise linear functions with indicator variables. *Operations Research Letters* 41(6):627–632.

Takriti S, Krasenbrink B, Wu LSY (2000) Incorporating fuel constraints and electricity spot prices into the stochastic unit commitment problem. *Operations Research* 48(2):268–280.

Van den Bergh K, Delarue E, Dhaeseleer W (2014) DC power flow in unit commitment models. *TMF Working Paper-Energy and Environment* EN2014-12, URL `https://www.mech.kuleuven.be/en/tme/research/energy_environment/Pdf/wpen2014-12.pdf`.

Wu L (2016) Accelerating NCUC via binary variable-based locally ideal formulation and dynamic global cuts. *IEEE Transactions on Power Systems* 31(5):4097–4107.

Yang L, Zhang C, Jian J, Meng K, Xu Y, Dong Z (2017) A novel projected two-binary-variable formulation for unit commitment in power systems. *Applied Energy* 187:732–745.

Online Supplement for

On Mixed Integer Programming Formulations for the Unit Commitment Problem

Bernard Knueven[1], James Ostrowski[2], and Jean-Paul Watson[3]

[1]Discrete Math & Optimization, Sandia National Laboratories, Albuquerque, NM 87185, bknueve@sandia.gov

[2]Industrial and Systems Engineering, University of Tennessee, Knoxville, TN 37996, jostrows@utk.edu

[3]Data Science & Cyber Analytics, Sandia National Laboratories, Livermore, CA 94551, jwatson@sandia.gov

November 16, 2018

A Ideal Formulation for Generator with Piecewise Production Costs and Start-up/Shutdown Ramping Limits

Theorem 1. *The system* (2), (4), (5), (43), (44), (46) *with variable bounds is an ideal formulation for a generator with minimum up/down times, piecewise production costs, and start-up/shutdown ramping limits if* $UT \geq 2$. *If* $UT = 1$, *then the system* (2), (4), (5), (43), (44), (48) *with variable bounds is an ideal formulation for a generator with piecewise production costs and start-up/shutdown ramping limits.*

Proof. When $UT = 2$, a straightforward extension of [12, Theorem 5] with the $p^l(t)$ variables playing the same role as the p_t variables in the proof of [12, Theorem 5] shows this is true for the system (2), (4), (5), (46) with variable bounds. An application of [12, Lemma 4] shows the addition of the equality constraints (43) and (44) do not affect integrality. Notice that generation limits on $p'(t)$ are redundant because of (43) with (46). Finally, the above is also true when $UT = 1$ with inequalities (48) in place of (46). □

Remark 1. *When the start-up cost formulation* (57),(58),(59) *from [19] is added to the formulation from Theorem 1 and start-up costs are non-decreasing, the resulting polytope has integer optimal vertices.*

Remark 1 is a direct result of Theorem 1 and Knueven et al. [17, Remark 1]. It implies that a 1-UC for a generator with minimum up/down times, piecewise production costs, start-up/shutdown ramping limits, and non-decreasing time-dependent start-up costs can be solved as a linear program.

B Other Formulations

This section details formulations choices in addition to those in the main text.

B.1 Additional formulations for minimum up-time/down-time

Given Garver's state variables, one possibility for writing the up-time/down-time is given by Dillon et al. [8] and more recently by Arroyo and Conejo [1]:

$$\sum_{i=t}^{t+UT-1} u(i) \geq UTv(t) \qquad t \in \{U+1, \ldots, T-UT+1\} \tag{70a}$$

$$\sum_{i=t}^{T} (u(i) - v(t)) \geq 0 \qquad t \in \{T-UT+2, \ldots, T\} \tag{70b}$$

$$\sum_{i=t}^{t+DT-1} (1-u(i)) \geq DTw(t) \qquad t \in \{D+1, \ldots, T-DT+1\} \tag{71a}$$

$$\sum_{i=t}^{T} (1-u(i)-w(t)) \geq 0 \qquad t \in \{T-DT+2, \ldots, T\}. \tag{71b}$$

Another common formulation is to just consider one binary variable to represent the state of generator g at time t, $u(t)$. Based on the logical constraint (2), the v and w variables are completely determined by the u variables, and so in some sense are redundant. However, results both theoretical and computational suggest this is not entirely true.

Takriti et al. [32] formulate the minimum up-time/down-time constraints as

$$u(t) - u(t-1) \leq u(\tau) \qquad \forall \tau \in \{t+1, \ldots, \min\{t+UT-1, T\}\}, t \in \mathcal{T} \tag{72}$$

$$u(t-1) - u(t) \leq 1 - u(\tau) \qquad \forall \tau \in \{t+1, \ldots, \min\{t+DT-1, T\}\}, t \in \mathcal{T}. \tag{73}$$

These constraints are simple, but could be up to quadratic in T if the minimum up-time or down-times are very long.

Carrion and Arroyo [5] formulate these same constraints as

$$\sum_{i=t}^{t+UT-1} u(i) \geq UT(u(t) - u(t-1)) \qquad t \in \{U+1, \ldots, T-UT+1\} \tag{74a}$$

$$\sum_{i=t}^{T} (u(i) - (u(t) - u(t-1))) \geq 0 \qquad t \in \{T-UT+2, \ldots, T\} \tag{74b}$$

$$\sum_{i=t}^{t+DT-1} (1 - u(i)) \geq DT(u(t-1) - u(t)) \qquad t \in \{D+1, \ldots, T-DT+1\} \tag{75a}$$

$$\sum_{i=t}^{T} (1 - u(i) - (u(t-1) - u(t))) \geq 0 \qquad t \in \{T-DT+2, \ldots, T\}, \tag{75b}$$

which are in the same form as (70) and (71), but with the v and w variables projected out.

However, unlike with the three- and two-binary formulations for minimum up-time/down-time, there is no compact convex hull description for these constraints in the u variables alone. The convex hull of the minimum up-time/down-time constraints has an exponential number of facets in the space of the u variables [21]. Hence the two- or three-binary formulations are often preferred as the minimum up-time/down-time constraints have a compact (linear) convex hull description which can be directly incorporated into UC MIP formulations.

B.2 Additional Generation and Ramping Limits from Carrion and Arroyo [5]

To enforce the shutdown ramp limits, Carrion and Arroyo [5] define the constraint

$$\overline{p}_g(t) \leq \overline{P}_g u_g(t+1) + SD_g(u_g(t) - u_g(t+1)) \qquad t \in \mathcal{T} \setminus \{T\}, \tag{76}$$

which is the same as constraint (19) with the shutdown variable w removed. Similarly, Carrion and Arroyo [5] formulate the ramping limits as

$$\overline{p}(t) - p(t-1) \leq RU u(t-1) + SU\big(u(t) - u(t-1)\big) + \overline{P}\big(1 - u(t)\big) \tag{77}$$

$$p(t-1) - p(t) \leq RD u(t) + SD\big(u(t-1) - u(t)\big) + \overline{P}\big(1 - u(t-1)\big), \tag{78}$$

which eliminate the variables v and w from (24) and (25), respectively.

B.3 Additional Ramping Inequalities from Damcı-Kurt et al. [7]

Like Ostrowski et al. [24], Damcı-Kurt et al. [7] also give polynomial classes of ramp-up and ramp-down inequalities which hold under certain conditions. In some ways these are complementary to those given

by Ostrowski et al. [24], as they hold under somewhat complementary conditions, when $RD = RU$ and $SU = SD$. Both ramping inequalities are extensions of (33) and (34). When $SU \geq \underline{P} + RU$ ($RU \leq SU - \underline{P}$) we have

$$p(t+j) - p(t) \leq (\underline{P} + jRU)u(t+j) + \sum_{i=1}^{j} \min\{(SU - \underline{P} - iRU), (\overline{P} - \underline{P} - jRU)\}v(t+i) - \underline{P}u(t), \tag{79a}$$

which holds for $\forall j \in \left\{1, \ldots, \min\left\{T - t, \frac{SU-\underline{P}}{RU}\right\}\right\}, t \in \mathcal{T}$. Note this is in contrast to inequalities (28) and (29), which in addition to requirements on UT and DT also require $RU > SD - \underline{P}$. Damcı-Kurt et al. [7] also show (79a) is a facet of the ramp-up polytope if and only if $\underline{P} + jRU < \overline{P}$. There is an analogous class of ramp-down inequalities, which are valid when $SD \geq \underline{P} + RD$ ($RD \leq SD - \underline{P}$)

$$p(t) - p(t+j) \leq (\underline{P} + jRD)u(t) - \underline{P}u(t+j) + \sum_{i=1}^{j} \min\{(SD - \underline{P} - (j-i+1)RD), (\overline{P} - \underline{P} - jRD)\}w(t+i), \tag{79b}$$

$\forall j \in \left\{1, \ldots, \min\left\{T - t, \frac{SD-\underline{P}}{RD}\right\}\right\}, t \in \mathcal{T}$. Like its ramp-up counterpart (79a), (79b) is a facet of the ramp-down polytope if and only if $\underline{P} + jRD < \overline{P}$. For both inequalities (79a) and (79b), it is not often the case that $\left\lfloor \frac{SU-\underline{P}}{RU} \right\rfloor \geq 2$ or $\left\lfloor \frac{SD-\underline{P}}{RD} \right\rfloor \geq 2$, and when these quantities are 1 these two inequalities are just (33) and (34) respectively. Hence the inequalities (79a) and (79b) may not be very useful in practice.

B.4 The Generator Polytope

Knueven et al. [16] presented the first perfect formulations for a generator with ramping constraints as well as time-dependent start-up costs, work that was independently discovered by Frangioni and Gentile [10, 11] and Guan et al. [13]. While the formulations are very similar, all having on the order of $|\mathcal{T}|^3$ and constraints, they differ in how they "link" the underlying economic dispatch polytopes. Knueven et al. [16] shows that only $\mathcal{O}(|\mathcal{T}|)$ many linking constraints are needed to describe the instances with no time-dependent start-up costs, and Guan et al. [13] gives the same result for instances with time-dependent start-up costs. We present here a formulation from Knueven et al. [16] which directly incorporates reserve capability. Note that any of these formulations can be extended to include most ancillary service products while still maintaining integrality, so long as the dispatch is a polytope when the on/off schedule is fixed. That is, there is a perfect formulation for Π_g, in the sense that the vertices of said formulation are integer in the binary variables. First, we need define an additional set and variable. Let $[t, t') \in \mathcal{Y}_g$ be the feasible intervals of operation for generator g with respect to its minimum uptime, that is, $[t, t') \in \mathcal{T} \times \mathcal{T}$ such that $t' \geq t + UT_g$, including

times (as necessary) before and after the planning period $\mathcal{T}$, and $y_g(t,t')$ be the binary indicator arc for start-up at time t, shutdown at time t', committed for $i \in [t,t')$, $[t,t') \in \mathcal{Y}_g$, for generator $g \in \mathcal{G}$. Then put broadly, said formulation is

$$A^{[i,j]}p^{[i,j]} + \overline{A}^{[i,j]}\overline{p}^{[i,j]} \leq b^{[i,j]}y(i,j) \qquad \forall [i,j) \in \mathcal{Y} \tag{80a}$$

$$\sum_{[i,j)\in\mathcal{Y}} p^{[t,t')}(t) = p(t) \qquad \forall t \in \mathcal{T} \tag{80b}$$

$$\sum_{[i,j)\in\mathcal{Y}} \overline{p}^{[t,t')}(t) = \overline{p}(t) \qquad \forall t \in \mathcal{T} \tag{80c}$$

$$\sum_{\{[k,l)\in\mathcal{X}|l=t\}} x(k,l) = \sum_{\{[i,j)\in\mathcal{Y}|i=t\}} y(i,j) \qquad \forall t \in \mathcal{T} \tag{80d}$$

$$\sum_{\{[i,j)\in\mathcal{Y}|j=t\}} y(i,j) = \sum_{\{[k,l)\in\mathcal{X}|k=t\}} x(k,l) \qquad \forall t \in \mathcal{T}, \tag{80e}$$

where the $p^{[i,j]}(t)$ ($\overline{p}^{[i,j]}(t)$) represent the power (power available) at time t given the generator started-up at time i and shutdown at time j, and the polytope $\{p^{[i,j]}, \overline{p}^{[i,j]} \mid A^{[i,j]}p^{[i,j]} + \overline{A}^{[i,j]}\overline{p}^{[i,j]} \leq b^{[i,j]}\}$ represents the physical (minimum power, ramp up/down limits, maximum power) when the generator is turned on at time i and turned off at time j. So long as the power and ancillary services provided can be represented as a (bounded) polytope when the commitment status is fixed, (80) is a perfect formulation for said generator [16]. Constraints (80b) and (80c) serve to calculate the total power produced (or available) for the generator. Constraints (80d) and (80e) ensure that an off-arc is followed by an on-arc and visa versa. Notice that time-dependent start-up costs and fixed running costs can be accounted for by placing the appropriate coefficients on the $x(i,j)$ and $y(i,j)$ variables respectively. Piecewise production costs can be handled by considering $f^{[i,j]}(p^{[i,j]})$, where $f^{[i,j]}$ is a piecewise convex function. (Note such production costs should be incorporated into constraints (80a).)

While this extended formulation could be directly considered in a full-scale UC problem, its size, which is $\mathcal{O}(T^3)$, poses computational challenges. Namely, the extra copies of the continuous variables are not well-handled by linear programming solvers, in addition to increasing the size of the formulation. Knueven et al. [16] use it as a basis for a cut-generation routine for this reason.

However, there may be some cases where incorporating (80) directly in the UC formulation is worth while. As shown in Knueven et al. [18], if there are several copies of the same generator at the same location, sometimes (80) is advantageous and can be directly incorporated into the formulation, so long as the multiple generators are aggregated. Knueven et al. [18] demonstrates this aggregation can be done while maintaining optimality and feasibility. Such a formulation may be useful especially in capacity expansion problems, where one may have the option of building many generators of the same type. Further, since the dispatch decisions are often relaxed as part of a two-stage framework, having a convex hull representation provides the best

approximation for dispatch. For the same reason, (80) may also be useful as part of the pricing problem, as it ensures convex hull prices are obtained [14]. Though in this context it may still be best to solve the pricing linear program using some sort of decomposition technique. Finally, we note that a version of (80) can be used in a two-stage stochastic setting by replicating (80a)–(80c) for each scenario, giving the convex hull for generator scheduling under uncertainty.

Guan et al. [13] introduce three extended formulations for ramping. The first which is similar to (80) except it replaces the shortest path polytope (80d)–(80e) with an integer polytope directly taken from the dual of a modified version of the dynamic program for 1-UC suggested by Frangioni and Gentile [9]. They demonstrate this extended formulation has the property of having integer extreme points when production costs are convex. Additionally, Guan et al. [13] gives two other related extended formulations, one for a traditional deterministic setting an the other for a stochastic setting. We discuss the deterministic formulation below; the stochastic formulation is similar.

As in Guan et al. [13], consider the case when $S = SU = SD$ and $R = RU = RD$, and there are no reserves, so we can assume $r_t = 0$ or $p_t = \overline{p}_t$, for all $t \in \mathcal{T}$. Further define $\alpha_1 = \max\{t \in \mathcal{T} \mid \underline{P} + tR \leq \overline{P}\}$ and $\alpha_2 = \max\{t \in \mathcal{T} \mid S + tR \leq \overline{P}\}$ and let

$$\mathcal{Q} = \{0, (\underline{P} + tR)_{t=0}^{\alpha_1}, (S + tR)_{t=0}^{\alpha_2}, (\overline{P} - tR)_{t=0}^{\alpha_1}\}. \tag{81}$$

In this case, $\mathcal{Q}$ are the p-components of the vertices of the generator polytope [13]. Of course, if we add the additional reserve variables or drop the assumptions on the ramp-rates, we may have more vertices, and so need to enlarge the set $\mathcal{Q}$. Guan et al. [13] make such an extension to piecewise production costs. Given this, one can define a state-space for a given time t which is dependent on UT, DT, and $|\mathcal{Q}|$ as follows. $\mathscr{S}_0(t)$ are all the states when the generator is off-line at time t, which is defined by the 4-tuple ($p(t)$, $u(t)$, $v(t)$, $d(t)$), where $p(t) = u(t) = v(t) = 0$ as the generator is not operating, and $d(t)$ is how many time periods the generator has been off at time t, up to DT. $\mathscr{S}_1(t)$ are all the states when the generator is on-line at time t, again defined by a 4-tuple ($p(t)$, $u(t)$, $v(t)$, $d(t)$), when $p(t) \in \mathcal{Q}$, and $d(t)$ is how many time periods the generator has been on-line up to UT. Let $\mathscr{S}(t) = \mathscr{S}_0(t) \cup \mathscr{S}_1(t)$. Then we can put in the feasible transition arcs between $\mathscr{S}(t)$ and $\mathscr{S}(t+1)$ which respect the ramping, start-up/shutdown limits, and minimum up-time/down-time constraints, and similarly between $\mathscr{S}(t)$ and $\mathscr{S}(t-1)$. Guan et al. [13] show that this flow formulation is integer in the variables for the state-transition arcs, and hence integer in the p, u, and v variables as well (see [13] for the full description). Additionally, the number of nodes in a state $\mathscr{S}(t)$ is $\mathcal{O}(DT + 3 \cdot UT\lceil(\overline{P} - \underline{P})/R\rceil)$, so this formulation may be useful for generators whose UT, DT, and/or $\lceil(\overline{P} - \underline{P})/R\rceil$ are small. Notice that the formulation (80) has the property that the set $\mathcal{Y}$ (and hence the number of variables and constraints) grows larger at UT gets smaller, so in some sense these two extended formulations are complementary. However, this formulation from [13] is not as extensible as that

of (80), in that a full vertex description in the continuous variables p (and $\overline{p}$, if included) is needed to specify the formulation. This may be especially problematic when the assumption $R = RU = RD$ does not hold.

B.5 Additional Variable Upper Bounds

Ostrowski et al. [24] stated inequality (37) as

$$p(t) \leq \overline{P}u(t + K(t)) + \sum_{i=1}^{K(t)} (SD + (i-1)RD)\, w(t+i) - \sum_{i=1}^{K(t)} \overline{P}v(t+i), \tag{82}$$

where $K(t) := \max\{\tau \in \{1, \ldots, UT\} \mid SD + (\tau - 1)RD < \overline{P} \text{ and } \tau + t < T\}$. Note that the $K(t) = K^{SD}(t) + 1$ for given t, where like for (37), $K^{SD}(t) = \min\{T^{RD}, UT - 1, T - t - 1\}$. To see that this is equivalent to (37), we will show that (2) can be applied to (82) to obtain (37). Note that by (2), $v(t+i) = u(t+i) - u(t+i-1) + w(t+i)$. Applying this to the final sum in (82), we have

$$p(t) \leq \overline{P}u(t + K(t)) + \sum_{i=1}^{K(t)} \left(SD + (i-1)RD - \overline{P}\right) w(t+i) - \sum_{i=1}^{K(t)} \overline{P}(u(t+i) - u(t+i-1)). \tag{83}$$

Canceling the inside terms of the last sum leaves in its place $\overline{P}(u(t + K(t)) - u(t))$, which when canceled with the first term yields

$$p(t) \leq \overline{P}u(t) + \sum_{i=1}^{K(t)} \left(SD + (i-1)RD - \overline{P}\right) w(t+i), \tag{84}$$

which gives exactly (37) after pulling a negative out of and reindexing the sum as $K(t) = K^{SD}(t) + 1$.

Damcı-Kurt et al. [7] give two exponential classes of variable upper bound inequalities with polynomial time separation algorithms. However, such classes of inequalities require a separation procedure, which is usually implemented as a callback to the solver. Pan and Guan [25] also present a linear and two exponential classes of variable bound inequalities for the generator polytope with minimum up/down times and ramp-up/ramp-down constraints. Again we will not consider the exponential classes here, but the linear class is a form of the inequalities alluded to above. First, we note that [25] assumes no difference between ramp-up and ramp-down, so let $R = RU = RD$ and $S = SU = SD$. Then we have

$$p(t) \leq Su(t) + (\overline{P} - S)(u(t+1) - v(t+1)) - \sum_{i=1}^{k-1} (\overline{P} - S - (i-1)R)v(t-i+1), \tag{85}$$

which is valid for $k \in \{1, \ldots, \min\{UT, T^R + 2\}\}$ and $t \in \{k, \ldots, T-1\}$, where $T^R = \left\lfloor \frac{\overline{P}-S}{R} \right\rfloor$. Pan and Guan [25] prove this is facet of the generator polytope when $k = \min\{UT, T^R + 2\}$ and (1) $UT \leq 3$ or (2)

$UT \geq 4$ and $t = T - 1$. Using the transformation given by (2) we can relate (85) to the those above. As $u(t+1) - v(t+1) = u(t) - w(t+1)$, we can re-arrange (85) as (re-indexing the sum as well):

$$p(t) \leq \overline{P}u(t) + (\overline{P} - S)w(t+1) - \sum_{i=0}^{\min\{UT-2, T^R\}} (\overline{P} - S - iR)v(t-i). \tag{86}$$

Further, now it is clear which S plays the role of SU and SD, and similarly for R, so we arrive at the following valid inequality

$$\overline{p}(t) \leq \overline{P}u(t) + (\overline{P} - SD)w(t+1) - \sum_{i=0}^{\min\{UT-2, T^{RU}\}} (\overline{P} - SU - iRU)v(t-i), \tag{87}$$

which is just (38).

Finally we outline the extension of (39) to when $UT = T^{RU} + T^{RD} + 1$. In this case, we can derive a couple of inequalities in the spirit of (23)

$$\begin{aligned} p'(t) \leq (\overline{P} - \underline{P})u(t) - \sum_{i=0}^{T^{RU}-1} (\overline{P} - (SU + iRU))v(t-i) - \sum_{i=0}^{T^{RD}} (\overline{P} - (SD + iRD))w(t+1+i) \\ - \left[(SD + T^{RD}RD) - (SU + T^{RU}RU)\right]^+ v(t - T^{RU}) \end{aligned} \tag{88a}$$

$$\begin{aligned} p'(t) \leq (\overline{P} - \underline{P})u(t) - \sum_{i=0}^{T^{RU}} (\overline{P} - (SU + iRU))v(t-i) - \sum_{i=0}^{T^{RD}-1} (\overline{P} - (SD + iRD))w(t+1+i) \\ - \left[(SU + T^{RU}RU) - (SD + T^{RD}RD)\right]^+ w(t + T^{RD} + 1). \end{aligned} \tag{88b}$$

When $UT \leq T^{RD} + T^{RD}$, the number of potential valid and strong inequalities for upper-bound continues to double.

B.6 Additional Piecewise Production Cost Formulations

Another possibility for modeling convex piecewise linear production costs is a relaxed SOS2 model. Let $\lambda^l \in [0,1]^T$, for $l \in \mathcal{L}$, represent the fraction of generation coming from piecewise segment l, and $\lambda^0 \in [0,1]^T$ represent the faction of generation coming from the unit operating at $\underline{P}$. Then another formulation for

convex piecewise linear production is

$$\sum_{l \in \mathcal{L} \cup \{0\}} (\overline{P}^l - \underline{P}) \lambda^l(t) = p'(t) \tag{89}$$

$$\sum_{l \in \mathcal{L} \cup \{0\}} (\overline{C}^l - \overline{C}^0) \lambda^l(t) = c^p(t) \tag{90}$$

$$\sum_{l \in \mathcal{L} \cup \{0\}} \lambda^l(t) = 1. \tag{91}$$

(The cost of operating the generator at minimum power is factored in to c^R.) Sridhar et al. [31] showed that if (91) is replaced with

$$\sum_{l \in \mathcal{L} \cup \{0\}} \lambda^l(t) = u(t), \tag{92}$$

then the resulting formulation is locally ideal, in the same sense as (42)–(44).

The formulation proposed by Chen and Wang [6] is also locally ideal, and comes from noticing that the coefficient on $\lambda^0(t)$ is 0 in both (89) and (90). Hence $\lambda^0(t)$ can be dropped from both equations without issue, and we can then project out $\lambda^0(t)$, leaving

$$\sum_{l \in \mathcal{L}} (\overline{P}^l - \underline{P}) \lambda^l(t) = p'(t) \tag{93}$$

$$\sum_{l \in \mathcal{L}} (\overline{C}^l - \overline{C}^0) \lambda^l(t) = c^p(t) \tag{94}$$

$$\sum_{l \in \mathcal{L}} \lambda^l(t) \leq u(t). \tag{95}$$

Chen and Wang [6] observed that projecting out $\lambda^0(t)$ had a dramatic effect on the root relaxation time for MISO's day-ahead UC.

B.7 Additional Start-up Cost Formulations

One class of start-up cost formulations use points on the epigraph of $c^{SU}(t)$ to calculate start-up costs, without needing additional variables. An example of such a formulation, introduced by Knueven et al. [19], uses the start-up and shutdown indicator variables v and w

$$c^{SU}(t) \geq C^s v(t) - \sum_{k=1}^{s-1} \left((C^s - C^k) \sum_{i=\underline{T}^k}^{\underline{T}^{k+1}-1} w(t-i) \right) \qquad s \in \mathcal{S} \tag{96}$$

$$c^{SU}(t) \geq 0. \tag{97}$$

It was shown in Silbernagl [29] that the formulation (52)–(54) has the same linear programming relaxation value as the formulation given by (96),(97).

One simple start-up cost formulation, introduced Nowak and Römisch [23] and used in [5], just relies on the auxiliary variable $c^{SU}(t)$ for each time period t and the status variable u:

$$c^{SU}(t) \geq C^s \left(u(t) - \sum_{i=1}^{\underline{T}^s} u(t-i) \right) \qquad \forall s \in \mathcal{S} \tag{98}$$

$$c^{SU}(t) \geq 0 \qquad \forall t \in \mathcal{T}. \tag{99}$$

Silbernagl et al. [30] showed constraint (98) could be strengthened by increasing the coefficients in the sum:

$$c^{SU}(t) \geq C^s \left(u(t) - \sum_{i=1}^{DT} u(t-i) \right) - \sum_{k=1}^{s-1} \left((C^s - C^k) \sum_{i=\underline{T}^k+1}^{\underline{T}^{k+1}} u(t-i) \right) \qquad \forall s \in \mathcal{S}. \tag{100}$$

Brandenberg et al. [4] shows the convex hull for non-decreasing start-up costs has an exponential number of facets in the u, c^{SU} space, but provides a linear-time separation algorithm. It is not difficult to show the inequalities (96) dominate (100) which dominate (98) [19].

Yang et al. [34] and Atakan et al. [2] both propose a different auxiliary variable, $\overline{c}^{SU}(t)$, which represents the start-up cost over a hot-start. Yang et al. [34] then writes the start-up costs as:

$$\overline{c}^{SU}(t) \geq (C^s - C^1) \left(v(t) - \sum_{i=1}^{\underline{T}^s} u(t-i) \right) \qquad \forall s \in \mathcal{S} \setminus \{1\} \tag{101}$$

$$\overline{c}^{SU}(t) \geq 0 \tag{102}$$

$$c^{SU}(t) = c^1 v(t) + \overline{c}^{SU}(t), \tag{103}$$

where (103) is substituted into the objective function. Note that Yang et al. [34] only considers two start-up types, though the above formulation is its natural extension to arbitrary start-up types. Substituting (103) into (101) and (102) we see that this formulation is dominated by (96),(97). Atakan et al. [2] proposes a similar formulation, and explicitly models arbitrary start-up types, replacing (101) with

$$\overline{c}^{SU}(t) \geq (C^s - C^1) \left(v(t) - \sum_{i=DT}^{\underline{T}^s} v(t-i) - \tilde{u}(t - \underline{T}^s) \right) \qquad \forall s \in \mathcal{S} \setminus \{1\}. \tag{104}$$

This same constraint can be written with $u(t)$ as:

$$\overline{c}^{SU}(t) \geq (C^s - C^1)\left(v(t) - \sum_{i=DT}^{\underline{T}^s-1} v(t-i) - u(t-\underline{T}^s)\right) \qquad \forall s \in \mathcal{S} \setminus \{1\}. \tag{105}$$

Hence we see that (105) dominates (101) and requires no more non-zeros. Notice that we can also replace (101) with a modified version of (96):

$$\overline{c}^{SU}(t) \geq (C^s - C^1)v(t) - \sum_{k=1}^{s-1}\left((C^s - C^k)\sum_{i=\underline{T}^k}^{\underline{T}^{k+1}-1} w(t-i)\right) \qquad \forall s \in \mathcal{S} \setminus \{1\} \tag{106}$$

and using (2) we can "push" $u(t-\underline{T}^s)$ through the sum in (105) to arrive at

$$\overline{c}^{SU}(t) \geq (C^s - C^1)\left(v(t) - u(t-DT) + \sum_{i=DT}^{\underline{T}^s-1} w(t-i)\right) \qquad \forall s \in \mathcal{S} \setminus \{1\}. \tag{107}$$

It is clear that (106) dominates (107), while requiring fewer non-zeros.

B.8 Additional Shutdown Cost Formulations

If the v variables are in the formulation but not the w variables, then the shutdown cost can be modeled using the implied shutdown status variable:

$$c^{SD}(t) = C^w(v(t) - u(t) - u(t-1)). \tag{108}$$

In either case $c^{SD}(t)$ can be substituted out of the objective function. Lastly, if neither the w nor v variables are in the model, then $c^{SD}(t)$ must remain a variable in the model, and we add the constraints

$$c^{SD}(t) \geq C^w(u(t-1) - u(t)) \tag{109}$$

$$c^{SD}(t) \geq 0. \tag{110}$$

C Other Formulations from the Literature

The first paper to consider a mostly complete UC formulation is Carrion and Arroyo [5]. The formulation given by that paper is shown in Table 1 and will be referred to as **CA**. Note that given the variables involved in this formulation, we may apply some of the transformations discussed above to arrive at the formulation given. For example, the formulation in Table 1 includes constraint (43), which has the term $p'_g(t)$. In this case, the transformation given by (12) is applied to arrive at a constraint valid for this model (and which

Table 1: Specification of the formulation proposed in Carrion and Arroyo [5] (**CA**)

Carrion-Arroyo (CA)	
objective:	(67)
variables:	$u_g, p_g, \overline{p}_g, p^l_g, c^{SU}_g, c^{SD}_g, p_{W,n}, f_k, \theta_n, s^+_n, s^-_n, s_n, s_R$
uptime/downtime:	(3), (74), (75)
generation limits:	(18), (76)
ramping limits:	(77), (78)
piecewise production:	(43), (44), (45)
start-up cost:	(97), (98)
shutdown cost:	(109), (110)
system constraints:	(62), (63), (64), (65)

Table 2: Specification of the "original" formulation from Ostrowski et al. [24] (**OAV-O**)

Ostrowski et al. "original" (OAV-O)	
objective:	(67)
variables:	$u_g, v_g, w_g, p_g, \overline{p}_g, c^p_g, c^{SU}_g, p_{W,n}, f_k, \theta_n, s^+_n, s^-_n, s_n, s_R$
uptime/downtime:	(2), (3), (70), (71)
generation limits:	(18), (19)
ramping limits:	(24), (25)
piecewise production:	(51)
start-up cost:	(97), (98)
shutdown cost:	(60)
system constraints:	(62), (63), (64), (65)

is the same as that in Carrion and Arroyo [5]). Note the only difference between the formulation given by Table 1 and that labeled "MILP-UC" in Carrion and Arroyo [5] is the addition of the network constraints and the slacks on nodal balance and reserves.

Carrion and Arroyo [5] also test a 3-binary formulation, however the formulation considered is not precisely specified. A possible variant of this formulation is considered in Ostrowski et al. [24], and is called the "original" formulation therein. Most of the generator description except for start-up costs, shutdown costs, and production costs are based on the formulation from Arroyo and Conejo [1]. As piecewise production costs are not specified in [24], we use the perspective formulation referenced therein, which is (51). Similarly [24] does not consider a network. The formulation considered is given in Table 2 and will be referred to as **OAV-O**. Another 3-binary formulation replaces (70) and (71) in Ostrowski et al. "original" with (72) and (73), respectively. This is called "Up/Downtime" in Ostrowski et al. [24], and we refer to it as **OAV-UD**. It is given in Table 3. Note that in all the formulations derived from [24], we add the perspective piecewise production (51), the systems constraints, as well as the upper-bound constraint (19), the last (which limits the reserves when the generator is turning-off) being necessary for this formulation to agree with [5].

Table 3: Specification of the "Up/Downtime" formulation from Ostrowski et al. [24] (**OAV-UD**)

Ostrowski et al. "Up/Downtime" (OAV-UD)	
objective:	(67)
variables:	$u_g, v_g, w_g, p_g, \overline{p}_g, c_g^p, c_g^{SU}, p_{W,n}, f_k, \theta_n, s_n^+, s_n^-, s_n, s_R$
uptime/downtime:	(2), (3), (4), (5)
generation limits:	(18), (19)
ramping limits:	(24), (25)
piecewise production:	(51)
start-up cost:	(97), (98)
shutdown cost:	(60)
system constraints:	(62), (63), (64), (65)

Table 4: Specification of a formulation from Ostrowski et al. [24] (**OAV**)

Ostrowski et al. (OAV)	
objective:	(67)
variables:	$u_g, v_g, w_g, p_g, \overline{p}_g, c_g^p, c_g^{SU}, p_{W,n}, f_k, \theta_n, s_n^+, s_n^-, s_n, s_R$
uptime/downtime:	(2), (3), (4), (5)
generation limits:	(18), (19)
ramp-up limits:	(24) if $RU_g \leq SD_g - \underline{P}_g$ or $UT_g < 2$, else (28)
ramp-down limits:	(25) if $RD_g \leq SU_g - \underline{P}_g$ or $UT_g < 2$, else (30) if $UT_g < 3$ or $DT_g < 2$, else (31)
piecewise production:	(51)
start-up cost:	(97), (98)
shutdown cost:	(60)
system constraints:	(62), (63), (64), (65)

Table 5: Specification of a tighter formulation from Ostrowski et al. [24] (**OAV-T**)

Ostrowski et al. tighter (OAV-T)	
objective:	(67)
variables:	$u_g, v_g, w_g, p_g, \overline{p}_g, c_g^p, c_g^{SU}, p_{W,n}, f_k, \theta_n, s_n^+, s_n^-, s_n, s_R$
uptime/downtime:	(2), (3), (4), (5)
generation limits:	(18), (19), (37)
ramp-up limits:	(24) if $RU_g \leq SD_g - \underline{P}_g$ or $UT_g < 2$, else (28)
ramp-down limits:	(25) if $RD_g \leq SU_g - \underline{P}_g$ or $UT_g < 2$, else (30) if $UT_g < 3$ or $DT_g < 2$, else (31)
2-ramp-up limits:	(29) if $RU_g > SD_g - \underline{P}_g$, $UT_g \geq 2$, and $DT_g \geq 2$
2-ramp-down limits:	(32) if $RD_g > SU_g - \underline{P}_g$, $UT_g \geq 3$, and $DT_g \geq 2$
piecewise production:	(51)
start-up cost:	(97), (98)
shutdown cost:	(60)
system constraints:	(62), (63), (64), (65)

Table 6: Specification of the formulation proposed in Atakan et al. [2] (**ALS**)

Atakan et al. (ALS)	
objective:	(67)
variables:	$\tilde{u}_g, v_g, w_g, p'_g, \overline{p}_g, c^p_g, \overline{c}^{SU}_g, p_{W,n}, f_k, \theta_n, s^+_n, s^-_n, s_n, s_R$
uptime/downtime:	(3), (9), (10), (11)
generation limits:	(16), (19)
ramp limits:	(35), (36)
piecewise production:	(49)
start-up cost:	(102), (103), (104)
shutdown cost:	(60)
system constraints:	(62), (63), (64), (65)

Because Ostrowski et al. [24] proposes adding the additional constraints (37), (28)–(32) as user cuts, a feature unique to CPLEX [15], we will consider two variants of the formulation proposed in Ostrowski et al. [24]. The first of which replaces the consecutive-period ramping constraints with their tighter counterparts (28), (30), (31), when possible, and the other also adds the upper bound constraint (37) and the two-period ramping constraints (29) and (32). The two formulations are in Tables 4 and 5 and will be referred to as **OAV** and **OAV-T**, respectively. Note we add the network constraints, the perspective piecewise production (51), and (19) to these models.

Recently Atakan et al. [2] presented a reformulation for UC using the state-transition variables discussed in Section 3.1.2. Other aspects of this formulation are the combination of the $p'_g(t)$ variables with the $\overline{p}_g(t)$ variables and the inclusion of the ramping constraints from Damcı-Kurt et al. [7]. Relying heavily on the transformations (8), (12), and (13), in Table 6 we give the formulation from Atakan et al. [2] with the addition of network constraints. We will refer to this formulation as **ALS** and it is given in Table 6.

D Detailed Summary of Instances

D.1 RTS-GMLC

The RTS-GMLC system [3] is an update to the RTS-96, and is publicly available on GitHub at `https://github.com/GridMod/RTS-GMLC`. As is, none of the generators have ramping constraints over an hourly time horizon. In order to create instances which are sensitive to various formulation changes, we considered a 3% reserve margin, let $SU_g = SD_g = \underline{P}_g$ for all $g \in \mathcal{G}$, and reduced the ramp rates by a factor of three. The later change is not overly restrictive, in that units marked as coal can ramp up/down in two to three hourly time periods, whereas the units marked as gas can ramp up/down in a single time period.

The RTS-GMLC system has 73 thermal generators, 81 renewable generators including wind, hydro, utility-scale photo-voltaic, and rooftop photo-voltaic generators. Each thermal generator has four piece-

wise production segments and between one and three start-up types. The rooftop photo-voltaic and hydro generation is modeled as must-take, but the wind and utility-scale photo-voltaic units are fully curtailable. The system also includes a network with 73 buses and 120 transmission lines. Hourly day-ahead data are provided for both load and renewable generation for the year 2020. For this test set we selected twelve days from the year, Jan 27, Feb 9, Mar 5, Apr 3, May 5, Jun 9, Jul 6, Aug 12, Sep 20, Oct 27, Nov 25, and Dec 23. Jan 27, Feb 9, Nov 25 and Dec 23 were selected because they contain significant wind-ramping events, Apr 3 and Jun 9 were selected because there is very little renewable generation online, and the remaining days were selected arbitrarily to have a test-set containing one day per month to capture seasonal variations. The initial generator status for all days is given from the provided PLEXOS solution. For each day we consider an instance with and without the network constraints, for a total of 24 instances.

D.2 CAISO

The "CAISO" instances have 410 schedulable thermal generators and another 200 must-run thermal generators. These instances are based on publicly-available market and regulatory data from the California Independent System Operator (CAISO). No network data is included. As the generator offer curve provided is quadratic, we approximate each curve using $L_g = 2$ for each $g \in \mathcal{G}$. Each generator only has two start-up categories. Five 48-hour demand scenarios are considered, one for each season based on historical data, and another, "Scenario400," representing a hypothetical scenario where wind is on average 40% of energy demand. Wind generation is treated as fully curtailable. The wind profile for this instance was collected from historical data and then scaled appropriately. Four different reserve margins were considered for each demand profile, 0%, 1%, 3%, and 5%. In total then we have 20 CAISO UC instances.

This system consists of mostly small and flexible generating units: only 20 of the 410 schedulable units have irredundant ramping constraints (that is, $RU_g > (\overline{P}_g - \underline{P}_g)$ and $RD_g > (\overline{P}_g - \underline{P}_g)$), and account for 75% of the schedulable capacity. Additionally, 370 of the schedulable units have $UT_g = DT_g = 1$, accounting for 66% of the schedulable capacity. These are the same instances considered in [19, 18].

D.3 FERC

The "FERC" instances are based on two sets of generators publicly available from the Federal Regulatory Energy Commission (FERC) in the United States [20]. Twelve 48-hour instances were constructed from publicly available load, reserve, and wind data from 2015 provided by PJM [26, 27]. One day was selected from each month so as to capture the seasonal variation, with the "Summer" generators being used for months April – September and the "Winter" generators for the remaining months. PJM was selected for the load profile because the FERC generator set is itself based on data from PJM. To create additional more interesting test instances, we scaled the provided wind profile by a factor of 15 to increase the average wind

Table 7: Summary computational results for RTS-GMLC instances.

Formulation	Time (s)	Opt gap (%)	Time outs	Times best	Times 2nd
CA	300.0	13.806%	24	0	0
OAV-O	172.8	0.3335%	13	0	0
OAV-UD	163.2	0.2541%	13	0	0
OAV	169.7	0.2352%	12	0	0
OAV-T	178.0	0.2498%	12	0	0
MLR	86.19	0.0165%	5	0	0
ALS	58.29	0.0122%	2	1	1
KOW	94.81	0.0165%	4	0	1
T	50.65	0.0121%	2	4	4
Co	43.11	0.0121%	**1**	1	4
R1	**32.37**	**0.0114%**	**1**	**14**	6
R2	36.94	0.0114%	**1**	4	**8**

energy supply to 30% of demand. In both cases, wind generation is treated as fully curtailable. Hence there are a total of 24 FERC instances, twelve "low-wind" instances which use the data as provided and twelve "high-wind" instances which scale the wind by a factor of 15. These are the same instances considered in [16, 19].

The Summer set of generators has 978 units and the Winter set has 934 units. Missing data is as in [16]. Piecewise production curves are based market data such that $1 \leq L_g \leq 10$, and each generator has at most two start-up types. Given the number of generators and the potential number of piecewise production points, this test set is very large as measured by the number of nonzeros in the constraint matrix, regardless of the formulation chosen. As compared to CAISO, this system has many fewer flexible generators; generators with irredundant ramping constraints comprise only 50% of units and 35% of capacity for both the Winter and Summer set of generators.

E Summary Computational Results, Including Other Formulations

E.1 RTS-GMLC

Summary computational results for the RTS-GMLC instances are reported in Table 7. As in the main text, the time limit was set at 300 seconds. Full results are in Tables 17 and 20. We note formulation **CA** is completely uncompetitive on these instances, and fails to find and certify quality solution (with a optimality gap less than 1%) for every instance within the time allotted. The **OAV** formulations all perform similarly, and are again uncompetitive, but at least manages to find and certify a quality solution in most instances.

Table 8: Summary computational results for CAISO instances.

Formulation	Time (s)	Opt gap (%)	Time outs	Times best	Times 2nd
CA	300.0	1.0987%	20	0	0
OAV-O	300.0	6.7647%	20	0	0
OAV-UD	300.0	6.2269%	20	0	0
OAV	300.0	3.6319%	20	0	0
OAV-T	300.0	6.1679%	20	0	0
MLR	117.1	0.0119%	2	0	1
ALS	260.4	0.0577%	12	0	0
KOW	79.02	0.0102%	2	4	**7**
T	**56.90**	**0.0100%**	**0**	**15**	3
Co	100.6	**0.0100%**	**0**	0	5
R1	147.4	0.0102%	1	0	1
R2	104.1	0.0100%	1	1	3

Formulation **ALS**, while clearly superior to **MLR** and **KOW** on this test set, is outperformed by **Co**, **R1**, and **R2**.

E.2 CAISO

Summary computational results for the CAISO instances are reported in Table 8. As in the main text, a time limit of 300 seconds was also set for these instances. Full results are in Tables 18 and 21. On these instances we see that the **CA** and **OAV** variants are uncompetitive. The CAISO generation set has mostly small, flexible generators with $UT = DT = 1$, so the poor representation of the start-up costs used for **ALS** is problematic, though it is still able to find and certify a quality solution in all cases by the time limit.

E.3 FERC

We report summary computational results for the FERC instances in Table 9. The time limit was set at 600 seconds, as in the main text. Full results are in Tables 19 and 22.

Here again we see that the **CA** and **OAV** variants are uncompetitive. Interestingly, however, we do see a difference in solution quality and verification at 600 seconds when comparing **OAV-O** to the other **OAV** variants, demonstrating the effectiveness of the uptime and downtime constraints from Rajan and Takriti [28]. The slightly weaker start-up cost formulation from Atakan et al. [2] is again the likely reason **ALS** performs slightly worse than the variants **MLR**, **Co**, **R1**, and **R2**.

Table 9: Summary computational results for FERC instances.

Formulation	Time (s)	Opt gap (%)	Time outs	Times best	Times 2nd
CA	600.0	43.333%	24	0	0
OAV-O	599.7	11.716%	23	0	0
OAV-UD	588.2	1.4575%	20	0	0
OAV	588.4	1.3104%	21	0	0
OAV-T	582.4	1.4389%	22	0	0
MLR	340.5	0.0555%	3	4	1
ALS	394.7	0.0933%	7	2	2
KOW	390.2	0.0117%	2	3	5
T	**268.6**	**0.0104%**	**1**	**8**	4
Co	309.5	0.0596%	3	4	5
R1	308.9	0.0480%	3	3	**6**
R2	373.1	0.0665%	4	0	1

Table 10: Summary of computational results, changing the power variable used.

	RTS-GMLC		CAISO		FERC	
	Time (s)	Opt gap (%)	Time (s)	Opt gap (%)	Time (s)	Opt gap (%)
T	50.65	0.0121%	56.90	0.0100%	268.6	0.0103%
CA: p_g [5]	55.59	0.0131%	63.86	0.0100%	415.6	0.0223%

F Analysis of the "Tight" Formulation

Because formulation **T** is the best performer across the test bed, we examined it further to determine which components are the most critical to its success. Approximately 30 variants of the Tight formulation were considered by swapping one component (power variables, reserve variables, uptime/downtime constraints, generation limits, ramp limits, piecewise production, start-up costs) for another considered in this paper. The motivation here is two-fold. First, this process may discover a better formulation, and second, the practitioner has a sense of what changes they should prioritize if considering a formulation change.

We first consider changing the power variable from $p'_g(t)$ to the simpler $p_g(t)$. A summary of the results are presented in Table 10, and the full results are in Tables 23–25 in Appendix G. As we can see, holding all else constant, using the variable $p_g(t)$ to represent total output leads to a degradation in overall performance.

Next we consider changing the variable used for reserve allocation. Formulation **T** uses $\overline{p}'_g(t)$, so we considered both $\overline{p}_g(t)$ from Carrion and Arroyo [5] and $r_g(t)$ from Morales-España et al. [22]. The full results are available in appendix Tables 26–28. Overall again it seems like the $\overline{p}'_g(t)$ variables are the best choice, but the results are more mixed than for the power variable selection.

For this experiment we considered two other ways of formulating the minimum uptime and downtime.

Table 11: Summary of computational results, changing the reserve variable used.

	RTS-GMLC		CAISO		FERC	
	Time (s)	Opt gap (%)	Time (s)	Opt gap (%)	Time (s)	Opt gap (%)
T	50.65	0.0121%	56.90	0.0100%	268.6	0.0103%
MLR: r_g [22]	76.91	0.0128%	80.01	0.0100%	230.4	0.0106%
CA: $\overline{p}_g$ [5]	52.41	0.0121%	50.77	0.0100%	397.2	0.0101%

Table 12: Summary of computational results, changing the uptime and downtime constraints used.

	RTS-GMLC		CAISO		FERC	
	Time (s)	Opt gap (%)	Time (s)	Opt gap (%)	Time (s)	Opt gap (%)
T	50.65	0.0121%	56.90	0.0100%	268.6	0.0103%
RT 2bin: (4)(7) [28]	48.29	0.0120%	51.30	0.0100%	235.1	0.0100%
DEKT: (70)(71) [8]	59.30	0.0124%	46.31	0.0100%	410.0	0.0163%

The first is simply the uptime/downtime polytope given by Rajan and Takriti [28] with just the unit on variable $u_g(t)$ and the start-up variable $v_g(t)$, given by (4) and (7). The other is the older formulation originally given by Dillon et al. [8] and more recently by Arroyo and Conejo [1], which was discussed in Section B.1. Summary results are reported in Table 12; full results are given in Tables 29–31. It is obvious that the DEKT formulation leads to an overall degradation in performance, whereas the 2bin variant of the uptime/downtime polytope seems to improve performance over the variant which included the turn-off variables. The "RT 2bin" formulation for the uptime/downtime constraints solved every instance of CAISO and FERC to within 0.01% of optimality within the time limit, while timing out on an additional RTS-GMLC instance over **T**. Still, its shifted geometric mean optimality gap is slightly less on RTS-GMLC while being faster on average.

In Table 13 we show the computational summary for changes to the generation limits for formulation **T**; the complete results are in Tables 32–34. As we can see, the MLR, GMR, and GMR+PG variants are all competitive with the generation limits used in **T**, which are essentially GMR+PG+(41). Conversely, the PG, AC, OAV, and CA variants result in degraded performance on at least two fo the three instance sets.

Table 14 summarizes the computational results for formulation **T** under changes to the ramping limits. Overall it is difficult to distinguish between the various formulations. However, the sparser MLR formulation from [22] has a definite advantage, whereas the denser ramping limits from the **OAV-T** formulation only serve to reduce performance. The performance of the MLR ramping inequalities is likely because the strong variable upper bound inequalities used in **T** make the ramping constraints mostly redundant. The complete results are in the appendix, Tables 35–37.

Table 13: Summary of computational results, changing the generation limits used.

	RTS-GMLC		CAISO		FERC	
	Time (s)	Opt gap (%)	Time (s)	Opt gap (%)	Time (s)	Opt gap (%)
T	50.65	0.0121%	56.90	0.0100%	268.6	0.0103%
MLR: (20)(21) [22]	51.29	0.0122%	52.44	0.0100%	254.8	0.0100%
GMR: (20)(23) [12]	51.37	0.0122%	52.42	0.0100%	254.1	0.0100%
PG: (38) [25]	57.22	0.0128%	88.97	0.0100%	299.2	0.0100%
GMR+PG: (23)(38)	50.10	0.0116%	50.70	0.0100%	255.0	0.0103%
AC: (19) [1]	72.94	0.0145%	93.44	0.0100%	362.1	0.0101%
OAV: (19)(37) [24]	75.44	0.0125%	96.72	0.0100%	229.7	0.0101%
CA: (18)(76) [5]	73.78	0.0179%	92.97	0.0100%	307.7	0.0100%

Table 14: Summary of computational results, changing the ramping limits used.

	RTS-GMLC		CAISO		FERC	
	Time (s)	Opt gap (%)	Time (s)	Opt gap (%)	Time (s)	Opt gap (%)
T	50.65	0.0121%	56.90	0.0100%	268.6	0.0103%
DKRA: (35)(36)(79)[7]	50.45	0.0119%	52.59	0.0100%	281.9	0.0100%
MLR: (26)(27) [22]	49.28	0.0119%	48.53	0.0100%	242.6	0.0100%
AC: (24)(25) [1]	51.67	0.0124%	53.59	0.0100%	313.7	0.0107%
OAV ramp limits [24]	51.27	0.0119%	59.60	0.0100%	268.3	0.0101%
OAV-T ramp limits [24]	53.76	0.0121%	59.94	0.0100%	324.0	0.0120%

Table 15: Summary of computational results, changing the production cost formulation used.

	RTS-GMLC		CAISO		FERC	
	Time (s)	Opt gap (%)	Time (s)	Opt gap (%)	Time (s)	Opt gap (%)
T	50.65	0.0121%	56.90	0.0100%	268.6	0.0103%
CA: (43)(44)(45) [5]	48.93	0.0119%	57.87	0.0100%	230.2	0.0100%
Wu: (42)(43)(44) [33]	49.64	0.0136%	55.55	0.0100%	323.9	0.0101%
KOW prod. costs [18]	50.28	0.0119%	52.63	0.0100%	282.2	0.0100%
CW: (93)(94)(95) [6]	50.00	0.0114%	47.68	0.0100%	320.7	0.0101%
SOS2: (89)(90)(91)	59.90	0.0146%	50.67	0.0100%	277.5	0.0100%
SLL: (89)(90)(92) [31]	46.83	0.0115%	48.25	0.0100%	304.1	0.0102%
Epi: (49)	57.33	0.0143%	68.24	0.0100%	277.3	0.0134%
HB: (50) [14]	57.27	0.0119%	71.53	0.0100%	364.5	0.0130%

Table 16: Summary of computational results, changing the start-up cost formulation used.

	RTS-GMLC		CAISO		FERC	
	Time (s)	Opt gap (%)	Time (s)	Opt gap (%)	Time (s)	Opt gap (%)
T	50.65	0.0121%	56.90	0.0100%	268.6	0.0103%
MLR: (52)(53)(54) [22]	49.23	0.0117%	66.37	0.0100%	291.9	0.0571%
KOW 3bin: (96)(97) [19]	49.25	0.0121%	104.3	0.0106%	326.9	0.0788%
A-K: (102)(103)(106) [2, 19]	49.65	0.0120%	55.86	0.0100%	276.4	0.0609%
MLR proj: (52)(55)(56)	44.15	0.0121%	65.47	0.0100%	289.3	0.0520%

The literature has many possibilities for formulating piecewise production costs; Table 15 summarized the computational results under changes to the production cost formulation for **T**. The full results are in the appendix, Tables 38–40. It is clear from Table 15 that the SOS2 and Epi variants result in performance degradation, and HB does not perform as well as we might expect. Gurobi seems to prefer formulations with additional variables, as even the non-ideal CA variant out-performs HB across the board. Interestingly, CA does surprisingly well, only timing out on the difficult RTS-GMLC instance "2020-04-03 NC." This may be in part because CA is sparse: the limits on the $p_g^l(t)$ variables are just variable bounds and hence are not additional rows in the simplex tableau.

Lastly, we consider the effect changing the start-up cost formulation has on the performance of formulation **T**. The summary results are in Table 16, and the full results are in the appendix, Tables 41–43. On the RTS-GMLC and CAISO instances, none of the other formulations are a significant improvement over **T**, and on the FERC instances the start-up costs formulation from Knueven et al. [19] allows **T** to achieve a high-quality solution in 10 minutes on all instances.

G Full Computational Results

In this appendix we report the full computational results for the formulations and instances tested.

Table 17: Computational results for RTS-GMLC instances. Wall clock times are reported in seconds. When the 300 second time limit is reached, the terminating optimality gap is reported in parentheses. The best value for each instance is bold-faced. Each instance is named by the date from which the beginning of the 48-hour load profile was selected and whether the system with considered with (NC) or without (CP) a network.

Instance	**MLR** (2013)	**ALS** (2018)	**KOW** (2018)	**T**	**Co**	**R1**	**R2**
2020-01-27 CP	(0.056%)	219.7	(0.073%)	**88.8**	101.5	94.8	99.7
2020-02-09 CP	49.8	**20.4**	47.6	23.0	28.0	21.3	23.3
2020-03-05 CP	91.5	34.7	92.2	**25.3**	26.6	25.9	40.2
2020-04-03 CP	(0.047%)	(0.020%)	(0.032%)	42.6	51.2	51.2	**39.1**
2020-05-05 CP	37.3	34.9	56.7	**19.5**	25.0	25.8	20.9
2020-06-09 CP	14.6	12.1	18.6	5.8	6.3	**4.7**	6.4
2020-07-06 CP	13.3	10.8	13.2	6.8	6.8	**5.3**	9.7
2020-08-12 CP	29.0	12.1	14.1	12.2	**6.0**	6.8	7.4
2020-09-20 CP	42.4	11.6	39.5	**7.4**	12.7	8.3	8.5
2020-10-27 CP	79.6	39.2	59.7	24.3	21.4	**21.1**	29.0
2020-11-25 CP	115.0	47.0	176.2	33.4	34.3	**26.7**	35.7
2020-12-23 CP	35.1	20.7	53.9	19.4	21.7	**13.4**	15.5
2020-01-27 NC	103.2	89.1	188.4	157.6	53.7	56.3	**38.6**
2020-02-09 NC	193.8	192.1	206.5	212.6	60.9	**55.8**	56.6
2020-03-05 NC	(0.017%)	300.0	217.8	(0.021%)	292.4	**113.5**	230.1
2020-04-03 NC	(0.048%)	(0.054%)	(0.051%)	(0.050%)	(0.061%)	**(0.043%)**	(0.044%)
2020-05-05 NC	197.1	205.2	(0.039%)	212.8	249.2	**67.6**	108.6
2020-06-09 NC	37.1	26.6	38.4	49.8	18.9	19.2	**16.0**
2020-07-06 NC	40.0	25.5	55.7	39.3	22.9	**16.1**	18.9
2020-08-12 NC	41.4	42.3	49.4	67.3	56.5	37.8	**26.2**
2020-09-20 NC	81.1	51.9	135.8	69.3	40.8	**39.4**	39.8
2020-10-27 NC	(0.037%)	222.7	295.2	153.7	191.9	**135.4**	168.9
2020-11-25 NC	206.7	93.5	209.9	164.9	100.3	**64.0**	108.8
2020-12-23 NC	219.3	211.6	236.9	226.1	244.3	**82.1**	89.8

Table 18: Computational results for CAISO instances. Wall clock times are reported in seconds. When the 300 second time limit is reached, the terminating optimality gap is reported in parentheses. The best value for each instance is bold-faced. Each instance is named by the date or hypothetical scenario from which the beginning of the 48-hour load profile was selected, followed by the reserve level, considered as a percentage of load.

Instance	**MLR** (2013)	**ALS** (2018)	**KOW** (2018)	**T**	**Co**	**R1**	**R2**
2014-09-01 0%	72.5	189.0	39.1	51.7	37.2	71.2	**37.2**
2014-12-01 0%	60.7	(0.014%)	**33.7**	45.1	66.7	122.8	64.0
2015-03-01 0%	36.4	207.5	**27.4**	32.1	90.9	118.3	38.7
2015-06-01 0%	23.7	190.4	**12.1**	19.1	43.3	87.8	47.3
Scenario400 0%	98.9	(0.139%)	50.4	**31.0**	92.3	162.6	146.4
2014-09-01 1%	81.6	163.8	56.5	**25.4**	35.8	88.8	41.6
2014-12-01 1%	116.7	(0.012%)	85.0	**84.5**	103.2	138.8	92.2
2015-03-01 1%	95.1	(0.012%)	39.6	**36.4**	87.7	123.3	131.9
2015-06-01 1%	93.9	176.2	69.9	**38.3**	54.5	98.2	77.7
Scenario400 1%	163.4	(0.283%)	99.6	**66.5**	131.6	207.5	140.3
2014-09-01 3%	297.1	(0.010%)	198.7	**83.5**	128.3	142.2	127.1
2014-12-01 3%	165.2	(0.021%)	**73.4**	106.8	152.8	176.3	104.9
2015-03-01 3%	83.2	241.7	88.0	**67.4**	109.9	114.5	88.5
2015-06-01 3%	166.8	284.3	159.2	**57.8**	124.9	107.3	160.9
Scenario400 3%	(0.017%)	(0.324%)	(0.010%)	**103.8**	261.9	273.1	(0.010%)
2014-09-01 5%	191.8	(0.025%)	132.3	**92.7**	138.6	198.4	111.8
2014-12-01 5%	268.1	(0.046%)	147.4	**129.9**	156.9	235.4	187.0
2015-03-01 5%	97.6	(0.018%)	75.7	**54.6**	145.1	176.6	140.3
2015-06-01 5%	145.8	260.3	113.8	**56.7**	147.1	246.6	136.7
Scenario400 5%	(0.041%)	(0.169%)	(0.014%)	**106.9**	165.6	(0.015%)	279.7

Table 19: Computational results for FERC instances. Wall clock times are reported in seconds. When the 600 second time limit is reached, the terminating optimality gap is reported in parentheses. The best value for each instance is bold-faced. Each instance is named by the date from which the beginning of the 48-hour load profile was selected and whether it is low-wind (LW) (wind supply is 2% of energy demand for the year) or high-wind (HW) (wind supply is scaled to be 30% of energy demand for the year).

Instance	**MLR** (2013)	**ALS** (2018)	**KOW** (2018)	**T**	**Co**	**R1**	**R2**
2015-01-01 LW	265.3	348.1	310.5	107.6	**105.0**	185.3	161.4
2015-02-01 LW	543.2	(0.022%)	266.3	**133.5**	508.0	570.2	438.2
2015-03-01 LW	423.0	**221.9**	(0.049%)	244.0	237.6	282.3	337.4
2015-04-01 LW	414.1	240.0	311.2	411.6	**184.7**	279.4	398.2
2015-05-01 LW	160.4	**128.8**	310.4	221.6	190.5	136.4	182.6
2015-06-01 LW	**120.6**	266.4	311.2	282.6	128.4	159.2	276.9
2015-07-01 LW	555.9	338.1	521.2	429.6	**237.4**	469.8	509.8
2015-08-01 LW	551.2	365.8	**273.6**	281.5	401.5	358.7	527.1
2015-09-01 LW	541.9	542.6	**394.8**	541.8	501.6	403.8	439.8
2015-10-01 LW	165.4	287.0	320.1	201.9	**141.1**	148.5	217.6
2015-11-02 LW	166.2	419.2	317.5	**166.0**	282.2	217.8	368.9
2015-12-01 LW	217.3	251.5	383.8	**114.5**	118.5	154.9	152.9
2015-01-01 HW	(0.793%)	(1.379%)	415.4	**210.4**	(1.151%)	(0.895%)	(1.263%)
2015-02-01 HW	(0.256%)	(0.430%)	435.6	**136.0**	(0.055%)	(0.027%)	(0.076%)
2015-03-01 HW	411.5	(0.016%)	559.7	379.2	420.5	**277.5**	573.9
2015-04-01 HW	508.5	369.8	595.3	**244.6**	296.6	252.3	290.3
2015-05-01 HW	**122.3**	277.7	246.7	244.4	258.0	235.5	191.5
2015-06-01 HW	**254.6**	385.7	263.6	351.2	435.8	319.3	409.1
2015-07-01 HW	**223.9**	(0.016%)	(0.010%)	548.1	(0.020%)	493.3	549.2
2015-08-01 HW	391.2	591.5	448.1	**361.7**	436.9	386.3	459.5
2015-09-01 HW	(0.075%)	(0.191%)	**439.5**	(0.018%)	554.5	(0.024%)	(0.044%)
2015-10-01 HW	486.1	499.8	(0.012%)	351.6	331.0	**294.3**	336.8
2015-11-02 HW	586.9	(0.025%)	343.2	**321.1**	492.8	512.1	(0.021%)
2015-12-01 HW	346.7	483.6	497.5	287.3	385.9	**283.0**	526.6

Table 20: Computational results for RTS-GMLC instances, older formulations. Wall clock times are reported in seconds. When the 300 second time limit is reached, the terminating optimality gap is reported in parentheses. Each instance is named by the date from which the beginning of the 48-hour load profile was selected and whether the system with considered with (NC) or without (CP) a network.

Instance	**CA** (2006)	**OAV-O** (2012)	**OAV-UD** (2012)	**OAV** (2012)	**OAV-T** (2012)
2020-01-27 CP	(29.439%)	(1.617%)	(1.363%)	(1.295%)	(1.161%)
2020-02-09 CP	(7.566%)	103.5	63.5	62.5	75.3
2020-03-05 CP	(11.437%)	204.0	163.8	154.0	169.5
2020-04-03 CP	(11.256%)	(0.044%)	(0.017%)	(0.031%)	(0.037%)
2020-05-05 CP	(9.583%)	144.0	69.1	77.0	101.3
2020-06-09 CP	(2.676%)	42.7	38.0	37.8	47.6
2020-07-06 CP	(2.536%)	59.9	62.6	64.3	89.4
2020-08-12 CP	(3.548%)	59.1	43.7	44.3	56.8
2020-09-20 CP	(9.302%)	60.2	53.0	56.4	66.8
2020-10-27 CP	(18.483%)	(0.180%)	(0.019%)	(0.155%)	(0.099%)
2020-11-25 CP	(23.601%)	(1.220%)	(0.654%)	(0.829%)	(0.790%)
2020-12-23 CP	(8.972%)	88.3	80.8	114.0	169.2
2020-01-27 NC	(35.790%)	(0.531%)	(0.448%)	(0.547%)	(0.489%)
2020-02-09 NC	(18.107%)	(0.828%)	(0.545%)	(0.372%)	(0.480%)
2020-03-05 NC	(13.130%)	(0.807%)	(0.571%)	(0.635%)	(0.579%)
2020-04-03 NC	(16.058%)	(0.487%)	(0.355%)	(0.084%)	(0.262%)
2020-05-05 NC	(16.950%)	(0.312%)	(0.260%)	(0.165%)	(0.252%)
2020-06-09 NC	(5.735%)	100.0	108.4	88.5	117.6
2020-07-06 NC	(3.136%)	117.4	132.0	220.7	126.3
2020-08-12 NC	(7.401%)	110.1	174.3	224.6	204.9
2020-09-20 NC	(13.968%)	(0.016%)	(0.011%)	273.3	179.6
2020-10-27 NC	(26.777%)	(0.786%)	(0.713%)	(0.619%)	(0.703%)
2020-11-25 NC	(35.007%)	(0.674%)	(0.553%)	(0.540%)	(0.665%)
2020-12-23 NC	(10.101%)	(0.417%)	(0.493%)	(0.266%)	(0.369%)

Table 21: Computational results for CAISO instances, older formulations. Wall clock times are reported in seconds. When the 300 second time limit is reached, the terminating optimality gap is reported in parentheses. Each instance is named by the date or hypothetical scenario from which the beginning of the 48-hour load profile was selected, followed by the reserve level, considered as a percentage of load.

Instance	**CA** (2006)	**OAV-O** (2012)	**OAV-UD** (2012)	**OAV** (2012)	**OAV-T** (2012)
2014-09-01 0%	(0.266%)	(0.249%)	(0.299%)	(0.260%)	(0.286%)
2014-12-01 0%	(0.540%)	(0.301%)	(0.273%)	(0.244%)	(0.257%)
2015-03-01 0%	(1.073%)	(0.414%)	(0.261%)	(0.476%)	(0.406%)
2015-06-01 0%	(0.248%)	(0.199%)	(0.217%)	(0.210%)	(0.211%)
Scenario400 0%	(2.684%)	(63.420%)	(52.212%)	(1.852%)	(50.837%)
2014-09-01 1%	(0.358%)	(0.608%)	(0.390%)	(0.697%)	(2.334%)
2014-12-01 1%	(0.489%)	(0.344%)	(0.297%)	(0.346%)	(0.359%)
2015-03-01 1%	(0.960%)	(0.334%)	(0.363%)	(0.465%)	(0.597%)
2015-06-01 1%	(0.318%)	(0.305%)	(0.352%)	(0.266%)	(0.275%)
Scenario400 1%	(3.182%)	(44.939%)	(23.811%)	(16.637%)	(50.386%)
2014-09-01 3%	(0.278%)	(0.188%)	(4.311%)	(5.619%)	(4.056%)
2014-12-01 3%	(0.560%)	(0.480%)	(0.404%)	(0.217%)	(0.571%)
2015-03-01 3%	(1.649%)	(0.356%)	(0.307%)	(12.475%)	(0.458%)
2015-06-01 3%	(0.458%)	(2.655%)	(1.931%)	(7.124%)	(9.985%)
Scenario400 3%	(3.158%)	(17.791%)	(38.164%)	(7.291%)	(9.758%)
2014-09-01 5%	(0.353%)	(0.194%)	(4.865%)	(0.286%)	(1.633%)
2014-12-01 5%	(0.750%)	(13.422%)	(1.922%)	(3.532%)	(0.411%)
2015-03-01 5%	(1.342%)	(0.811%)	(0.626%)	(0.726%)	(0.677%)
2015-06-01 5%	(0.365%)	(0.327%)	(0.319%)	(0.356%)	(0.342%)
Scenario400 5%	(3.048%)	(8.326%)	(8.579%)	(16.152%)	(6.425%)

Table 22: Computational results for FERC instances, older formulations. Wall clock times are reported in seconds. When the 600 second time limit is reached, the terminating optimality gap is reported in parentheses. Each instance is named by the date from which the beginning of the 48-hour load profile was selected and whether it is low-wind (LW) (wind supply is 2% of energy demand for the year) or high-wind (HW) (wind supply is scaled to be 30% of energy demand for the year).

Instance	**CA** (2006)	**OAV-O** (2012)	**OAV-UD** (2012)	**OAV** (2012)	**OAV-T** (2012)
2015-01-01 LW	(2.710%)	(0.552%)	(0.093%)	(0.083%)	(0.137%)
2015-02-01 LW	(2.593%)	(1.268%)	(0.471%)	(0.779%)	(0.878%)
2015-03-01 LW	(1.747%)	(0.264%)	(0.016%)	(0.071%)	(0.115%)
2015-04-01 LW	(23.563%)	(2.157%)	(0.013%)	(0.013%)	(0.040%)
2015-05-01 LW	(2.151%)	592.1	566.5	468.7	355.4
2015-06-01 LW	(4.241%)	(0.949%)	529.2	540.6	(0.096%)
2015-07-01 LW	(38.678%)	(1.635%)	(0.029%)	(0.042%)	(0.194%)
2015-08-01 LW	(4.372%)	(1.458%)	(0.692%)	(0.750%)	(1.003%)
2015-09-01 LW	(11.635%)	(3.155%)	(0.559%)	(0.644%)	(0.689%)
2015-10-01 LW	(34.530%)	(3.988%)	(0.085%)	(0.282%)	(0.913%)
2015-11-02 LW	(57.216%)	(4.354%)	(2.145%)	(0.820%)	(1.267%)
2015-12-01 LW	(28.359%)	(1.672%)	(0.569%)	(0.247%)	(0.899%)
2015-01-01 HW	(89.979%)	(14.934%)	(5.845%)	(5.765%)	(5.596%)
2015-02-01 HW	(77.601%)	(6.419%)	(3.069%)	(3.723%)	(3.871%)
2015-03-01 HW	(15.793%)	(6.696%)	(1.935%)	(2.150%)	(2.383%)
2015-04-01 HW	(92.072%)	(66.194%)	(6.103%)	(6.252%)	(6.239%)
2015-05-01 HW	(58.044%)	(0.123%)	510.5	533.1	495.2
2015-06-01 HW	(90.847%)	(11.658%)	(0.775%)	(0.619%)	(1.623%)
2015-07-01 HW	(73.523%)	(7.871%)	(1.236%)	(1.788%)	(1.059%)
2015-08-01 HW	(89.531%)	(26.264%)	(3.219%)	(1.932%)	(3.238%)
2015-09-01 HW	(66.341%)	(43.264%)	(4.737%)	(3.331%)	(1.774%)
2015-10-01 HW	(99.977%)	(36.145%)	524.8	(0.038%)	(0.082%)
2015-11-02 HW	(97.372%)	(40.326%)	(3.014%)	(2.306%)	(2.004%)
2015-12-01 HW	(86.932%)	(27.849%)	(0.737%)	(0.147%)	(0.742%)

Table 23: Computational results for RTS-GMLC instances. Wall clock times are reported in seconds. When the 300 second time limit is reached, the terminating optimality gap is reported in parentheses. Each instance is named by the date from which the beginning of the 48-hour load profile was selected and whether the system with considered with (NC) or without (CP) a network. We replace the variable $p'_g(t)$ in formulation **T** with that listed in each heading.

Instance	**T**	CA [5] p_g
2020-01-27 CP	88.8	94.4
2020-02-09 CP	23.0	23.7
2020-03-05 CP	25.3	26.9
2020-04-03 CP	42.6	71.4
2020-05-05 CP	19.5	34.2
2020-06-09 CP	5.8	8.2
2020-07-06 CP	6.8	7.3
2020-08-12 CP	12.2	13.1
2020-09-20 CP	7.4	10.6
2020-10-27 CP	24.3	24.9
2020-11-25 CP	33.4	35.4
2020-12-23 CP	19.4	21.2
2020-01-27 NC	157.6	100.2
2020-02-09 NC	212.6	244.7
2020-03-05 NC	(0.021%)	183.3
2020-04-03 NC	(0.050%)	(0.044%)
2020-05-05 NC	212.8	(0.051%)
2020-06-09 NC	49.8	48.9
2020-07-06 NC	39.3	68.2
2020-08-12 NC	67.3	48.2
2020-09-20 NC	69.3	78.0
2020-10-27 NC	153.7	195.1
2020-11-25 NC	164.9	122.8
2020-12-23 NC	226.1	271.8

Table 24: Computational results for CAISO instances. Wall clock times are reported in seconds. When the 300 second time limit is reached, the terminating optimality gap is reported in parentheses. Each instance is named by the date or hypothetical scenario from which the beginning of the 48-hour load profile was selected, followed by the reserve level, considered as a percentage of load. We replace the variable $p'_g(t)$ in formulation **T** with that listed in each heading.

Instance	**T**	CA [5] p_g
2014-09-01 0%	51.7	59.9
2014-12-01 0%	45.1	33.6
2015-03-01 0%	32.1	34.5
2015-06-01 0%	19.1	22.4
Scenario400 0%	31.0	52.0
2014-09-01 1%	25.4	43.9
2014-12-01 1%	84.5	57.9
2015-03-01 1%	36.4	53.3
2015-06-01 1%	38.3	58.0
Scenario400 1%	66.5	68.4
2014-09-01 3%	83.5	82.4
2014-12-01 3%	106.8	98.6
2015-03-01 3%	67.4	85.3
2015-06-01 3%	57.8	96.5
Scenario400 3%	103.8	104.2
2014-09-01 5%	92.7	78.3
2014-12-01 5%	129.9	140.0
2015-03-01 5%	54.6	59.8
2015-06-01 5%	56.7	74.5
Scenario400 5%	106.9	85.9

Table 25: Computational results for FERC instances. Wall clock times are reported in seconds. When the 600 second time limit is reached, the terminating optimality gap is reported in parentheses. Each instance is named by the date from which the beginning of the 48-hour load profile was selected and whether it is low-wind (LW) (wind supply is 2% of energy demand for the year) or high-wind (HW) (wind supply is scaled to be 30% of energy demand for the year). We replace the variable $p'_g(t)$ in formulation **T** with that listed in each heading.

Instance	**T**	CA [5] p_g
2015-01-01 LW	107.6	304.2
2015-02-01 LW	133.5	246.6
2015-03-01 LW	244.0	414.5
2015-04-01 LW	411.6	472.2
2015-05-01 LW	221.6	360.8
2015-06-01 LW	282.6	473.3
2015-07-01 LW	429.6	329.5
2015-08-01 LW	281.5	480.2
2015-09-01 LW	541.8	581.1
2015-10-01 LW	201.9	312.0
2015-11-02 LW	166.0	366.9
2015-12-01 LW	114.5	210.6
2015-01-01 HW	210.4	420.1
2015-02-01 HW	136.0	441.7
2015-03-01 HW	379.2	457.2
2015-04-01 HW	244.6	375.0
2015-05-01 HW	244.4	383.6
2015-06-01 HW	351.2	503.1
2015-07-01 HW	548.1	(0.273%)
2015-08-01 HW	361.7	(0.015%)
2015-09-01 HW	(0.018%)	(0.039%)
2015-10-01 HW	351.6	571.8
2015-11-02 HW	321.1	498.1
2015-12-01 HW	287.3	335.1

Table 26: Computational results for RTS-GMLC instances. Wall clock times are reported in seconds. When the 300 second time limit is reached, the terminating optimality gap is reported in parentheses. Each instance is named by the date from which the beginning of the 48-hour load profile was selected and whether the system with considered with (NC) or without (CP) a network. We replace the variable $\overline{p}'_g(t)$ in formulation **T** with that listed in each heading.

Instance	**T**	MLR [22] r_g	CA [5] $\overline{p}_g$
2020-01-27 CP	88.8	(0.021%)	90.9
2020-02-09 CP	23.0	53.6	18.0
2020-03-05 CP	25.3	48.8	21.7
2020-04-03 CP	42.6	(0.029%)	48.5
2020-05-05 CP	19.5	42.0	15.9
2020-06-09 CP	5.8	11.9	6.8
2020-07-06 CP	6.8	16.0	6.8
2020-08-12 CP	12.2	12.9	9.0
2020-09-20 CP	7.4	26.9	14.2
2020-10-27 CP	24.3	50.8	23.2
2020-11-25 CP	33.4	79.7	36.3
2020-12-23 CP	19.4	56.7	20.5
2020-01-27 NC	157.6	97.3	152.8
2020-02-09 NC	212.6	212.8	193.2
2020-03-05 NC	(0.021%)	162.5	(0.020%)
2020-04-03 NC	(0.050%)	(0.046%)	(0.050%)
2020-05-05 NC	212.8	227.0	248.6
2020-06-09 NC	49.8	46.2	66.1
2020-07-06 NC	39.3	52.1	44.1
2020-08-12 NC	67.3	56.2	56.0
2020-09-20 NC	69.3	65.6	111.4
2020-10-27 NC	153.7	192.4	178.4
2020-11-25 NC	164.9	147.4	146.2
2020-12-23 NC	226.1	213.4	210.0

Table 27: Computational results for CAISO instances. Wall clock times are reported in seconds. When the 300 second time limit is reached, the terminating optimality gap is reported in parentheses. Each instance is named by the date or hypothetical scenario from which the beginning of the 48-hour load profile was selected, followed by the reserve level, considered as a percentage of load. We replace the variable $\overline{p}'_g(t)$ in formulation **T** with that listed in each heading.

Instance	**T**	MLR [22] r_g	CA [5] $\overline{p}_g$
2014-09-01 0%	51.7	40.8	36.8
2014-12-01 0%	45.1	33.4	35.3
2015-03-01 0%	32.1	29.3	30.7
2015-06-01 0%	19.1	13.8	17.6
Scenario400 0%	31.0	30.3	34.8
2014-09-01 1%	25.4	61.4	28.5
2014-12-01 1%	84.5	82.0	60.9
2015-03-01 1%	36.4	38.4	45.2
2015-06-01 1%	38.3	68.5	40.8
Scenario400 1%	66.5	191.8	62.2
2014-09-01 3%	83.5	242.9	67.9
2014-12-01 3%	106.8	71.9	98.1
2015-03-01 3%	67.4	99.5	77.4
2015-06-01 3%	57.8	120.4	35.8
Scenario400 3%	103.8	126.8	86.0
2014-09-01 5%	92.7	114.1	70.8
2014-12-01 5%	129.9	158.1	58.8
2015-03-01 5%	54.6	123.1	56.7
2015-06-01 5%	56.7	173.6	104.9
Scenario400 5%	106.9	266.0	67.8

Table 28: Computational results for FERC instances. Wall clock times are reported in seconds. When the 600 second time limit is reached, the terminating optimality gap is reported in parentheses. Each instance is named by the date from which the beginning of the 48-hour load profile was selected and whether it is low-wind (LW) (wind supply is 2% of energy demand for the year) or high-wind (HW) (wind supply is scaled to be 30% of energy demand for the year). We replace the variable $\overline{p}'_g(t)$ in formulation **T** with that listed in each heading.

Instance	**T**	MLR [22] r_g	CA [5] $\overline{p}_g$
2015-01-01 LW	107.6	175.7	310.0
2015-02-01 LW	133.5	108.1	297.1
2015-03-01 LW	244.0	254.0	420.4
2015-04-01 LW	411.6	364.3	577.4
2015-05-01 LW	221.6	110.1	304.0
2015-06-01 LW	282.6	200.9	243.1
2015-07-01 LW	429.6	(0.013%)	548.3
2015-08-01 LW	281.5	191.8	456.0
2015-09-01 LW	541.8	465.6	543.1
2015-10-01 LW	201.9	131.5	296.0
2015-11-02 LW	166.0	120.6	356.8
2015-12-01 LW	114.5	112.8	281.5
2015-01-01 HW	210.4	223.8	340.2
2015-02-01 HW	136.0	290.3	286.3
2015-03-01 HW	379.2	193.6	394.9
2015-04-01 HW	244.6	270.0	447.2
2015-05-01 HW	244.4	103.8	294.0
2015-06-01 HW	351.2	181.7	496.3
2015-07-01 HW	548.1	(0.021%)	534.1
2015-08-01 HW	361.7	443.1	478.8
2015-09-01 HW	(0.018%)	294.5	(0.012%)
2015-10-01 HW	351.6	362.8	355.5
2015-11-02 HW	321.1	335.4	478.6
2015-12-01 HW	287.3	219.6	544.7

Table 29: Computational results for RTS-GMLC instances. Wall clock times are reported in seconds. When the 300 second time limit is reached, the terminating optimality gap is reported in parentheses. Each instance is named by the date from which the beginning of the 48-hour load profile was selected and whether the system with considered with (NC) or without (CP) a network. We replace the uptime/downtime constraints from **T** with those listed.

Instance	**T**	RT 2bin [28] (4)(7)	DEKT [8] (70)(71)
2020-01-27 CP	88.8	90.9	105.8
2020-02-09 CP	23.0	18.7	23.9
2020-03-05 CP	25.3	24.0	26.3
2020-04-03 CP	42.6	49.1	53.9
2020-05-05 CP	19.5	24.3	26.8
2020-06-09 CP	5.8	6.2	6.8
2020-07-06 CP	6.8	9.4	10.6
2020-08-12 CP	12.2	7.6	12.4
2020-09-20 CP	7.4	9.6	11.3
2020-10-27 CP	24.3	22.7	27.9
2020-11-25 CP	33.4	31.7	53.0
2020-12-23 CP	19.4	18.1	16.6
2020-01-27 NC	157.6	135.7	180.8
2020-02-09 NC	212.6	(0.011%)	283.2
2020-03-05 NC	(0.021%)	(0.018%)	(0.020%)
2020-04-03 NC	(0.050%)	(0.050%)	(0.052%)
2020-05-05 NC	212.8	120.9	169.6
2020-06-09 NC	49.8	52.9	55.9
2020-07-06 NC	39.3	38.3	43.6
2020-08-12 NC	67.3	43.8	43.1
2020-09-20 NC	69.3	97.4	124.7
2020-10-27 NC	153.7	192.4	214.2
2020-11-25 NC	164.9	127.6	(0.015%)
2020-12-23 NC	226.1	102.9	227.2

Table 30: Computational results for CAISO instances. Wall clock times are reported in seconds. When the 300 second time limit is reached, the terminating optimality gap is reported in parentheses. Each instance is named by the date or hypothetical scenario from which the beginning of the 48-hour load profile was selected, followed by the reserve level, considered as a percentage of load. We replace the uptime/downtime constraints from **T** with those listed.

Instance	**T**	RT 2bin [28] (4)(7)	DEKT [8] (70)(71)
2014-09-01 0%	51.7	42.0	55.6
2014-12-01 0%	45.1	23.3	39.5
2015-03-01 0%	32.1	23.6	31.3
2015-06-01 0%	19.1	12.0	18.2
Scenario400 0%	31.0	38.5	32.0
2014-09-01 1%	25.4	28.0	25.9
2014-12-01 1%	84.5	56.9	34.5
2015-03-01 1%	36.4	16.9	33.2
2015-06-01 1%	38.3	41.7	32.5
Scenario400 1%	66.5	86.7	40.7
2014-09-01 3%	83.5	83.4	51.5
2014-12-01 3%	106.8	57.5	68.6
2015-03-01 3%	67.4	61.5	66.7
2015-06-01 3%	57.8	95.4	38.5
Scenario400 3%	103.8	108.1	91.7
2014-09-01 5%	92.7	71.0	59.0
2014-12-01 5%	129.9	100.9	98.7
2015-03-01 5%	54.6	71.9	33.3
2015-06-01 5%	56.7	95.0	75.0
Scenario400 5%	106.9	102.8	107.8

Table 31: Computational results for FERC instances. Wall clock times are reported in seconds. When the 600 second time limit is reached, the terminating optimality gap is reported in parentheses. Each instance is named by the date from which the beginning of the 48-hour load profile was selected and whether it is low-wind (LW) (wind supply is 2% of energy demand for the year) or high-wind (HW) (wind supply is scaled to be 30% of energy demand for the year). We replace the uptime/downtime constraints from **T** with those listed.

Instance	**T**	RT 2bin [28] (4)(7)	DEKT [8] (70)(71)
2015-01-01 LW	107.6	102.9	197.5
2015-02-01 LW	133.5	88.0	268.1
2015-03-01 LW	244.0	211.7	318.1
2015-04-01 LW	411.6	369.7	271.8
2015-05-01 LW	221.6	117.1	192.0
2015-06-01 LW	282.6	187.6	345.1
2015-07-01 LW	429.6	389.7	480.3
2015-08-01 LW	281.5	275.0	374.8
2015-09-01 LW	541.8	422.1	(0.012%)
2015-10-01 LW	201.9	125.4	350.9
2015-11-02 LW	166.0	140.1	213.3
2015-12-01 LW	114.5	135.5	427.3
2015-01-01 HW	210.4	254.2	(0.030%)
2015-02-01 HW	136.0	175.8	380.7
2015-03-01 HW	379.2	277.3	471.3
2015-04-01 HW	244.6	275.8	580.4
2015-05-01 HW	244.4	184.4	433.0
2015-06-01 HW	351.2	246.8	395.3
2015-07-01 HW	548.1	410.4	(0.026%)
2015-08-01 HW	361.7	421.6	(0.034%)
2015-09-01 HW	(0.018%)	474.6	(0.026%)
2015-10-01 HW	351.6	401.5	(0.019%)
2015-11-02 HW	321.1	330.3	583.3
2015-12-01 HW	287.3	286.0	(0.075%)

Table 32: Computational results for RTS-GMLC instances. Wall clock times are reported in seconds. When the 300 second time limit is reached, the terminating optimality gap is reported in parentheses. Each instance is named by the date from which the beginning of the 48-hour load profile was selected and whether the system with considered with (NC) or without (CP) a network. We replace the generation limits except (17) from **T** with those listed.

Instance	**T**	MLR [22] (20)(21)	GMR [12] (20)(23)	PG [25] (38)	GMR+PG (23)(38)	AC [1] (19)	OAV [24] (19)(37)	CA [5] (18)(76)
2020-01-27 CP	88.8	146.7	147.3	108.0	146.8	177.3	147.3	149.5
2020-02-09 CP	23.0	23.2	23.5	24.6	23.8	28.3	34.1	32.5
2020-03-05 CP	25.3	27.6	27.8	33.1	32.3	31.9	39.3	30.0
2020-04-03 CP	42.6	70.7	72.8	149.4	40.2	(0.025%)	(0.016%)	175.5
2020-05-05 CP	19.5	23.7	23.9	31.0	20.0	26.0	27.2	43.2
2020-06-09 CP	5.8	6.4	6.3	6.6	6.2	8.8	9.4	9.2
2020-07-06 CP	6.8	10.6	10.7	10.8	7.0	11.1	15.1	7.1
2020-08-12 CP	12.2	10.6	10.7	13.9	9.3	14.6	21.0	26.0
2020-09-20 CP	7.4	7.7	7.9	12.0	9.0	9.8	15.8	15.6
2020-10-27 CP	24.3	20.5	20.6	21.7	26.6	33.8	47.7	42.7
2020-11-25 CP	33.4	30.8	30.5	35.0	28.9	48.3	52.5	51.7
2020-12-23 CP	19.4	20.4	20.4	35.7	22.1	29.6	24.4	28.2
2020-01-27 NC	157.6	89.1	88.4	103.6	139.9	172.1	158.5	193.7
2020-02-09 NC	212.6	109.7	108.7	98.5	264.4	255.7	224.5	243.5
2020-03-05 NC	(0.021%)	(0.018%)	(0.018%)	(0.012%)	129.3	(0.017%)	(0.016%)	258.5
2020-04-03 NC	(0.050%)	(0.054%)	(0.054%)	(0.075%)	(0.049%)	(0.054%)	(0.059%)	(0.052%)
2020-05-05 NC	212.8	262.4	265.5	296.2	263.6	(0.052%)	279.9	293.3
2020-06-09 NC	49.8	54.7	54.2	52.9	46.1	92.9	68.2	85.1
2020-07-06 NC	39.3	44.2	43.5	93.6	44.3	64.9	87.0	71.4
2020-08-12 NC	67.3	53.3	53.3	48.8	50.8	57.8	50.2	54.8
2020-09-20 NC	69.3	117.7	116.9	74.3	114.7	121.0	110.8	119.8
2020-10-27 NC	153.7	152.8	152.5	175.7	149.8	234.9	212.3	204.2
2020-11-25 NC	164.9	149.4	150.0	107.7	175.5	191.2	143.8	140.8
2020-12-23 NC	226.1	122.4	121.8	125.3	94.2	270.1	273.2	(0.157%)

Table 33: Computational results for CAISO instances. Wall clock times are reported in seconds. When the 300 second time limit is reached, the terminating optimality gap is reported in parentheses. Each instance is named by the date or hypothetical scenario from which the beginning of the 48-hour load profile was selected, followed by the reserve level, considered as a percentage of load. We replace the generation limits except (17) from **T** with those listed.

Instance	**T**	MLR [22] (20)(21)	GMR [12] (20)(23)	PG [25] (38)	GMR+PG (23)(38)	AC [1] (19)	OAV [24] (19)(37)	CA [5] (18)(76)
2014-09-01 0%	51.7	31.6	31.8	46.6	46.3	50.0	76.2	50.5
2014-12-01 0%	45.1	39.1	39.3	35.8	31.7	37.4	43.7	38.5
2015-03-01 0%	32.1	40.3	41.0	53.8	36.2	44.7	45.4	49.5
2015-06-01 0%	19.1	20.2	20.3	19.6	21.4	18.4	18.8	18.0
Scenario400 0%	31.0	40.6	39.8	46.6	45.4	57.9	61.8	61.3
2014-09-01 1%	25.4	26.7	26.2	45.2	21.9	48.4	44.2	73.2
2014-12-01 1%	84.5	76.2	75.9	140.8	81.3	141.8	153.1	98.0
2015-03-01 1%	36.4	33.9	33.7	66.3	35.6	57.8	67.5	54.8
2015-06-01 1%	38.3	38.5	38.6	74.6	40.1	132.7	76.4	142.8
Scenario400 1%	66.5	46.1	46.4	84.4	35.8	132.9	149.4	121.5
2014-09-01 3%	83.5	54.6	54.9	168.1	62.7	158.6	165.5	156.2
2014-12-01 3%	106.8	119.9	117.7	139.4	72.7	154.5	151.6	145.1
2015-03-01 3%	67.4	64.6	64.4	105.0	79.0	128.6	140.1	121.1
2015-06-01 3%	57.8	62.8	62.9	206.6	38.3	91.0	58.5	98.0
Scenario400 3%	103.8	109.7	110.3	175.7	102.6	167.0	227.1	(0.011%)
2014-09-01 5%	92.7	58.9	58.6	164.4	71.0	106.2	126.1	138.3
2014-12-01 5%	129.9	106.0	106.7	130.6	64.1	208.7	149.4	106.6
2015-03-01 5%	54.6	38.8	38.8	116.8	58.6	108.0	156.1	105.6
2015-06-01 5%	56.7	54.4	54.9	117.3	55.5	162.4	181.9	150.1
Scenario400 5%	106.9	128.8	128.1	168.9	128.1	221.9	224.6	170.5

Table 34: Computational results for FERC instances. Wall clock times are reported in seconds. When the 600 second time limit is reached, the terminating optimality gap is reported in parentheses. Each instance is named by the date from which the beginning of the 48-hour load profile was selected and whether it is low-wind (LW) (wind supply is 2% of energy demand for the year) or high-wind (HW) (wind supply is scaled to be 30% of energy demand for the year). We replace the generation limits except (17) from **T** with those listed.

Instance	**T**	MLR [22] (20)(21)	GMR [12] (20)(23)	PG [25] (38)	GMR+PG (23)(38)	AC [1] (19)	OAV [24] (19)(37)	CA [5] (18)(76)
2015-01-01 LW	107.6	106.3	106.5	167.6	107.9	183.5	123.3	163.0
2015-02-01 LW	133.5	93.3	93.1	199.9	86.8	302.1	241.1	238.7
2015-03-01 LW	244.0	196.2	193.7	243.4	194.1	327.2	328.2	536.5
2015-04-01 LW	411.6	383.2	382.3	423.5	366.4	600.0	253.3	387.0
2015-05-01 LW	221.6	177.4	177.4	201.7	213.1	253.1	103.3	212.3
2015-06-01 LW	282.6	304.1	303.6	443.8	287.4	340.0	171.1	406.9
2015-07-01 LW	429.6	398.4	400.6	528.5	508.5	594.0	463.9	407.6
2015-08-01 LW	281.5	386.5	381.9	357.3	364.7	386.5	133.0	415.2
2015-09-01 LW	541.8	437.7	436.9	354.3	407.3	(0.013%)	(0.013%)	544.9
2015-10-01 LW	201.9	126.1	123.8	226.1	181.1	302.3	176.0	138.2
2015-11-02 LW	166.0	148.2	146.2	243.8	124.7	219.7	163.2	106.6
2015-12-01 LW	114.5	115.1	114.9	198.5	131.4	334.0	256.3	229.0
2015-01-01 HW	210.4	273.7	272.8	222.3	254.6	401.1	211.7	280.6
2015-02-01 HW	136.0	171.3	171.7	248.8	152.7	353.6	188.2	268.9
2015-03-01 HW	379.2	248.6	246.2	351.1	247.9	327.2	540.4	290.3
2015-04-01 HW	244.6	289.7	288.5	216.1	239.0	321.7	192.4	510.7
2015-05-01 HW	244.4	349.8	349.4	297.4	288.4	374.3	184.1	420.4
2015-06-01 HW	351.2	369.7	369.8	308.7	326.3	410.1	146.5	282.7
2015-07-01 HW	548.1	424.1	429.7	544.9	(0.018%)	572.6	344.6	400.9
2015-08-01 HW	361.7	402.4	406.6	392.2	432.3	469.0	348.6	484.0
2015-09-01 HW	(0.018%)	462.0	463.2	435.0	(0.010%)	475.4	243.1	412.9
2015-10-01 HW	351.6	342.9	329.7	326.2	318.2	331.0	369.2	346.5
2015-11-02 HW	321.1	301.3	300.5	359.1	244.0	298.1	142.7	186.6
2015-12-01 HW	287.3	269.3	278.3	278.8	239.2	312.6	227.9	345.5

Table 35: Computational results for RTS-GMLC instances. Wall clock times are reported in seconds. When the 300 second time limit is reached, the terminating optimality gap is reported in parentheses. Each instance is named by the date from which the beginning of the 48-hour load profile was selected and whether the system with considered with (NC) or without (CP) a network. We replace the ramping limits from **T** with those listed.

Instance	**T**	DKRA [7] (35)(36)(79)	MLR [22] (26)(27)	AC [1] (24)(25)	**OAV** [24] ramp limits	**OAV-T** [24] ramp limits
2020-01-27 CP	88.8	99.8	90.8	86.9	96.9	87.0
2020-02-09 CP	23.0	35.3	28.7	26.8	26.0	32.6
2020-03-05 CP	25.3	20.7	28.0	32.2	27.6	33.6
2020-04-03 CP	42.6	53.8	38.8	66.8	44.7	68.2
2020-05-05 CP	19.5	22.8	23.5	24.4	23.6	22.7
2020-06-09 CP	5.8	6.4	6.6	6.3	6.0	7.3
2020-07-06 CP	6.8	9.6	6.2	7.0	10.3	10.4
2020-08-12 CP	12.2	10.6	9.3	10.7	10.7	10.3
2020-09-20 CP	7.4	11.2	8.2	8.3	8.1	9.6
2020-10-27 CP	24.3	19.2	29.5	26.5	31.2	26.5
2020-11-25 CP	33.4	32.9	33.2	26.8	38.9	42.7
2020-12-23 CP	19.4	20.3	18.7	24.6	18.9	16.5
2020-01-27 NC	157.6	137.4	167.3	143.5	79.1	139.6
2020-02-09 NC	212.6	259.2	220.1	217.3	242.1	(0.015%)
2020-03-05 NC	(0.021%)	(0.015%)	(0.018%)	(0.019%)	(0.015%)	(0.020%)
2020-04-03 NC	(0.050%)	(0.049%)	(0.048%)	(0.058%)	(0.050%)	(0.045%)
2020-05-05 NC	212.8	138.9	133.4	143.8	225.2	242.5
2020-06-09 NC	49.8	53.4	45.9	51.3	52.9	50.4
2020-07-06 NC	39.3	42.2	59.5	33.1	47.8	47.6
2020-08-12 NC	67.3	61.6	50.3	53.3	46.4	46.9
2020-09-20 NC	69.3	67.9	63.1	109.2	110.0	65.4
2020-10-27 NC	153.7	178.7	186.0	165.4	151.5	175.1
2020-11-25 NC	164.9	129.8	132.1	121.2	145.0	119.5
2020-12-23 NC	226.1	91.0	116.4	196.0	108.5	116.7

Table 36: Computational results for CAISO instances. Wall clock times are reported in seconds. When the 300 second time limit is reached, the terminating optimality gap is reported in parentheses. Each instance is named by the date or hypothetical scenario from which the beginning of the 48-hour load profile was selected, followed by the reserve level, considered as a percentage of load. We replace the ramping limits from **T** with those listed.

Instance	**T**	DKRA [7] (35)(36)(79)	MLR [22] (26)(27)	AC [1] (24)(25)	**OAV** [24] ramp limits	**OAV-T** [24] ramp limits
2014-09-01 0%	51.7	57.0	42.3	41.1	62.0	61.6
2014-12-01 0%	45.1	32.0	30.9	35.2	24.2	25.1
2015-03-01 0%	32.1	36.2	34.8	39.4	34.8	36.7
2015-06-01 0%	19.1	20.2	17.1	21.9	22.7	22.1
Scenario400 0%	31.0	36.3	15.9	35.0	37.7	37.5
2014-09-01 1%	25.4	36.5	32.8	32.3	48.9	50.2
2014-12-01 1%	84.5	73.8	71.7	62.1	69.6	69.5
2015-03-01 1%	36.4	35.6	27.5	42.5	40.6	41.0
2015-06-01 1%	38.3	41.5	45.3	55.2	56.5	58.5
Scenario400 1%	66.5	63.4	68.2	39.1	44.5	44.2
2014-09-01 3%	83.5	55.5	77.2	69.6	76.4	76.2
2014-12-01 3%	106.8	89.5	71.0	82.2	110.9	111.1
2015-03-01 3%	67.4	63.5	68.0	76.0	71.3	70.8
2015-06-01 3%	57.8	35.3	71.4	54.3	36.7	36.8
Scenario400 3%	103.8	102.8	93.8	97.2	101.7	98.2
2014-09-01 5%	92.7	68.7	58.6	59.3	86.8	87.3
2014-12-01 5%	129.9	84.5	72.0	116.0	201.7	202.7
2015-03-01 5%	54.6	43.6	51.4	47.4	57.4	57.5
2015-06-01 5%	56.7	72.7	70.9	62.7	76.7	77.2
Scenario400 5%	106.9	101.7	55.4	101.5	118.6	120.5

Table 37: Computational results for FERC instances. Wall clock times are reported in seconds. When the 600 second time limit is reached, the terminating optimality gap is reported in parentheses. Each instance is named by the date from which the beginning of the 48-hour load profile was selected and whether it is low-wind (LW) (wind supply is 2% of energy demand for the year) or high-wind (HW) (wind supply is scaled to be 30% of energy demand for the year). We replace the ramping limits from **T** with those listed.

Instance	**T**	DKRA [7] (35)(36)(79)	MLR [22] (26)(27)	AC [1] (24)(25)	**OAV** [24] ramp limits	**OAV-T** [24] ramp limits
2015-01-01 LW	107.6	114.4	107.9	132.5	111.9	119.3
2015-02-01 LW	133.5	107.1	139.3	139.4	98.5	99.7
2015-03-01 LW	244.0	259.5	124.2	293.5	223.7	263.7
2015-04-01 LW	411.6	395.9	342.1	(0.017%)	400.0	359.8
2015-05-01 LW	221.6	224.9	166.3	263.9	229.1	277.9
2015-06-01 LW	282.6	341.5	302.3	358.1	328.6	449.0
2015-07-01 LW	429.6	595.3	203.5	484.4	514.1	(0.032%)
2015-08-01 LW	281.5	417.9	385.2	376.1	401.6	438.5
2015-09-01 LW	541.8	568.1	399.3	584.4	392.7	568.4
2015-10-01 LW	201.9	212.3	390.1	160.9	132.2	127.0
2015-11-02 LW	166.0	138.7	137.6	177.6	126.8	133.6
2015-12-01 LW	114.5	161.8	148.3	174.6	144.4	162.7
2015-01-01 HW	210.4	250.3	276.0	251.5	242.1	303.2
2015-02-01 HW	136.0	156.5	172.6	178.0	149.5	351.6
2015-03-01 HW	379.2	293.0	342.7	494.1	339.4	(0.013%)
2015-04-01 HW	244.6	282.4	250.9	296.4	258.1	308.0
2015-05-01 HW	244.4	255.0	117.2	278.8	227.8	246.3
2015-06-01 HW	351.2	464.6	373.0	431.6	386.1	437.5
2015-07-01 HW	548.1	522.3	282.8	579.0	489.1	(0.022%)
2015-08-01 HW	361.7	398.3	562.9	476.5	456.2	(0.011%)
2015-09-01 HW	(0.018%)	373.6	413.8	(0.019%)	(0.012%)	(0.021%)
2015-10-01 HW	351.6	349.3	346.1	368.3	326.7	454.1
2015-11-02 HW	321.1	348.8	192.7	409.5	340.7	396.2
2015-12-01 HW	287.3	268.6	272.9	256.9	319.0	372.4

Table 38: Computational results for RTS-GMLC instances. Wall clock times are reported in seconds. When the 300 second time limit is reached, the terminating optimality gap is reported in parentheses. Each instance is named by the date from which the beginning of the 48-hour load profile was selected and whether the system with considered with (NC) or without (CP) a network. We replace the production cost formulation from **T** with those listed.

Instance	**T**	CA [5] (43)(44)(45)	Wu [33] (42)(43)(44)	**KOW** [18] prod. costs	CW [6] (93)(94)(95)	SOS2 (89)(90)(91)	SLL [31] (89)(90)(92)	Epi (49)	HB [14] (50)
2020-01-27 CP	88.8	75.8	102.3	99.8	82.0	84.0	78.0	87.7	72.9
2020-02-09 CP	23.0	20.2	23.8	35.5	21.4	33.1	20.6	38.6	28.3
2020-03-05 CP	25.3	22.4	21.5	20.3	23.0	24.6	22.2	28.1	30.4
2020-04-03 CP	42.6	53.6	51.3	53.8	42.7	45.4	55.3	67.7	49.7
2020-05-05 CP	19.5	30.8	24.9	22.5	15.9	29.1	17.1	33.9	23.3
2020-06-09 CP	5.8	6.5	6.9	6.3	5.8	6.5	5.7	6.8	6.3
2020-07-06 CP	6.8	7.9	7.9	9.5	8.8	11.7	7.6	13.2	11.1
2020-08-12 CP	12.2	6.3	8.4	10.7	7.6	8.5	7.5	8.8	12.1
2020-09-20 CP	7.4	8.1	11.3	11.2	8.2	12.2	8.9	8.1	11.7
2020-10-27 CP	24.3	30.5	25.0	18.6	23.2	25.0	26.6	23.8	22.6
2020-11-25 CP	33.4	32.9	31.2	32.0	33.5	30.9	36.4	39.2	57.5
2020-12-23 CP	19.4	13.3	24.0	20.1	22.2	35.1	22.1	26.2	18.9
2020-01-27 NC	157.6	202.1	93.7	137.7	164.0	163.6	129.1	191.5	140.7
2020-02-09 NC	212.6	176.7	156.9	258.4	207.1	255.6	209.7	102.1	187.2
2020-03-05 NC	(0.021%)	210.5	125.8	(0.016%)	258.9	247.2	182.5	279.3	172.7
2020-04-03 NC	(0.050%)	(0.054%)	(0.067%)	(0.049%)	(0.043%)	(0.076%)	(0.047%)	(0.072%)	(0.055%)
2020-05-05 NC	212.8	125.2	(0.039%)	139.0	141.3	(0.055%)	254.6	(0.051%)	299.7
2020-06-09 NC	49.8	60.1	47.1	54.0	61.2	80.6	58.1	63.5	54.5
2020-07-06 NC	39.3	61.6	43.6	42.4	51.0	82.6	41.5	45.2	87.0
2020-08-12 NC	67.3	45.8	67.2	61.1	69.1	61.6	42.0	51.5	75.9
2020-09-20 NC	69.3	77.1	67.2	68.4	73.9	125.4	77.0	121.8	113.8
2020-10-27 NC	153.7	203.6	205.8	179.3	183.5	229.2	184.3	180.3	184.1
2020-11-25 NC	164.9	86.9	212.5	130.4	155.2	136.9	113.2	123.0	125.0
2020-12-23 NC	226.1	276.3	114.0	91.1	235.7	156.8	97.0	239.1	229.1

Table 39: Computational results for CAISO instances. Wall clock times are reported in seconds. When the 300 second time limit is reached, the terminating optimality gap is reported in parentheses. Each instance is named by the date or hypothetical scenario from which the beginning of the 48-hour load profile was selected, followed by the reserve level, considered as a percentage of load. We replace the production cost formulation from **T** with those listed.

Instance	**T**	CA [5] (43)(44)(45)	Wu [33] (42)(43)(44)	**KOW** [18] prod. costs	CW [6] (93)(94)(95)	SOS2 (89)(90)(91)	SLL [31] (89)(90)(92)	Epi (49)	HB [14] (50)
2014-09-01 0%	51.7	53.5	55.5	56.2	45.0	29.6	41.8	33.2	28.4
2014-12-01 0%	45.1	33.1	36.8	31.6	27.8	26.1	24.9	19.2	21.3
2015-03-01 0%	32.1	41.2	37.0	36.0	21.4	35.7	25.6	30.7	35.0
2015-06-01 0%	19.1	26.2	21.3	20.5	14.6	18.0	15.6	17.4	18.8
Scenario400 0%	31.0	34.7	29.7	35.6	27.2	36.3	28.0	62.8	43.9
2014-09-01 1%	25.4	27.1	24.5	36.9	22.5	25.2	26.2	38.3	45.2
2014-12-01 1%	84.5	77.9	45.5	72.3	54.8	34.5	42.6	110.1	112.5
2015-03-01 1%	36.4	55.9	34.6	36.2	25.4	45.7	24.6	48.6	32.9
2015-06-01 1%	38.3	59.5	47.2	42.0	37.1	64.3	37.8	59.7	68.8
Scenario400 1%	66.5	53.9	72.8	62.4	81.3	49.7	43.2	47.0	74.5
2014-09-01 3%	83.5	76.6	57.5	55.9	64.9	75.8	79.6	128.5	102.8
2014-12-01 3%	106.8	41.0	86.5	88.9	61.2	63.1	69.9	92.9	134.9
2015-03-01 3%	67.4	79.4	57.8	64.3	66.8	66.7	66.7	64.8	110.8
2015-06-01 3%	57.8	42.9	75.5	35.0	33.0	40.4	38.6	170.1	156.4
Scenario400 3%	103.8	99.9	102.8	105.0	105.7	117.1	149.5	132.8	114.1
2014-09-01 5%	92.7	63.5	80.8	68.9	62.0	76.7	49.1	139.0	81.5
2014-12-01 5%	129.9	134.5	93.7	84.6	85.6	77.2	118.4	131.7	159.6
2015-03-01 5%	54.6	77.2	64.8	44.1	56.7	54.1	42.9	71.1	62.3
2015-06-01 5%	56.7	100.6	86.6	72.9	84.4	87.7	128.2	127.4	137.0
Scenario400 5%	106.9	99.8	130.4	102.1	156.2	127.8	130.9	134.3	269.5

Table 40: Computational results for FERC instances. Wall clock times are reported in seconds. When the 600 second time limit is reached, the terminating optimality gap is reported in parentheses. Each instance is named by the date from which the beginning of the 48-hour load profile was selected and whether it is low-wind (LW) (wind supply is 2% of energy demand for the year) or high-wind (HW) (wind supply is scaled to be 30% of energy demand for the year). We replace the production cost formulation from **T** with those listed.

Instance	**T**	CA [5] (43)(44)(45)	Wu [33] (42)(43)(44)	**KOW** [18] prod. costs	CW [6] (93)(94)(95)	SOS2 (89)(90)(91)	SLL [31] (89)(90)(92)	Epi (49)	HB [14] (50)
2015-01-01 LW	107.6	118.8	164.6	114.4	268.4	183.8	226.5	94.2	319.3
2015-02-01 LW	133.5	109.5	194.4	110.7	212.5	143.0	160.9	75.0	149.7
2015-03-01 LW	244.0	241.6	266.4	255.9	296.0	241.6	340.5	331.7	432.4
2015-04-01 LW	411.6	281.7	391.5	395.7	470.7	382.5	287.7	494.0	527.6
2015-05-01 LW	221.6	152.9	265.3	233.7	297.2	201.1	253.2	308.7	370.3
2015-06-01 LW	282.6	247.0	538.6	341.8	305.4	321.8	293.9	491.8	380.8
2015-07-01 LW	429.6	481.0	503.1	594.8	461.6	563.3	364.3	(0.040%)	(0.025%)
2015-08-01 LW	281.5	243.6	393.4	416.0	363.5	306.0	334.7	387.9	487.2
2015-09-01 LW	541.8	328.1	(0.012%)	568.3	(0.013%)	463.1	551.1	(0.016%)	(0.013%)
2015-10-01 LW	201.9	222.1	182.3	206.8	244.6	232.6	238.0	152.6	251.8
2015-11-02 LW	166.0	139.5	170.1	138.5	216.2	176.0	210.8	93.9	248.4
2015-12-01 LW	114.5	135.7	225.8	161.7	272.6	177.0	189.4	90.6	256.0
2015-01-01 HW	210.4	196.0	285.2	249.5	237.9	194.8	210.0	162.2	279.5
2015-02-01 HW	136.0	172.5	207.6	156.8	267.0	227.8	233.9	180.6	307.5
2015-03-01 HW	379.2	249.7	500.0	291.9	298.7	293.0	433.2	367.1	(0.020%)
2015-04-01 HW	244.6	276.9	330.4	284.6	217.8	180.4	207.9	293.7	237.2
2015-05-01 HW	244.4	164.8	216.7	251.7	232.0	211.3	266.6	226.3	251.5
2015-06-01 HW	351.2	332.2	354.2	458.7	338.2	387.0	364.4	487.2	343.6
2015-07-01 HW	548.1	371.6	570.6	521.7	514.2	527.3	527.2	(0.039%)	(0.042%)
2015-08-01 HW	361.7	290.1	487.1	398.9	407.8	388.5	370.7	(0.015%)	543.8
2015-09-01 HW	(0.018%)	464.6	317.6	370.2	563.5	474.5	(0.014%)	(0.022%)	(0.022%)
2015-10-01 HW	351.6	293.2	364.4	349.2	338.4	391.2	325.5	309.6	417.4
2015-11-02 HW	321.1	208.6	481.0	353.5	351.7	259.4	388.0	158.2	259.6
2015-12-01 HW	287.3	230.4	386.1	272.1	293.3	251.6	362.8	365.5	313.5

Table 41: Computational results for RTS-GMLC instances. Wall clock times are reported in seconds. When the 300 second time limit is reached, the terminating optimality gap is reported in parentheses. Each instance is named by the date from which the beginning of the 48-hour load profile was selected and whether the system with considered with (NC) or without (CP) a network. We replace the start-up cost formulation from **T** with those listed.

Instance	**T**	MLR [22] (52)(53)(54)	KOW 3bin [19] (96)(97)	A-K [2, 19] (102)(103)(106)	MLR proj (52)(55)(56)
2020-01-27 CP	88.8	97.1	107.3	160.6	72.7
2020-02-09 CP	23.0	21.4	21.0	22.0	23.1
2020-03-05 CP	25.3	24.8	25.9	27.0	18.8
2020-04-03 CP	42.6	57.8	60.3	46.3	75.0
2020-05-05 CP	19.5	25.2	26.5	28.0	19.9
2020-06-09 CP	5.8	5.3	6.2	5.7	5.2
2020-07-06 CP	6.8	7.3	6.4	5.8	6.6
2020-08-12 CP	12.2	8.3	12.4	10.7	8.7
2020-09-20 CP	7.4	12.7	9.1	8.3	10.1
2020-10-27 CP	24.3	21.6	21.8	27.3	20.9
2020-11-25 CP	33.4	32.1	28.3	29.8	32.8
2020-12-23 CP	19.4	14.5	13.8	14.1	12.5
2020-01-27 NC	157.6	101.8	111.9	90.4	79.8
2020-02-09 NC	212.6	229.3	286.2	224.8	218.2
2020-03-05 NC	(0.021%)	(0.012%)	(0.014%)	(0.019%)	(0.021%)
2020-04-03 NC	(0.050%)	(0.049%)	(0.055%)	(0.050%)	(0.051%)
2020-05-05 NC	212.8	255.7	117.9	266.5	168.9
2020-06-09 NC	49.8	50.6	51.0	41.0	47.6
2020-07-06 NC	39.3	40.5	39.5	39.2	34.8
2020-08-12 NC	67.3	64.3	42.4	40.9	54.1
2020-09-20 NC	69.3	75.8	89.9	82.7	77.2
2020-10-27 NC	153.7	133.7	106.8	126.3	106.2
2020-11-25 NC	164.9	136.3	148.7	139.3	91.4
2020-12-23 NC	226.1	135.9	282.1	259.2	138.9

Table 42: Computational results for CAISO instances. Wall clock times are reported in seconds. When the 300 second time limit is reached, the terminating optimality gap is reported in parentheses. Each instance is named by the date or hypothetical scenario from which the beginning of the 48-hour load profile was selected, followed by the reserve level, considered as a percentage of load. We replace the start-up cost formulation from **T** with those listed.

Instance	**T**	MLR [22] (52)(53)(54)	KOW 3bin [19] (96)(97)	A-K [2, 19] (102)(103)(106)	MLR proj (52)(55)(56)
2014-09-01 0%	51.7	47.5	60.2	24.9	18.5
2014-12-01 0%	45.1	41.0	57.6	38.6	40.6
2015-03-01 0%	32.1	40.4	53.9	23.2	40.3
2015-06-01 0%	19.1	31.9	50.1	19.1	39.6
Scenario400 0%	31.0	67.0	159.9	65.9	79.6
2014-09-01 1%	25.4	38.7	64.8	33.6	40.1
2014-12-01 1%	84.5	87.9	122.9	72.9	90.7
2015-03-01 1%	36.4	49.8	58.9	49.6	65.3
2015-06-01 1%	38.3	56.7	87.3	29.7	39.2
Scenario400 1%	66.5	71.9	270.5	66.1	132.8
2014-09-01 3%	83.5	71.9	120.7	51.6	111.5
2014-12-01 3%	106.8	92.7	129.2	108.5	96.2
2015-03-01 3%	67.4	73.5	65.1	53.9	66.3
2015-06-01 3%	57.8	54.3	46.8	43.8	31.2
Scenario400 3%	103.8	120.1	(0.015%)	203.4	107.6
2014-09-01 5%	92.7	107.1	156.0	66.2	73.5
2014-12-01 5%	129.9	130.2	171.0	98.4	92.6
2015-03-01 5%	54.6	73.1	115.7	68.7	85.1
2015-06-01 5%	56.7	41.0	106.7	73.8	88.3
Scenario400 5%	106.9	177.3	(0.017%)	147.3	146.1

Table 43: Computational results for FERC instances. Wall clock times are reported in seconds. When the 600 second time limit is reached, the terminating optimality gap is reported in parentheses. Each instance is named by the date from which the beginning of the 48-hour load profile was selected and whether it is low-wind (LW) (wind supply is 2% of energy demand for the year) or high-wind (HW) (wind supply is scaled to be 30% of energy demand for the year). We replace the start-up cost formulation from **T** with those listed.

Instance	**T**	MLR [22] (52)(53)(54)	KOW 3bin [19] (96)(97)	A-K [2, 19] (102)(103)(106)	MLR proj (52)(55)(56)
2015-01-01 LW	107.6	221.1	254.5	185.6	203.3
2015-02-01 LW	133.5	562.2	(0.015%)	519.6	413.3
2015-03-01 LW	244.0	350.9	237.5	313.9	283.1
2015-04-01 LW	411.6	190.3	293.5	113.7	281.6
2015-05-01 LW	221.6	89.8	90.3	81.3	75.3
2015-06-01 LW	282.6	110.0	112.3	110.9	117.2
2015-07-01 LW	429.6	286.5	421.3	470.4	322.1
2015-08-01 LW	281.5	215.2	298.2	251.3	260.5
2015-09-01 LW	541.8	530.6	(0.010%)	276.7	452.0
2015-10-01 LW	201.9	188.5	155.4	198.6	217.6
2015-11-02 LW	166.0	257.8	441.1	354.7	283.0
2015-12-01 LW	114.5	212.1	163.1	177.3	210.2
2015-01-01 HW	210.4	(1.099%)	(1.335%)	(1.191%)	(0.984%)
2015-02-01 HW	136.0	(0.057%)	(0.218%)	(0.058%)	(0.048%)
2015-03-01 HW	379.2	389.7	533.8	447.0	492.0
2015-04-01 HW	244.6	342.7	447.2	268.7	240.4
2015-05-01 HW	244.4	163.1	154.5	178.9	141.0
2015-06-01 HW	351.2	163.2	201.1	177.3	206.3
2015-07-01 HW	548.1	337.1	431.5	283.7	370.3
2015-08-01 HW	361.7	382.9	427.7	338.4	356.6
2015-09-01 HW	(0.018%)	479.4	(0.051%)	466.2	428.7
2015-10-01 HW	351.6	395.1	352.7	320.6	391.0
2015-11-02 HW	321.1	578.6	(0.091%)	383.3	560.3
2015-12-01 HW	287.3	293.5	389.4	412.6	264.0

References

[1] José M Arroyo and Antonio J Conejo. Optimal response of a thermal unit to an electricity spot market. *IEEE Transactions on Power Systems*, 15(3):1098–1104, 2000.

[2] Semih Atakan, Guglielmo Lulli, and Suvrajeet Sen. A state transition MIP formulation for the unit commitment problem. *IEEE Transactions on Power Systems*, 33(1):736–748, 2018.

[3] C. Barrows, A. Bloom, A. Ehlen, J. Jorgenson, D. Krishnamurthy, J. Lau, B. McBennett, M. O'Connell, E. Preston, A.-S. Staid, and J.-P. Watson. The IEEE reliability test system: A proposed 2018 update, 2018. Working Paper.

[4] René Brandenberg, Matthias Huber, and Matthias Silbernagl. The summed start-up costs in a unit commitment problem. *EURO Journal on Computational Optimization*, pages 1–36, 2015.

[5] M. Carrion and J. M. Arroyo. A computationally efficient mixed-integer linear formulation for the thermal unit commitment problem. *IEEE Transactions on Power Systems*, 21(3):1371–1378, Aug 2006. ISSN 0885-8950.

[6] Yonghong Chen and Fengyu Wang. MIP formulation improvement for large scale security constrained unit commitment with configuration based combined cycle modeling. *Electric Power Systems Research*, 148:147–154, 2017.

[7] Pelin Damcı-Kurt, Simge Küçükyavuz, Deepak Rajan, and Alper Atamtürk. A polyhedral study of production ramping. *Mathematical Programming*, 158(1-2):175–205, 2016.

[8] Tharam S Dillon, Kurt W Edwin, H-D Kochs, and RJ Taud. Integer programming approach to the problem of optimal unit commitment with probabilistic reserve determination. *IEEE Transactions on Power Apparatus and Systems*, (6):2154–2166, 1978.

[9] A. Frangioni and C. Gentile. Solving nonlinear single-unit commitment problems with ramping constraints. *Operations Research*, 54(4):767–775, 2006.

[10] A Frangioni and C Gentile. An extended MIP formulation for the single-unit commitment problem with ramping constraints. In *17th British-French-German conference on Optimization*, London, June 2015.

[11] A Frangioni and C Gentile. New MIP formulations for the single-unit commitment problems with ramping constraints. IASI Research Report 15-06, 2015.

[12] C Gentile, G Morales-Espana, and A Ramos. A tight MIP formulation of the unit commitment problem with start-up and shut-down constraints. *EURO Journal on Computational Optimization*, 5(1–2):177–201, 2017.

[13] Yongpei Guan, Kai Pan, and Kezhuo Zhou. Polynomial time algorithms and extended formulations for unit commitment problems. *IISE Transactions*, 50(8):735–751, 2018.

[14] Bowen Hua and Ross Baldick. A convex primal formulation for convex hull pricing. *IEEE Transactions on Power Systems*, 32(5):3814–3823, 2017.

[15] International Business Machines Corporation. IBM CPLEX Optimizer, 2018. URL `https://www-01.ibm.com/software/commerce/optimization/cplex-optimizer/`.

[16] Ben Knueven, Jim Ostrowski, and Jianhui Wang. The ramping polytope and cut generation for the unit commitment problem. *INFORMS Journal on Computing*, 2017. To appear.

[17] Ben Knueven, Jim Ostrowski, and Jean-Paul Watson. Online supplement for a novel matching formulation for startup costs in unit commitment. 2018.

[18] Ben Knueven, Jim Ostrowski, and Jean-Paul Watson. Exploiting identical generators in unit commitment. *IEEE Transactions on Power Systems*, 33(4), 2018.

[19] Bernard Knueven, James Ostrowski, and Jean-Paul Watson. A novel matching formulation for startup costs in unit commitment, 2018. URL `http://www.optimization-online.org/DB_FILE/2017/03/5897.pdf`.

[20] Eric Krall, Michael Higgins, and Richard P O'Neill. RTO unit commitment test system. *Federal Energy Regulatory Commission*, 2012. URL `https://ferc.gov/legal/staff-reports/rto-COMMITMENT-TEST.pdf`.

[21] J. Lee, J. Leung, and F. Margot. Min-up/min-down polytopes. *Discrete Optimization*, 1(1):77–85, June 2004. ISSN 1572-5286.

[22] G. Morales-España, J. M. Latorre, and A. Ramos. Tight and compact MILP formulation for the thermal unit commitment problem. *IEEE Transactions on Power Systems*, 28(4):4897–4908, 2013.

[23] Matthias P Nowak and Werner Römisch. Stochastic lagrangian relaxation applied to power scheduling in a hydro-thermal system under uncertainty. *Annals of Operations Research*, 100(1-4):251–272, 2000.

[24] James Ostrowski, Miguel F Anjos, and Anthony Vannelli. Tight mixed integer linear programming formulations for the unit commitment problem. *IEEE Transactions on Power Systems*, 27(1):39, 2012.

[25] Kai Pan and Yongpei Guan. A polyhedral study of the integrated minimum-up/-down time and ramping polytope. *arXiv preprint arXiv:1604.02184*, 2016. URL `https://arxiv.org/pdf/1604.02184`.

[26] PJM. PJM - ancillary services. http://pjm.com/markets-and-operations/ancillary-services.aspx, 2016. Accessed: 2016-01-07.

[27] PJM. PJM - system operations. http://www.pjm.com/markets-and-operations/ops-analysis.aspx, 2016. Accessed: 2016-01-07.

[28] D. Rajan and S. Takriti. Minimum up/down polytopes of the unit commitment problem with start-up costs. *IBM Research Report*, RC23628 (W0506-050), 2005.

[29] Matthias Silbernagl. *A polyhedral analysis of start-up process models in unit commitment problems.* PhD thesis, Technische Universität München, 2016.

[30] Matthias Silbernagl, Matthias Huber, and René Brandenberg. Improving accuracy and efficiency of start-up cost formulations in MIP unit commitment by modeling power plant temperatures. *IEEE Transactions on Power Systems*, 31(4):2578–2586, 2016.

[31] Srikrishna Sridhar, Jeff Linderoth, and James Luedtke. Locally ideal formulations for piecewise linear functions with indicator variables. *Operations Research Letters*, 41(6):627–632, 2013.

[32] Samer Takriti, Benedikt Krasenbrink, and Lilian S-Y Wu. Incorporating fuel constraints and electricity spot prices into the stochastic unit commitment problem. *Operations Research*, 48(2):268–280, 2000.

[33] Lei Wu. Accelerating NCUC via binary variable-based locally ideal formulation and dynamic global cuts. *IEEE Transactions on Power Systems*, 31(5):4097–4107, 2016.

[34] Linfeng Yang, Chen Zhang, Jinbao Jian, Ke Meng, Yan Xu, and Zhaoyang Dong. A novel projected two-binary-variable formulation for unit commitment in power systems. *Applied Energy*, 187:732–745, 2017.